FRACTIONATION AND CHARACTERIZATION OF POLYOLEFINS

1976

TOSHIO OGAWA

FRACTIONATION AND CHARACTERIZATION OF POLYOLEFINS

1976

TOSHIO OGAWA

Chapter 1 INTRODUCTION

The rapid development in polymer industry has supplied a large amount of synthetic resins of various types to market. Nowadays these materials are quite indispensable to our life. Among these, polyolefins such as polyethylene and polypropylene belong to the most important class, the production exceeding 40 % of the total amount of all synthetic polymers.[1]

When we follow up the trace of past development in polymer industry, it is noticeable that streneous efforts have been made to increase the number of commercial grades, to improve the quality, and to reduce the cost of production. In what manner were such development and improvement made ? Let us consider polypropylene products as a familiar example.[2-4] Especially we consider high impact polypropylene of which the properties have been made effectively improved to date. Homopolypropylene products have a number of desirable properties such as high yield strength and stiffness, and good surface hardness that make them a material of most versatile utility among modern thermoplastic polymers. However, they also have certain inferior properties: below room temperature their impact strength decreases, and the products become brittle. This property gives trouble when molding articles are used in a cold northern district. From the viewpoint of physical properties, this is due to the relatively high glass transition temperature of polypropylene products. Therefore, this poor performance at low temperature must be improved by lowering the transition temperature. Needless to say, the improved product must satisfy the conditions not only for impact strength but also

for other various properties, especially stiffness and melt flow characteristics. For this purpose, improvements by copolymerization were attempted, since this method was considered not to exert great effects upon properties other than the impact one. Propylene was copolymerized with a small amount of ethylene, which is similar to propylene in physical properties. The impact strength could be improved in this manner, but other properties such as stiffness and surface hardness became worse. Further, the impact strength and other properties varied in a complicated way, depending on copolymerization and purification conditions, even though the ethylene content of products was kept constant. It turned out very difficult to prepare a product which is well-balanced among the above properties. Apparently not only the chemical composition but also other molecular characteristics, such as the average molecular weight, molecular weight distribution, compositional distribution and mode of monomer arrangements should be referred to for copolymerization products. The detailed characterization of products becomes indispensable for the research and development of various commercial grades, which are going to come to market.

1.1 Importance of fractionation experiment

Synthetic polymers have the essential character termed as "the polymolecularity." Accordingly the following six molecular characteristics should be taken into consideration for the case of homopolymer products.

(1) Average molecular weights (number average $\bar{M}n$, weight average $\bar{M}w$, z-average $\bar{M}z$, etc);

(2) Molecular weight distribution;

(3) Average stereoregularity;

(4) Distribution of stereoregularity;

(5) Average chain branching;

(6) Distribution of chain branching.

In the above, some intramolecular characteristics such as the distribution of chain branching and stereoregularity along single polymer chain are ignored to avoid complexity. Needless to say, the elucidation of all of these characteristics are not always necessary for the characterization of a given homopolymer product to understand its use-properties. As an example, the characteristics (1) to (4) will provide sufficient information for describing commercial crystalline polypropylene.

For the case of copolymers the following additional characteristics should be referred to:

(7) Average chemical composition;

(8) Compositional distribution;

(9) Mode of monomer arrangement.

Furthermore, copolymerization products are usually contaminated more or less with homopolymers. The characterization of such copolymerization products becomes much more complicated than that of homopolymer products.

The molecular characteristics mentioned above may be determined by various methods such as osmometry, light scattering, infrared spectroscopy (IR) and high resolution nuclear magnetic resonance (NMR). However, these methods would only provide quantities averaged over all polymer chains present in a given sample. On the other hand, solution

and precipitation fractionations, gel permeation chromatography (GPC), thin layer chromatography (TLC) and density-gradient ultracentrifugation can be used for separation of component species from a whole sample according to the difference in certain molecular chracteristics such as molecular weight, composition, and stereoregularity. However, in practice, experimental difficulties would arise from high temperature operation, when one has to carry out the above experiments for crystalline polypropylene and ethylene-propylene copolymerization produtcs. For instance, TLC and density-gradient ultracentrifugation are very difficult to operate at high temperature, and inappropriate for preparative purpose. On the other hand, GPC is applicable even at high temperature and, in practice, allows collection of fractions having different molecular weight.[6,7] However, the amount of each fraction obtainable with GPC is usually too small to be subjected to other tests. From the above viewpoint, precipitation and solution fractionation techniques are most useful especially for obtaining fractions of crystalline polymers in a substantial quantity, since these can be easily operated at high temperature. This is the reason why we have intended to apply column fractionation techniques for the present study.

Now we will consider the advantages and disadvantages of these fractionation techniques. The first disadvantage to be mentioned is that the precipitation fractionation often causes so-called tailing effect in separating each fraction.[8,9] Moreover, it is not operated continuously. The tailing effect is known to be less significant on solution fractionation.[9] The latter disadvantage can be improved by incorporating a continuous column fractionation technique. Consequently solution fractionation is much more suitable than

precipitation fractionation for the purpose of separating crystalline polymer into well-defined fractions. Thus the present dissertation mainly concerns results on characterization of polypropylenes and ethylene-propylene copolymerization products and their fractions obtained by solution fractionation technique.

1.2 Outline of this dissertation

Chapter 2 is concerned with the phase equilibrium related to molecular weight fractionation of crystalline polypropylene. This fractionation must be carried out under the condition that two liquid phases, namely sol and gel phases, exist in equilibrium.[10-13] In order to find this condition for polypropylene-solvent-nonsolvent system, phase diagram and cloud point were determined. Some fractionation apparatus were constructed and tested. Some other fractionation conditions, such as polymer deposition onto the support and elution technique, were examined to search appropriate ones for crystalline polypropylene.[14] The molecular weight distrbution was determined by solution fractionation under specified conditions. The distribution curves obtained were compared with those by GPC.[15] In addition, some statistical parameters such as the skewness and kurtosis were also calculated. On the basis of theories developed by Tung,[16] Koningsveld and Staverman,[17] and Kamide et al.,[9] simulation was performed for the fractionation of crystalline polypropylene. Experimental results will be discussed on the theoretical basis.

We attempted and succeeded to fractionate larger amount of polypropylene per unit column volume than that ever reported.[14] It motivated us to do more detailed investigation on the separation conditions.

In particular, condition of polymer deposition onto support and choice of solvent and nonsolvent as eluent were considered to be very important in case of crystalline polypropylene. The deposited states of the polymer are studied in detail in Chapter 3.[18] Effects of solvent-nonsolvent combinations on molecular weight distributions of fractions were investigated and the results will be described in Chapter 4.[19]

Information concerning stereoregularity is also very important in characterizing crystalline polypropylene.[13] The stereoregularity, averaged over all polymer chains present in a given sample, can be determined by IR[20] or NMR.[21] However, the determination of stereoregularity distribution is not so easy as that of average quantities. As a method for determining the distribution, fractionation in a solid-liquid phase equilibrium, which is known as a structural fractionation technique,[10] was found to be recommendable. Thus the fractionation behavior in this equilibrium was investigated and will be discussed in Chapter 5 from thermodynamic point of view.[22]

Chapters 6 and 7 deal with fractionation of ethylene-propylene copolymerization products. The compositional distribution is one of the most interesting molecular characteristics concerning the above products, especially those including a considerable amount of homopolymer components. At present the study of determining the above characteristics is still at an immature stage.[23-25] Therefore, in Chapter 6, experimental conditions for the fractionation, such as solvent-nonsolvent pair and fractionation temperature, are discussed.[26] Samples having high ethylene content (20-50 ethylene wt%) were fractionated. On the basis of these experimental results, hypothetical fractionations of the products were carried out by means of computer. Chapter 7 will describe these results in detail

by classifying the products into various types.

Chapter 8 concerns a rapid determination of number-average molecular weight. One-point intrinsic viscosity method has been widely adopted for this purpose.[29-31] However, this is an indirect method. In practice, washing of viscometer takes much trouble especially in crystalline polyolefins, because of high temperature operation. On the other hand, measurements of osmotic pressure became rapid and easy by recent development of high speed membrane osmometer. Thus a one-point method for the determination of number-average molecular weight was investigated, which uses a high speed membrane osmometer.

REFERENCES

1. "Plastics Age Encyclopedia (1974)," Plastics Age Inc., Tokyo, 1973
2. "Encyclopedia of Polymer Science and Technology," Volume 11, p.597, Interscience Pub., 1969
3. T.O.J. Kresser, "Polypropylene," Reinhold Pub., 1960
4. K. Takagi and H. Sasaki, "Polypropylene Resins," Academic Press, 1967
5. T. Ogawa and T. Inaba, J. Appl. Polym. Sci., in press
6. N. Donkai, Chemistry (KAGAKU), 227(1970)
7. J.L. Waters, J. Chromatog., 55, 213(1971)
8. A. Nakajima and M. Hosono, "Molecular Properties of Polymers II," p.427, Kagakudojin (1969)
9. K. Kamide and K. Sugamiya, Makromol. Chem., 156, 259(1972)
10. M.J.R. Cantow ed., "Polymer Fractionation," Academic Press, 1967
11. W.H. Stockmayer and M. Fixman, Ann. N.Y. Acad. Sci., 57, 342(1953)
12. L.H. Tung, J. Polym. Sci., 20, 495(1956)
13. P.W.O. Wijga, J. van Schooten and J. Boerma, Makromol. Chem., 36, 115(1970)
14. T. Ogawa, Y. Suzuki, S. Tanaka and S. Hoshino, Kobunshi Kagaku, 27, 356(1970)
15. T. Ogawa, Y. Suzuki and T. Inaba, J. Polym. Sci., Part A-1, 10, 737(1972)
16. L.H. Tung, J. Polym. Sci., 61, 449(1962)
17. R. Koningsveld and A.J. Staverman, J. Polym. Sci., Part A-2, 6, 305, 325, 349, 367, 383(1968)
18. T. Ogawa, S. Tanaka and T. Inaba, J. Appl. Polym. Sci., 17, 779(1973)
19. T. Ogawa, S. Tanaka and S. Hoshino, J. Appl. Polym. Sci., 16, 2257(1972)

20. J.P. Luongo, J. Appl. Polym. Sci., 3, 302(1960)

21. E. Lonbardi, A. Segre, A. Zambelli, A. Marinangelli and G. Natta, J. Polym. Sci., Part C, Polymer Symposia, No. 16, 2539(1967)

22. T. Ogawa and S. Hoshino, J. Appl. Polym. Sci., 17, 2235(1973)

23. G.W. Phillips and W.L. Carrick, J. Amer. Chem. Soc., 84, 920(1962)

24. V.I. Pilipovskii, I.K. Kartsev, G.V. Vinogradov and S.A. Shibalovskaya, Soviet Plast., No.5, 1(1969)

25. V.A. Klyushinikov, N.N. Andreeva, A.I. Barkova, Z.V. Akkhipova and L. Shaloeva, Soviet Plast., No.1, 5(1969)

26. T. Ogawa, S. Tanaka and T. Inaba, J. Appl. Polym. Sci., 17, 319(1973)

27. T. Ogawa and T. Inaba, J. Polym. Sci., Polym. Phys. Ed., 12, 785(1974)

28. T. Ogawa, S. Tanaka and T. Inaba, J. Appl. Polym. Sci., 18, 1351(1974)

29. M.L. Huggins, Ind. Eng. Chem., 35, 980(1943)

30. R.Z. Naar, H.H. Zabusky and R.F. Heitmiller, J. Appl. Polym. Sci., 7, 330(1963)

31. J.H. Elliot, K.H. Horowitz and T. Hoodock, J. Appl. Polym. Sci., 14, 2947(1970)

32. T. Ogawa, S. Tanaka and S. Hoshino, J. Appl. Polym. Sci., 17, 2435(1973)

Chapter 2 DETERMINATION OF MOLECULAR WEIGHT DISTRIBUTION FOR CRYSTALLINE POLYPROPYLENE BY COLUMN FRACTIONATION

The column method is in principle a type of solution fractionation. It is widely used for the determination of molecular weight distributions because of its ease in operation and low cost, compared with other determination methods. This chapter concerns a study on the molecular weight distribution of crystalline polypropylenes as determined by the column method. The fractionation by a column method is considerably affected by experimental conditions such as polymer deposition, fractionation temperature, packing of the support into the column, choice of solvent-nonsolvent system, elution rate, and device for polymer recovering. Information on the thermodynamic state, which serves as the basis of investigating the above conditions, has not been fully obtained for crystalline polymers. Thus the phase diagram was determined for a crystalline polypropylene-solvent-nonsolvent system. The result showed that the system was in liquid-liquid phase equilibrium state in the vicinity of 160°C. Further the other fractionation conditions were investigated in detail. Crystalline polypropylenes were fractionated under specified conditions, and their molecular weight distributions were determined.

The features of molecular weight distribution curves obtained by the column method were examined in detail. That is, the ratio ($\bar{M}w/\bar{M}n$) of the number and weight average molecular weights was calculated for each experimental distribution curve, and was compared with that from osmometry and light scattering, and from GPC. The ratio deduced with the column method

was found to be smaller than that with other methods. To explain this finding we first examined effects of thermal degradation upon the resultant molecular weight distribution. Such a degradation might occur during fractionation and be serious for higher molecular weight fractions. The second examination was made for errors in constructing the final distribution curve from amounts and average molecular weights of recovered fractions. Such errors will be generated because each fraction has polydispersity to some extent in molecular weight. It was experimentally proved that the narrow distributions found by the column method were caused largely by the latter reason mentioned above.

Tung,[1] Koningsveld and Staverman,[2] and Kamide et al.[3,4] have presented accurate simulation methods for fractionation based on liquid-liquid phase equilibrium, and succeeded in analyzing fractionation processes by means of computer. This chapter contains a result on such a simulation treatment for fractionation of polypropylene, which was made under the conditions similar to experimental ones as close as possible. The origin of the small value of $\bar{M}_w/\bar{M}_n$ for whole polymer was again traced from the theoretical point of view.

2.1 Phase diagram in crystalline polypropylene-solvent-nonsolvent systems

Phase diagram of crystalline polymer-solvent-nonsolvent system is schematically presented in Figure 1.[2,5] As is evident from the figure, two types of phase equilibria, i.e., liquid-liquid and solid-liquid types are present. Fractionation is performed in either liquid-liquid or solid-liquid phase equilibrium. When one attempts to determine which

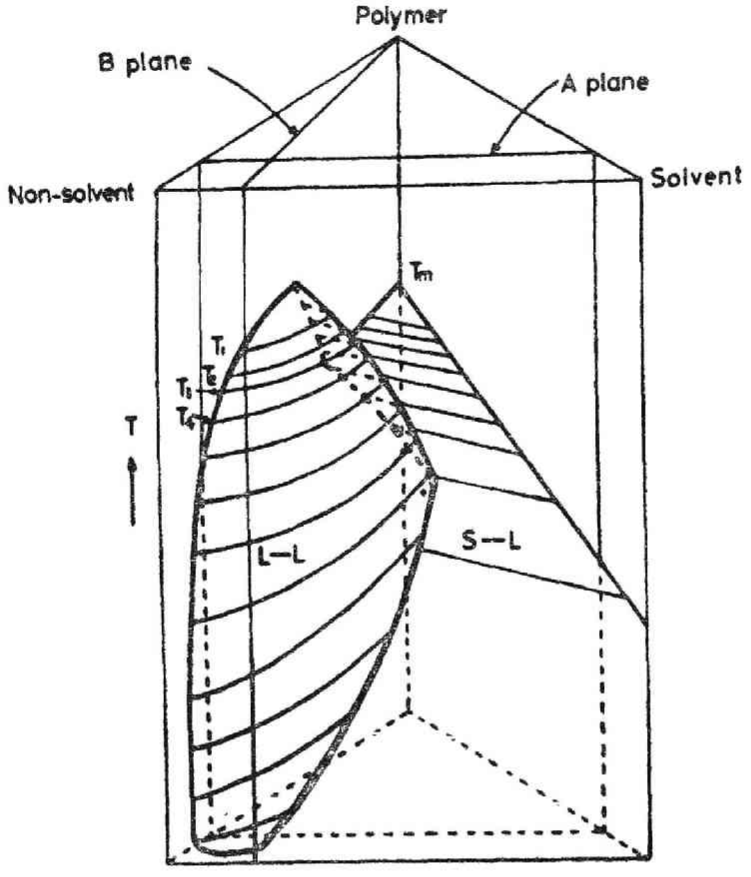

Fig. 1 Schematic presentation of phase diagram of crystalline polymer-solvent-nonsolvent ternary system.

T_1, T_2, T_3, ------ : isothermal lines on which the phase equilibrium is realized;

T_m : melting point of polymer in the solvent free state;

L-L : liquid-liquid phase equilibrium;

S-L : solid-liquid phase equilibrium.

type of phase equilibrium is attained, the phase diagram should be viewed from the various directions of cloud point behavior. Namely the cloud point should be examined at least as a function of solvent-nonsolvent ratio (A plane in Figure 1), and as a function of polymer concentration (B plane in Figure 1). The cloud point in the A plane was determined on crystalline polypropylene-decalin (or tetralin)-butyl carbitol system. The results are shown in Figure 2. The cloud point is depressed steeply with increase of solvent concentration. On the other hand, as shown in Figures 3 and 4, the cloud point in the B plane has a maximum and decreases monotonously beyond the maximum. These behavior very closely resemble those of liquid-liquid type in amorphous polymer-solvent binary system.[6] Furthermore the phase diagram was determined in this region. The result shows that only liquid-liquid type is present, as in Figure 5.[7] The cloud point behavior studied above correspond to those in binodial curve of the phase diagram. In other words, the sample polymer can be fractionated according to molecular weight under these conditions.

2.2 Computer simulation of fractionation

2.2.1 Theoretical background

The partition of polymer species between two liquid phases, i.e., the concentrated (gel) and dilute (sol) phases, is the basis for fractionation. In principle, we can solve the problems of fractionation by equating chemical potentials between the two liquid phases. A mixture of a good solvent and a nonsolvent is used as a fractionation medium. Polymer fractions are obtained by varying the ratio of solvent and nonsolvent, instead of varying temperature as in the case of a single solvent system.

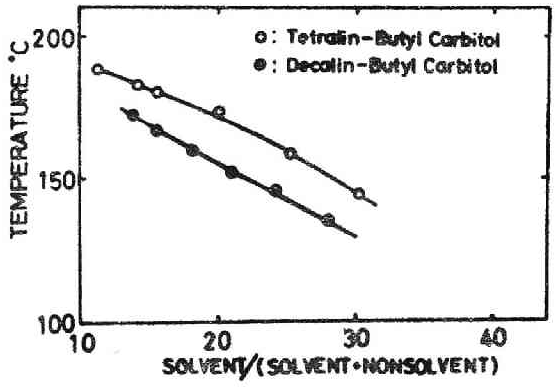

Fig. 2 Cloud points of crystalline polypropylene in two kinds of solvent-nonsolvent (butyl carbitol) systems.
Polymer concentration : 1.0 wt% polymer/(solvent+nonsolvent).

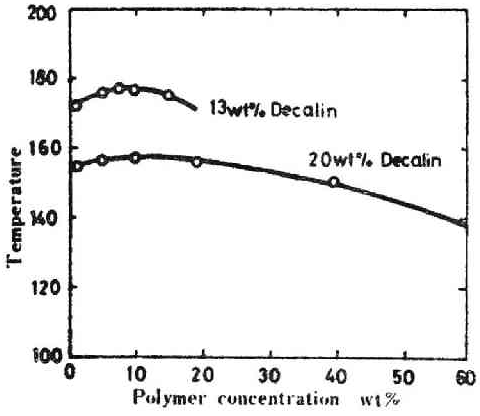

Fig. 3 Dependence of cloud point on polymer concentration with fixed decalin contents in decalin-butyl carbitol system.

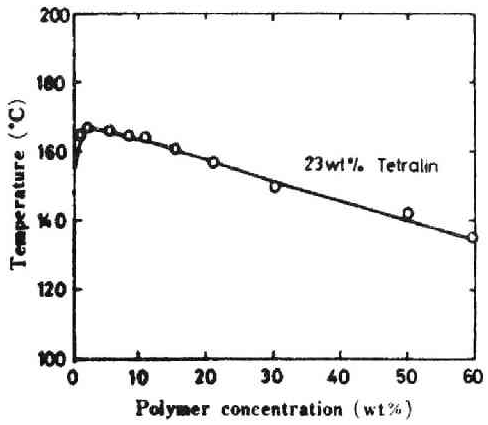

Fig. 4 Dependence of cloud point on polymer concentration in tetralin-butyl carbitol system.

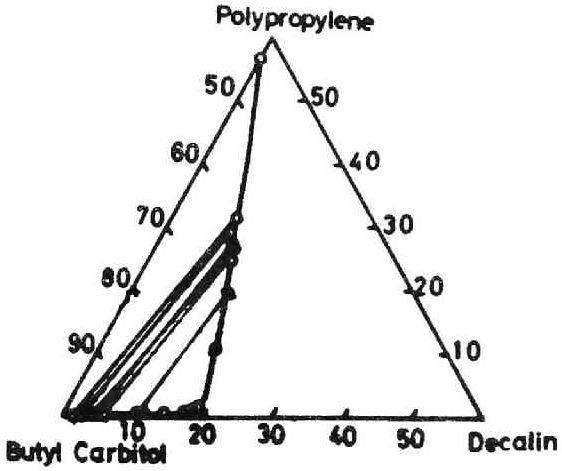

Fig. 5 Phase diagram of crystalline polypropylene-decalin-butyl carbitol system. A polymer sample having a broad molecular weight distribution ($\bar{M}w = 36.4 \times 10^4$, $\bar{M}n = 7.98 \times 10^4$) was used. It has been already confirmed from cloud point behavior that the phase diagram of polypropylenes having molecular weight higher than 5×10^4 can be approximated by this figure.

However, precise theoretical treatment of phase equilibrium for polymer-solvent-nonsolvent system is very complicated. No complete calculation method for fractionation in this system has been found so far. As a first approximation, it seems admissible to study the fractionation carried out by lowering temperature in solvent-polymer systems, in stead of that by adding nonsolvent.[5,14] The fractionation thus approximated corresponds to the most inefficient case in polymer-solvent-nonsolvent systems, although the fractionation is ideal.

According to the Flory-Huggins theory, the partial molar free energy of mixing for solvent $\Delta\mu_1$ and that for X-mer $\Delta\mu_X$ are respectively given as,[1,7,8,15]

$$\Delta\mu_1 = RT[\ln (1 - \upsilon_p) + (1 - 1/\bar{X}n)\upsilon_p + \chi_o \upsilon_p^2] \qquad (1)$$

$$\Delta\mu_X = RT[\ln \upsilon_X - (X - 1) + \upsilon_p(1 - 1/\bar{X}n)X + \chi_o(1 - \upsilon_p)^2 X] \qquad (2)$$

Here R is the molar gas constant; T is the absolute temperature; υ_p is the volume fraction of the polymer in solution; X is the degree of polymerization; $\bar{X}n$ is the number average degree of polymerization: the molar volume of the monomer was assumed to be equal to that of the solvent; χ_o is the polymer-solvent interaction parameter; and υ_X is the volume fraction of the X-mer in the solution. When the two liquid phases are in thermodynamic equilibrium, the partial molar free energy of mixing for each species must be equal between the two phases:

$$\Delta\mu_1 = \Delta\mu_1' \tag{3}$$

$$\Delta\mu_X = \Delta\mu_X' \tag{4}$$

where the prime represents the concentrated phase. The result obtained from eqs.(1) to (4) has been expressed by Flory:[11]

$$\upsilon_X'/\upsilon_X = \exp(\sigma \cdot X) \tag{5}$$

where

$$\sigma = 2/(\upsilon_p' + \upsilon_p)\{\ln[(1 - \upsilon_p)/(1 - \upsilon_p')] + (1 - 1/\bar{X}n)\upsilon_p - (1 - 1/\bar{X}n')\upsilon_p'\} - \ln[(1 - \upsilon_p)/(1 - \upsilon_p')] \tag{6}$$

Since the X-mer is in the partition equilibrium between the two liquid phases, its amount in each phase must be determined. Now let f_X^O be the fraction of the X-mer in the original polymer, the fraction f_X^E of the X-mer in the dilute phase is given by

$$f_X^E = r f_X^O/[r + \exp(\sigma \cdot X)] \tag{7}$$

where $r = V/V'$: V and V' represent the volumes of the two phases. In fractionation r and σ must be previously known. This procedure will be described in the following section.

2.2.2 Calculation procedure

Molecular weight distribution of original polymer was approximated by a log normal distribution function,[16-18] namely,

$$W(\ln M) = 1/(2\pi\beta^2)^{1/2}\exp[\ -(1/2\ \beta^2)(\ln M - \ln M_o)^2] \qquad (8)$$

where W(ln M) is the weight distribution function as a function of ln M (M: molecular weight); β is the standard deviation for ln M; and ln Mo is the peak position of the log normal distribution curve. One gram of the original polymer (density = 1.0 g/cm^3) was hypothetically dissolved in (V + V' - 1) ml of solvent. The solution was brought to a temperature by cooling, at which phase separtion occurred, and the first fraction was obtained from the dilute phase. After this step of fractionation was completed, the next was performed for the concentrated phase which was obtained in the penultimate step, the volume of the solution being kept constant. The operation was repeated until the polymer species were almost completely removed from the solution. A schematic diagram of the fractionation is presented in Figure 6.

The actual calculation procedure is as follows. The flow chart for simulation of the above fractionation is shown in Figure 7. The molecular weight distribution curve for ln M from 7 to 18 was divided into 100 equal increments. Each increment f_X° in eq.(7) is expressed as W(ln M) in eq.(8), where X = M/m (m: molecular weight of a polymer chain unit). Then f_X° was normalized as follows:

$$\sum_{i=1}^{n} (f_X^\circ)_i = 1 \qquad (9)$$

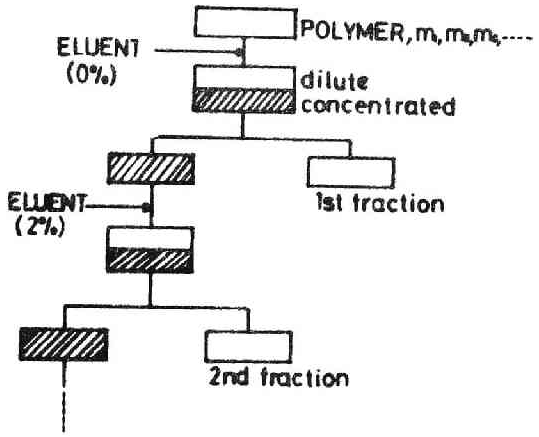

Fig. 6 Schematic representation of fractionation process, which was applied to the simulation.

where n is the number of increments.

For hypothetical fractionation, the parameters r and σ in eq.(7) must be known before each fractionation step is executed. In other words, the problem of the hypothetical fractionation is how to obtain a self-consistent r-σ pair. Now an actual fractionation is carried out by varying solvent concentration in medium. However, it is impossible to determine the pair directly from the solvent concentration. The value of the concentration, i.e., the medium composition must be converted into another variable. For this purpose, the relation between molecular weight and medium composition showing cloud point was determined by adding nonsolvent to polymer-solvent system at a constant temperature. The result is shown in Figure 8. The molecular weight showing cloud point was obtained from the solvent concentration for each fractionation point.

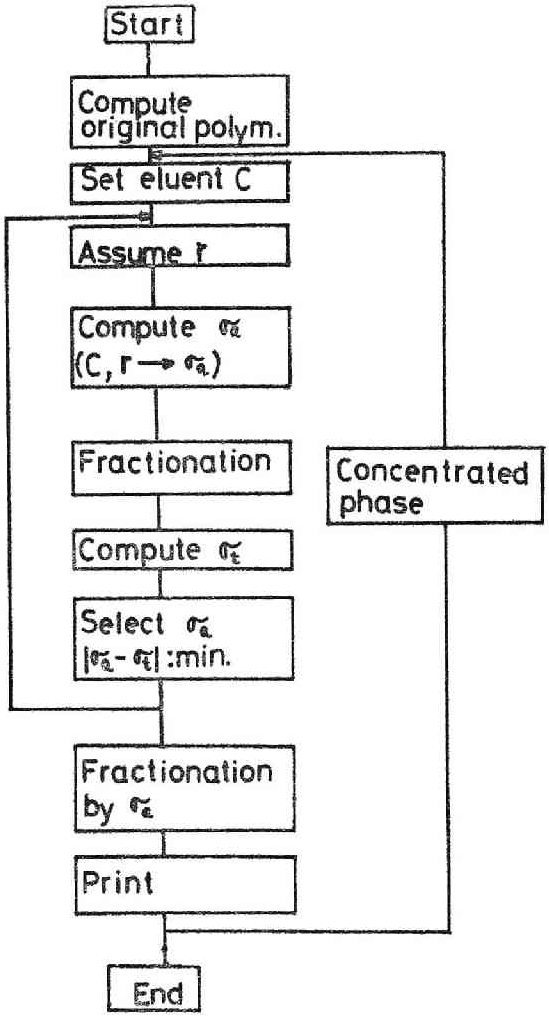

Fig. 7 Flow chart of the hypothetical fractionation for homopolymer.

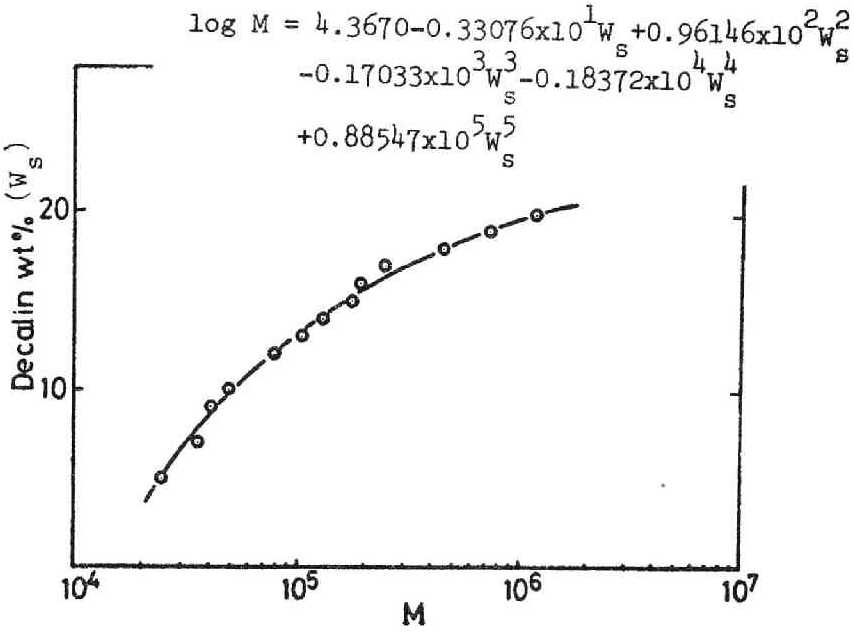

Fig. 8 Relation between the molecular weight and solvent conentration of the cloud point in decalin-butyl carbitol system at the temperature 161°C.

When $r/[r + \exp(\sigma \cdot X)]$ in eq.(7) is assumed to be constant for the molecular weight thus obtained, the variables r and σ can be determined by iterative method with electronic computer for each fractionation point. The hypothetical fractionation for all the increments was performed in the first place, using a certain $r\text{-}\sigma(\sigma_a)$ pair. The value $\sigma(\sigma_t)$ was recalculated by eq.(6), and was compared with σ_a. Thus, the r-σ pair was singled out, minimizing the absolute value of $(\sigma_a - \sigma_t)$. One step of fractionation was accomplised using this r-σ pair. The operation for the next step began in a similar manner to that for the penultimate step. An example thus calculated is shown in Table I and Figure 9.

Table I Results of hypothetical fractionation of polypropylene with decalin-butyl carbitol system at 161°C. Original polymer: $\bar{M}n = 7.47 \times 10^4$, $\bar{M}w = 35.5 \times 10^4$, $\bar{M}w/\bar{M}n = 4.76$. Initial polymer concentration: 0.50 %.

Fraction No.	Weight fraction	Solvent concentration (wt%)	$\bar{M}n \times 10^{-4}$	$\bar{M}w \times 10^{-4}$	$\bar{M}w/\bar{M}n$
1	0.0425	0.0	1.090	1.481	1.359
2	0.0126	2.0	1.624	1.896	1.168
3	0.0099	3.9	2.113	2.304	1.090
4	0.0142	5.8	2.584	2.767	1.071
5	0.0250	7.7	3.170	3.403	1.074
6	0.0420	9.5	3.978	4.321	1.086
7	0.0629	11.3	5.173	5.706	1.103
8	0.0862	13.1	6.989	7.827	1.120
9	0.1128	14.8	9.814	11.156	1.137
10	0.1434	16.5	14.506	16.803	1.158
11	0.1712	18.2	23.125	27.564	1.192
12	0.1669	19.9	41.386	51.739	1.250
13	0.0954	21.5	87.656	118.630	1.353
14	0.0114	23.1	239.086	345.811	1.446

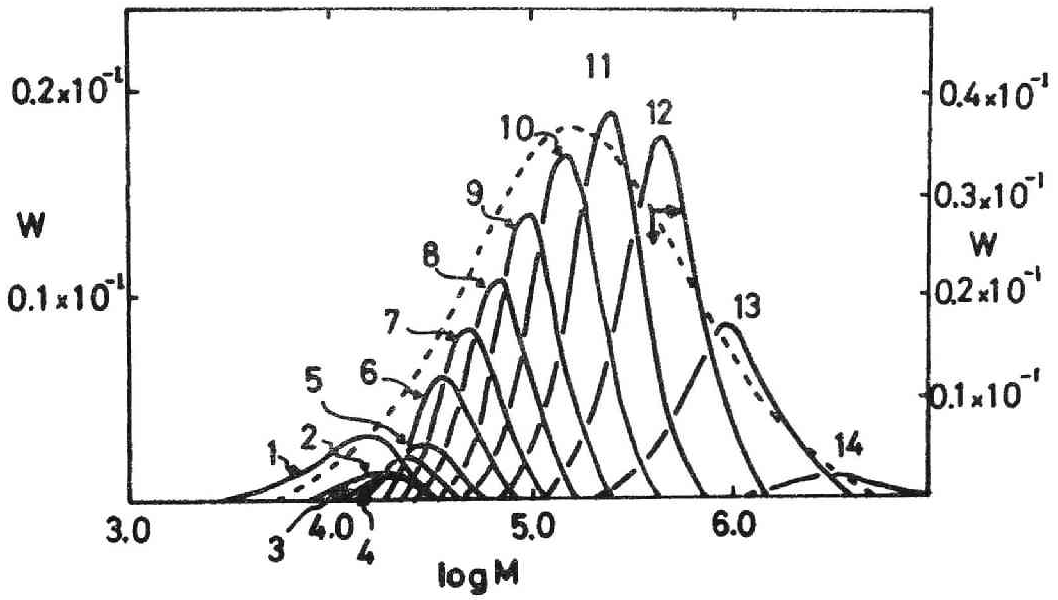

Fig. 9 Molecular weight distribution curves of the fractions obtained by the hypothetical fractionation (cf. Table I). Numbers indicate the order of the fractions.

------- : molecular weight distribution curve of the original polymer.

2.3 Fractionation apparatus

Various fractionation apparatus have been designed by many investigators.[12-20] At the beginning of our study an apparatus similar to that designed by Francis et al.[13] was used. However, some troubles happened during operation due to the complexity of the apparatus. A new small scale apparatus as shown in Figure 10 was designed and used subsequently. Good temperature control was achieved by refluxing appropriate solvent such as cyclohexanol. Channeling phenomenon and other troubles could be confined to the minimum. Most fractionation experiments in this dissertation were carried out by using this apparatus.

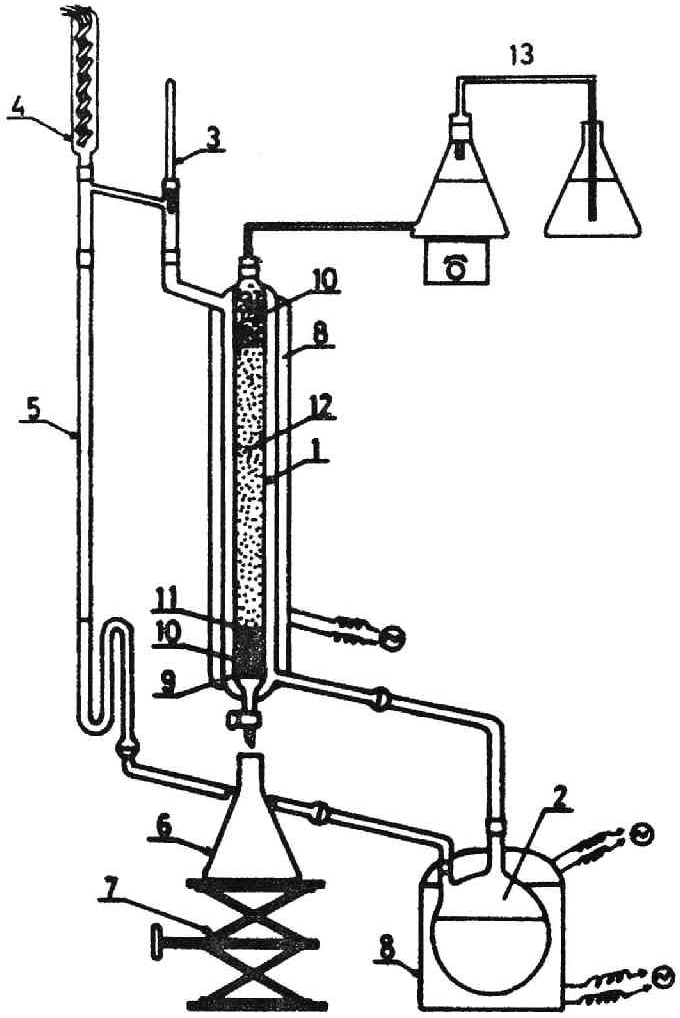

Fig. 10 Small scale fractionation apparatus: (1) column, 27mm-diam. x 830 mm-length(inside); (2) flask; (3) thermometer; (4) condenser; (5) reflux pipe; (6) adapter; (7) laboratory jack; (8) heating mantle; (9) sintered glass filter; (10) fiber glass; (11) Celite 545 (coarse); (12) Celite 545 coated with polymer; (13) solvent tank.

2.4 Fractionation experiment and characterization methods

Commercially available decalin and butyl carbitol [$C_4H_9O(CH_2CH_2O)_2H$] of high purity were used as solvent and nonsolvent, respectively. To prevent degradation of sample, 2,6-di-tert-butyl-p-cresol (Ionol) was added to solution throughout the fractionation processes. Silica particle (Celite 545) or glass powder was used as support. The supporting material was washed three or four times by decantation with water to eliminate fine powder filtrable through a glass filter of porosity G3, and further washed with acetone before filling into the column.

Considerable experience and skill are needed for good fractionation, although the column method is widely used as a routine technique. As is well known, the column fractionation procedure involves several steps[21] such as (1) deposition of polymer onto support, (2) packing the above support, (3) temperature control of the column, (4) elution of the polymer, (5) recovering each fraction, and (6) its characterization. Fractionation experiment was carried out following the above steps. For the polymer deposition, stationary method (see ref. 9) was adopted, by which polymer was deposited onto support without agitation. A decalin-butyl carbitol mixture (70 : 30 or 50 : 50 %) was used as medium for the deposition. Usually the column temperature was kept at 161°C by refluxing cyclohexanol. Each sample was fractionated to from 15 to 20 fractions. Eluted fractions were precipitated by adding large quantity of acetone, and dried at 55°C under reduced pressure.

Limiting viscosity number [η] of each fraction was determined by

the one-point method. Viscosity of 0.1 % decalin solution was measured at 135°C with an Ubbelohde type viscometer, and Huggins' constant adopted was 0.35 as determined by Sato.[13] Molecular weight was calculated with Kinsinger's equation,[22] $[\eta] = 1.10 \times 10^{-4} M^{0.80}$.

A Shimadzu GPC Model-1A was employed with the combination of four columns: Poramina 1300 which is the same as discussed previously,[23] and cross-linked polystyrene gels of 1×10^5, 1×10^4, and 1×10^3 Å permeability. The experimental conditions adopted were as follows: flow rate is 1.0 ml/min; polymer concentration 0.4 g/dl; solvent o-dichlorobenzene containing 0.2 % Ionol; and temperature 135°C. The resolution efficiency of this combined column was at least more than 400 theoretical number of plate per feet (TPF) with butyl stearate, which corresponds to above 700 TPF with acetone based on Ishida's experimental result.[24] A calibration curve was made by plotting log M versus elution count V_e data of fractions within molecular weight range of 2×10^4 to 1×10^6. The calibration curve outside this range was deduced from that of Pressure Chemical polystyrene, using the universal calibration of $\log([\eta]M)$ versus V_e relation.[25] The calibration curve is shown in Figure 11.

A Hewlett Packard Model-502 high speed membrane osmometer was employed to determine the number average molecular weight. The determination was made at 130°C on tetralin solutions containing 0.2 % Ionol with a Ultracellafilter (allerfeinst). The membrane was pretreated by immersing it successively in water, water-isopropanol (50 : 50 v/v), isopropanol, isopropanol-tetralin (75 : 25, 50 : 50, and 25 : 75 v/v) and finally tetralin. The solvent used was degassed above 100°C to avoid release of air bubbles in the cell. The membrane was also degassed in

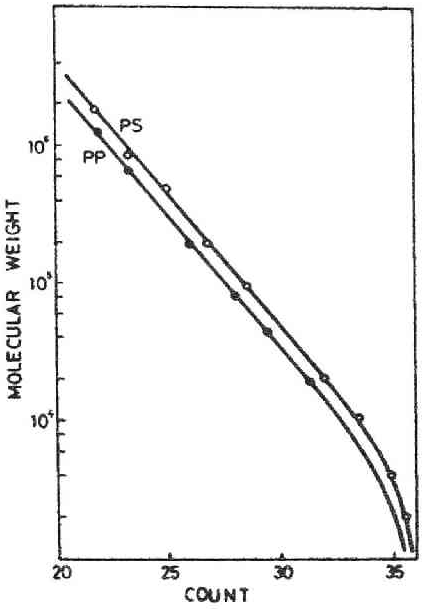

Fig. 11 Calibration curve for polypropylene (PP) and polystyrene (PS) at 135°C in o-dichlorobenzene: (○)experimental points for PS; (●) experimental points for PP.

tetralin under vacuum at 55°C for 5 hr, and allowed to stand for 30 min in the cell at 130°C before being clamped in the instrument. Such a treatment minimized the effect of permeation of low molecular weight species included in the sample, as demonstrated before.[26] Number average molecular weight was calculated by plotting $(\Pi/C)^{1/2}$ versus C (C: polymer concentration, Π: osmotic pressure).

A Sofica 42000M light scattering instrument was employed to determine the weight average molecular weight. The measurement was made at 140°C on α-chloronaphthalene solutions which had been prepared

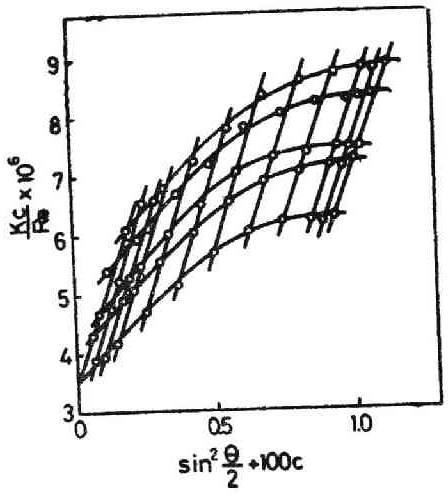

Fig. 12 An example of Zimm plot: sample C-1 in α-chloronaphthalene at 140°C.

under nitrogen atmosphere. To clean the sample solution optically we used a Millipore holder with two pieces of fluororesin filter VF-6 (Gelman Instrument Co.) and washed it at 140°C with 50-70 ml solvent. Scattering intensities were measured at eleven angles ranging from 30° to 150° and at four concentrations, i.e., 1, 2/3, 1/2, and 1/3 in relative concentration The value of -0.188 ml/g[27] was adopted for the refractive index increment (dn/dc) of crystalline polypropylene at 546 nm. Weight average molecualar weights were calculated from Zimm plot. An example of Zimm plot is shown in Figure 12.

2.5 Determination of molecular weight distribution

Molecular weight distribution curves were obtained by numerical differentiation of integral or cumulative curves, based on Rutledge's method.[28,29] From the distribution curves, number and weight average molecular weights were calculated, and then compared with the values obtained by osmometry and light scattering.

Molecular weight distributions of different samples can be most conveniently compared with one another by use of some statistical parameters which describe the distributions. It is considered that molecular weight distribution of crystalline polypropylene has a shape similar to a log normal distribution. Therefore, log M was used as a variable instead of M. Statistical parameters, such as standard deviation, skewness and kurtosis, were calculated from

$$\mu_n = \Sigma \, (\log M_i - \langle \log M_i \rangle)^n f_i \qquad (10)$$

Here, μ_n is the n-th moment around $\langle \log M_i \rangle$, and f_i is the weight fraction of the component with molecular weight M_i. The standard deviation σ, the skewness μ_3, and the kurtosis μ_4 are given by eqs.(11), (12) and (13), respectively.

$$\sigma = \mu_2^{1/2} \qquad (11)$$

$$\alpha_3 = \mu_3/\mu_2^{3/2} \qquad (12)$$

$$\alpha_4 = \mu_4/\mu_2^2 \qquad (13)$$

The standard deviation σ describes the breadth of molecular weight distribution, regardless of average molecular weight, and is different from D ($=\bar{M}w/\bar{M}n$) value. The skewness α_3 concerns the symmetry of distribution curve: $\alpha_3 = 0$ for a symmetric distribution, $\alpha_3 > 0$ for an extended trail toward higher molecular weight region, $\alpha_3 < 0$ for that toward lower molecular weight region. The kurtosis α_4 refers to the deviation from a log normal distribution: $\alpha_4 = 3.0$ for a log normal distribution, $\alpha_4 > 3.0$ for steep figure, and $\alpha_4 < 3.0$ for gentle figure. In these calculations, height (f_i) and log M_i were counted for each 0.1 interval in log M over whole range of the molecular weight distribution curve. These statistical parameters were calculated by using a FACOM 270-20/30 computer (Fujitsu Ltd.).

Commercial polypropylenes supplied from different manufacturers were examined. Two sets of distribution curves obtained for two samples by fractionation and GPC are shown in Figures 13 and 14. These figures indicate that a narrower distribution curve is obtainable from column fractionation data as compared with that from GPC. Table II shows the number and weight average molecular weights ($\bar{M}n$ and $\bar{M}w$) calculated from the curves together with those obtained by osmometry and light scattering. Table III shows the standard deviation, the skewness, and the kurtosis.

2.6 Evaluation of the distribution curve

As shown in Table II, $\bar{M}n$ obtained from the fractionation is close to that obtained by osmometry, and $\bar{M}w$ obtained from GPC is close to that obtained by light scattering. However, it is not easy to discuss the comparative merits of these methods only by identification of $\bar{M}n$ or $\bar{M}w$.

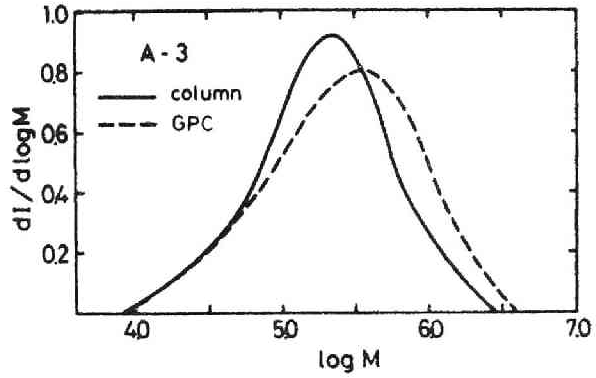

Fig. 13 Molecular weight distribution curves obtained by column fractionation (———) and GPC (-----). Sample A-3.

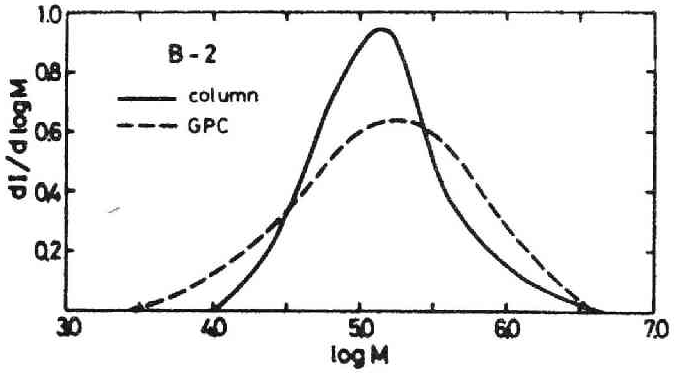

Fig. 14 Molecular weight distribution curves obtained by column fractionation (———) and GPC (-----). Sample B-2.

Table II. $\bar{M}n$, $\bar{M}w$ and D obtained by column fractionation, GPC, and osmometry and light scattering.

Sample	$\bar{M}n \times 10^{-4}$			$\bar{M}w \times 10^{-4}$			D ($=\bar{M}w/\bar{M}n$)		
	OS[a)]	Column	GPC	LS[b)]	Column	GPC	OS-LS	Column	GPC
A-1	9.86	9.16	8.71	36.4	31.3	27.5	3.69	3.42	3.16
A-2	10.1	10.9	13.0	44.4	33.6	47.2	4.38	3.09	3.63
B-1	5.27	6.44	9.40	26.7	15.3	36.2	5.07	2.38	3.65
B-2	6.27	7.16	4.75	33.3	22.6	31.2	5.31	3.16	6.58
B-3	7.34	----	10.5	42.5	----	46.3	5.79	----	4.41
C-1	7.98	7.50	5.27	36.4	17.3	24.2	4.56	2.30	4.60
Average							4.80	2.89	4.34

a) and b) indicate osmometry and light scattering, respectively.

Table III. Standard deviation, skewness and kurtosis obtained by column fractionation and GPC.

	Standard deviation		Skewness		Kurtosis	
Sample	Column	GPC	Column	GPC	Column	GPC
A-1	1.12	1.09	-0.462	-0.320	2.89	2.67
A-2	1.07	1.15	-0.321	-0.368	2.94	2.81
B-1	0.95	1.17	-0.133	-0.095	2.40	2.46
B-2	1.08	1.40	+0.237	-0.324	2.84	2.77
C-1	0.93	1.26	-0.054	-0.407	2.38	2.77

Thus the ratio of these values, namely, the D value was noted. Table II shows that the D value from the fractionation is on the average 40 % lower than that from the absolute methods, while only the deviation of ca. 10 % is observed in the case of GPC. The same behavior is also confirmed from the results of the standard deviation. Therefore, the molecular weight distribution obtained from GPC appears to be more accurate than that obtained from the fractionation.

The above results suggest that the fractionation gives a narrower molecular weight distribution than the true one. The origin of this narrow distribution will hereafter be pursued. This artifact should be attributed to several reasons such as thermal degradation during fractionation and overlapping of the molecular weight distribution curves of each fraction.

Table IV. Thermal stability of crystalline polypropylene at 160°C in decalin solution

Exposure time, hr	$\bar{M}n \times 10^{-4}$	$\bar{M}w \times 10^{-4}$	$\bar{M}w/\bar{M}n$
0	5.85	37.0	6.3
14	5.77	35.0	6.1
30	5.30	32.9	6.2
40	5.25	32.5	6.2
50	5.29	32.1	6.1

In the first place, the influence of thermal degradation was investigated. Decalin solutions of 1.0 wt% polypropylene containing 0.3 wt% Ionol as antioxidant were allowed to stand at 160°C for 5-50 hr in nitrogen atmosphere, aliquots were taken at prescribed time intervals, and then the molecular weight distributions were compared. As shown in Table IV, the D value did not vary over the period of 50 hr under these conditions. The influence of thermal degradation should be of little importance in practical fractionation.

Next, the influence of the polydispersity of each fraction upon the overall distribution was investigated. Each fraction has still a somewhat extended molecular weight distribution ($D = \sim 1.5$) and their distributions will overlap with one another. However, we usually construct the integral weight distribution curve without correcting such overlappings. Therefore, this effect was treated with a method reported by Hasely.[30] The corrected integral weight fraction is expressed by eq.(14)

$$A_i' = A_i - \sum_{j=1}^{i-1} \omega_j(M>\bar{M}_i) + \sum_{j=i+1}^{n} \omega_j(M<\bar{M}_i) \qquad (14)$$

where A_i' and A_i are the corrected and uncorrected integral weight fractions; $\omega_j(M>\bar{M}_i)$ is the weight fraction of polymer with molecular weight larger than M_i; and $\omega_j(M<\bar{M}_i)$ is that with molecular weight smaller than $\bar{M}_i$ in the j-th fraction.

When we correct the distribution curve of the original polymer with this method, the molecular weight distribution curve for each fraction, i.e., ω_j must be known in advance. As an example, the distributions of the fractions from sample C-1 were determined by GPC, and then adequately classified into four types of curves as shown in Figure 15. The corrected integral weight fractions A_i' were calculated by using the curves and plotted. The distribution curve thus obtained is shown in Figure 16. The corrected one is considerably broader than the uncorrected one, and becomes fairly close to that from GPC.

The same behavior can also be seen by the hypothetical fractionation of polymer having a log normal distribution. The true distribution curve and the curve obtained by Schulz's plot[31] from the fractions in simulation are shown in Figure 17. This figure leads to a value of 4.1 for the uncorrected curve as compared with that of 4.8 for the true one. This result coincides with the above experimental one.

Strictly speaking the simulated D value (D = 4.1) is still larger than the one expected by the experiment (D = 3.7, cf. Table II). As shown in Figure 18, this may be attributed to the slight difference of molecular weight distributions of fractions between the experiment and simulation,

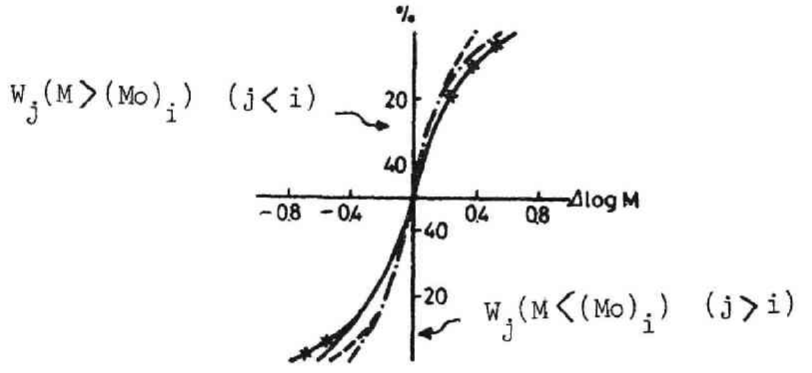

Fig. 15 Distribution curves of the fractions from sample C-1: (-----) fractions 5-9, (—— –) fractions 2-4 and 10-13, (———) fractions 14-16, (—×—×—) fraction 1. $\Delta \log M = (\log Mo)_i - (\log Mo)_j$, $(\log Mo)_i$ is the peak position of distribution curve of i-th fraction, and $(\log Mo)_j$ is that of j-th fraction.

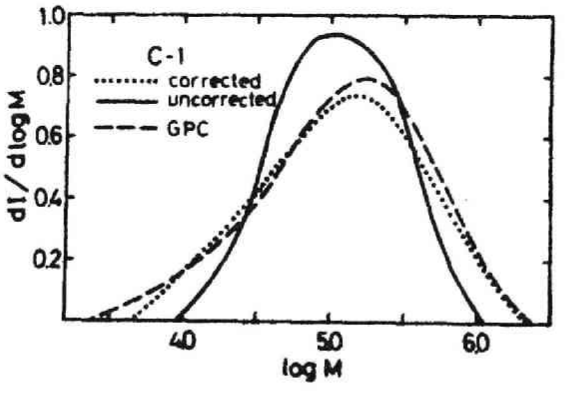

Fig. 16 Corrected and uncorrected molecular weight distribution curves obtained by the fractionation, and the distribution curve obtained by GPC. Sample C-1.

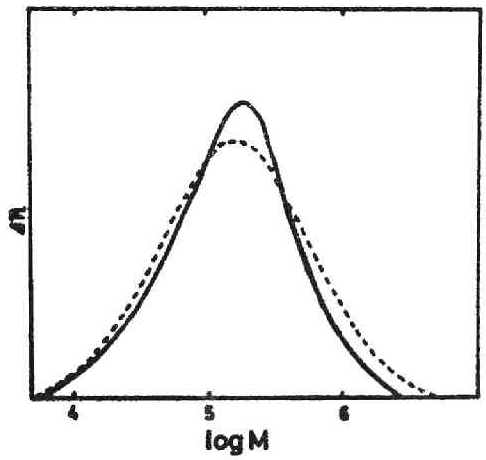

Fig. 17 Log normal distribution curve (-----) and the curve obtained from hypothetical fractions by Schulz's plot[31] (———).

Log normal distribution curve: $\bar{M}n = 7.47 \times 10^4$, $\bar{M}w = 35.6 \times 10^4$, $\bar{M}w/\bar{M}n = 4.76$.

The curve obtained from hypothetical fractions: $\bar{M}n = 7.83 \times 10^4$, $Mw = 32.1 \times 10^4$, $\bar{M}w/\bar{M}n = 4.10$.

especially in higher molecular weight region. That is, the experimental curve is influenced more considerably than the simulated one by the overlapping, because of broader distributions of experimental fractions. It is concluded that the apparent narrow molecular weight distribution obtained from the column fractionation is caused by the overlapping effect due to the polydispersity of each fraction.

The shape of the molecular weihgt distribution curve was examined. As shown in Table III, no significant difference in the skewness or

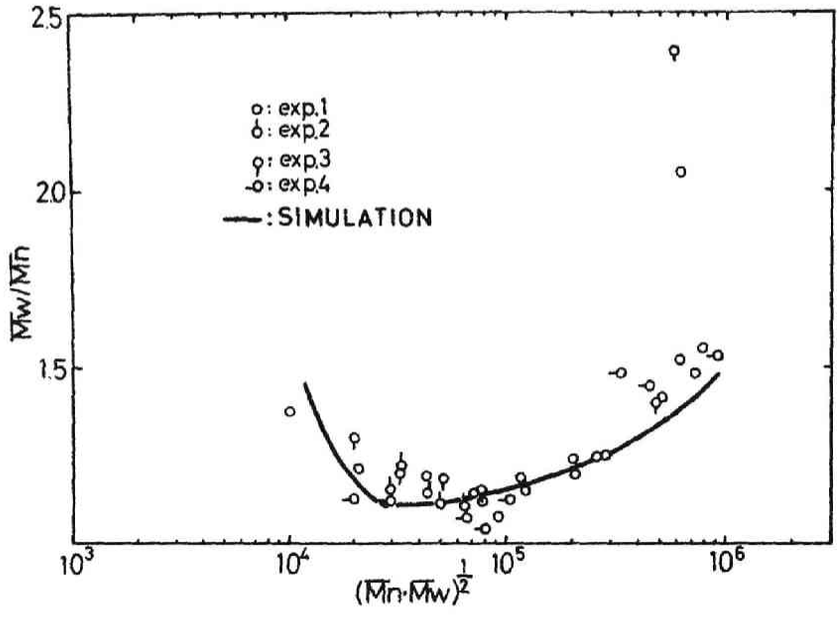

Fig. 18 Comparison of the experimental data with those by the simulation for the D value of fractions.

kurtosis is observed between the fractionation and GPC. The value of the kurtosis is nearly equal to 3.0, and that of the skewness generally gives negative value. Therefore, the molecular weight distribution of crystalline polypropylene can be approximated by a log normal distribution function, although it has slightly an extended trail in the lower molecular weight region.

1. L.H. Tung, J. Polym. Sci., 61, 449(1962)
2. R. Konigsveld and A.J. Staverman, J. Polym. Sci., A-2, 6, 305(1968)
3. K. Kamide and K. Sugamiya, Makromol. Chem., 139, 197(1970)
4. K. Kamide and K. Sugamiya, Makromol. Chem., 156, 259(1972)
5. T. Ogawa and S. Hoshino, Kobunshi kagaku, 28, 348(1971)
6. A.R. Shultz and P.J. Flory, J. Am. Chem. Soc., 74, 4760(1952)
7. T. Ogawa, S. Tanaka and T. Inaba, J. Appl. Polym. Sci., 17, 779(1973)
8. A. Saijyo, S. Hayashi, F. Hamada and A. Nakajima, Kobunshi Kagaku, 24, 775(1967)
9. T. Ogawa, Y. Suzuki, S. Tanaka and S. Hoshino, Kobunshi Kagaku, 27, 356(1970)
10. R. Koningsveld, in "Characterization of Macromolecular Structure", Proceedings of a Conference, April 5-7, 1967, Warrengton, National Academy of Sci., Washington, 1968
11. P.J. Flory, "Principles of Polymer Chemistry", Cornell University Press, 1953
12. H. Wesslau, Makromol. Chem., 20, 111(1956)
13. M. Sato, Kogyo Kagaku Zasshi, 65, 385(1962)
14. R.A. Mendelson, J. Polym. Sci., Part A, 1, 2361(1963)
15. R.S. Francis, R.C. Cooke, Jr., and J.H. Elliott, J. Polym. Sci., 31, 453(1958)
16. P.W. Wijga, J. van Schooten and J. Boerma, Makromol. Chem., 36, 115(1960)
17. T.E. Davis and R.L. Tobias, J. Polym. Sci., 50, 227(1961)
18. R.W. Ford and J.D. Ilavsky, J. Appl. Polym. Sci., 12, 2299(1968)
19. S. Hayashi, F. Hamada, A. Saijyo and A. Nakajima, Kobunshi Kagaku,

24, 769(1967)

20. R.T. Traskos, N.S. Schneider and A.S. Hoffman, J. Appl. Polym. Sci. 12, 509(1968)

21. N. Donkai and T. Kotaka, Kogyo Kagaku Zasshi, 71, 1039(1968)

22. J.R. Kinsinger and R.E. Hughes, J. Phys. Chem., 63, 2002(1959)

23. N. Baba and S. Sato, Japan Analyst, 20, 208(1971)

24. Y. Ishida, Y. Yoshida, K. Kawai and I. Kimura, Kobunshi Kagaku, 26, 498(1970)

25. T. Ogawa, S. Tanaka and S. Hoshino, Kobunshi Kagaku, 29, 6(1972)

26. T. Ogawa, S. Tanaka and S. Hoshino, Kobunshi Kagaku, 28, 8(1971)

27. E.E. Drott and R.A. Mendelson, Polym. Lett., 2, 187(1964)

28. G. Rutledge, Phys. Rev., 40, 252(1932)

29. H. Margenau and G.M. Murphy, "The Mathematics of Physic and Chemistry," van Nostrand, New York, 1943

30. E.A. Haseley, J. Polym. Sci., 35, 309(1959)

31. G.V. Schulz, Z. Physik. Chem., B43, 25(1939)

Chapter 3 POLYMER DEPOSITION ONTO SUPPORT IN COLUMN FRACTIONATION

Among various conditions which influence the efficiency of column fractionation, the method of polymer deposition onto support is important in achieving a good fractionation.[2-5] It has been believed that a better fractionation can be achieved by the so-called selective deposition, in which polymer components are deposited layer by layer onto the support in the order of decreasing molecular weight. However, techniques employed by various investigators to attain the selective deposition differ from one another. This raises a question whether or not the selective deposition is first of all the necessary condition. We have examined the effect of polymer deposition on the fractionation result, employing the various methods of deposition.

By the above investigation, it was found that the selective deposition is not essential for a good fractionation. The result different from the idea in the past is due to the fact that few information has been obtained so far on the state of the deposited polymer. The state of the polymer was examined with a microscope. As the result, we found that the polymer is not uniformly spread as a film[3] but deposited as small particles on the support surface. The influence of the particle size on fractionation result is examined, and importance of the particle size is pointed out.

3.1 Experimental procedure

3.1.1 Cloud point determination

The dependence of cloud point on molecular weight was examined for finding various depositing conditions. A Sofica 42000M light scattering instrument was used. The measurement was performed on 1.5 g/l polymer solution in decalin-butyl carbitol mixture. Variation of scattering intensity at 90° angle was recorded as the solution was cooled gradually (0.3°C/min) from 150°C. The cloud point was determined as A from scattering intensity versus temperature curve such as shown in Figure 1.[6]

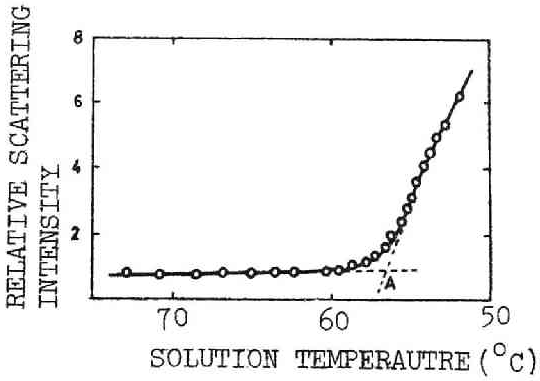

Fig. 1 The curve of scattering intensity vs. solution temperature

3.1.2 Polymer deposition and mixing of polymer with support

Two methods were adopted for packing polymer and support into the column: one is to pack the support on which polymer had been deposited in advance, and the other is to pack the mechanical mixture of polymer particles and support. The former was applied to two cases of the selective and nonselective depositions. In these cases, the stationary

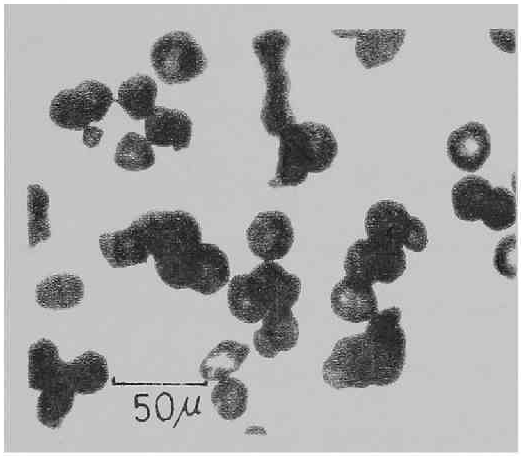

Fig. 2 Polymer particles (spherulite) precipitated from decalin solution (3 g/l). White light.

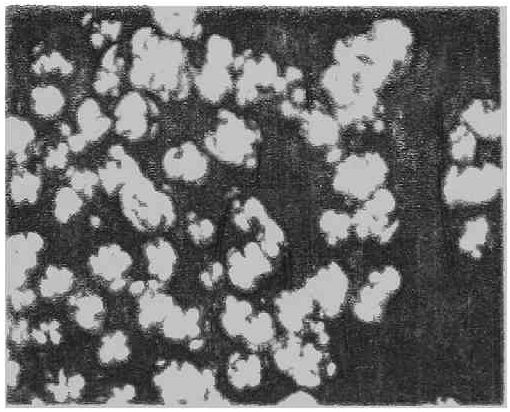

Fig. 3 Polymer particles (spherulite) precipitated from decalin solution (3 g/l). Polarized.

method (cf. Chapter 2) was adopted for the polymer deposition onto support. For the latter, two types of polymer particles were prepared in advance by the method described as follows, and by crashing polymer tips.

The polymer particles were first prepared by cooling of 0.3 g/l decalin solution of the fraction having low molecular weight ($\bar{M}n = 7.3 \times 10^4$, $\bar{M}w/\bar{M}n \leqq 1.3$). The polymer particles thus obtained were spherulite having a uniform size of approximately 30 μ in diameter. The photographs are shown in Figures 2 and 3. The polymer particles were immersed in a 2.5 % decalin solution of polymer having high molecular weight ($\bar{M}n = 3.2 \times 10^5$, $\bar{M}w/\bar{M}n \leqq 1.3$), whose temperature had been maintained just the precipitation temperature. When this solution was rapidly cooled, the polymer particles specially designed were obtained. The deposition method is hereafter called the reversed deposition. The mechanical mixture of the particles and support was packed in the column and fractionated. Figure 4 shows a schematic figure of a column, which was generally adopted in this study.

3.1.3 Fractionation experiment

Fractionation experiments on polypropylene sample deposited under various conditions were carried out to examine the effect of the depositing conditions. The molecular weight and the D value of the sample are $\bar{M}w = 3.7 \times 10^5$, and $\bar{M}w/\bar{M}n = 4.6$, respectively. The same apparatus as described in Chapter 2 (700 mm length x 27 mm diam.) was used.[7] Fractionation experiments were carried out in decalin-butyl carbitol system at 161°C. Decalin and butyl carbitol were of commercial grade. Eluent composition was varied stepwise from 0 to 23 wt% decalin by 300 g increments of eluent. The other experimental conditions and procedures are the same as described in Chapter 2.

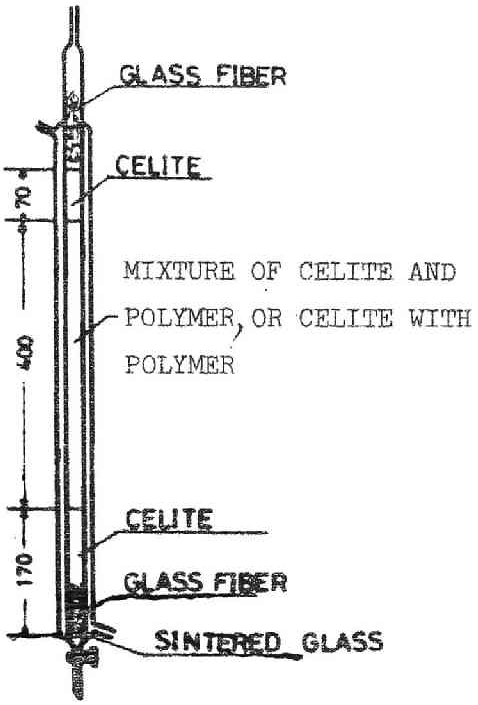

Fig. 4 Construction of the fractionation column.

3.2 Fractionation of polymer deposited under various conditions

It is doubtful whether or not the selective deposition is by all means necessary. The dependence of cloud point on molecular weight was first determined in decalin-butyl carbitol mixtures with various compositions, in order to seek favorable conditions for the selective or nonselective deposition. Figure 5 shows the result. This dependence was considerably large in 40 % decalin system (decalin : butyl carbitol = 40 : 60), but diminished as the solvent ratio increased, and ultimately disapeared

in the 100 % decalin system. The selective deposition can be attained in the 40 % decalin system and the nonselective deposition in the 100 % decalin system.

Fractionation experiments were carried out on the polymer deposited from the 40, 70, and 100 % decalin systems, in order to study the influence of the depositing conditions. The results are shown in Figure 6. All the three cases including the highly selective (40 % system) and the nonselective (100 % system) depositions give essentially an identical distribution curve. Figure 7 shows that the reversed deposition leads also to a satisfactory fractionation according to molecular weight over a wide range. The distribution curve is in fairly good agreement with that by GPC determined as reference. The D values (= $\bar{M}w/\bar{M}n$) of these fractions are

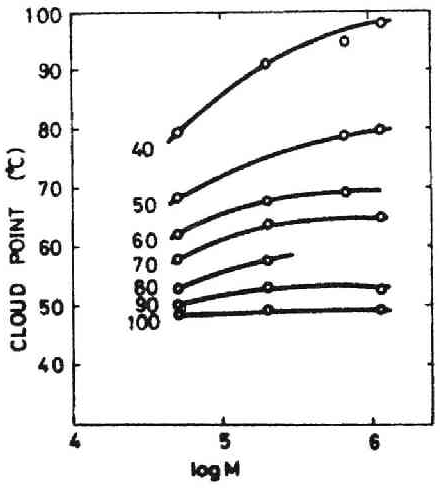

Fig. 5 Dependence of the cloud point on molecular weight in polypropylene-decalin-butyl carbitol system. The numbers indicate decalin per cent by volume at room temperature.

shown in Figure 8. Any difference cannot be confirmed among these fractionations. Therefore, these results indicate that the selective deposition is not the essential factor to attain good fractionation.

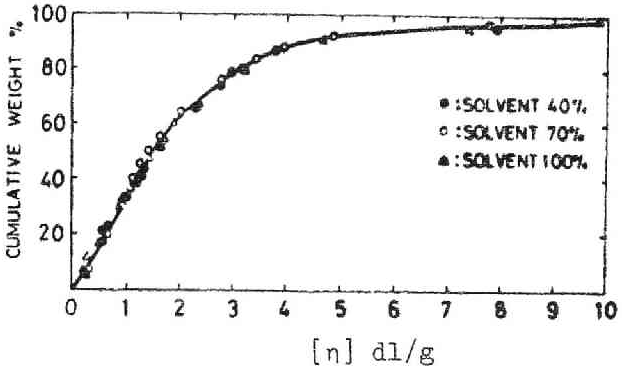

Fig. 6 Cumulative weight distribution curve obtained from the polymer deposited in the 40, 70 and 100 % decalin systems.

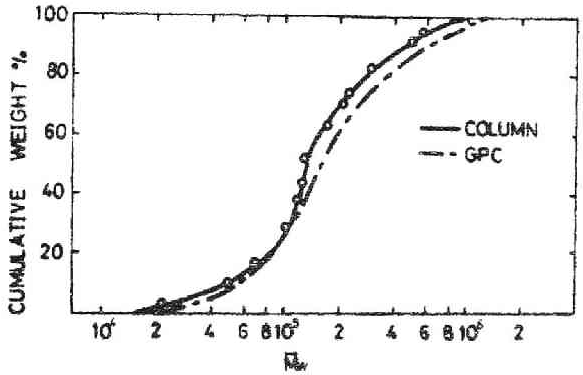

Fig. 7 Cumulative weight distribution curve obtained in the reversed deposition. A Shimadzu GPC Model-1A was used.[7]

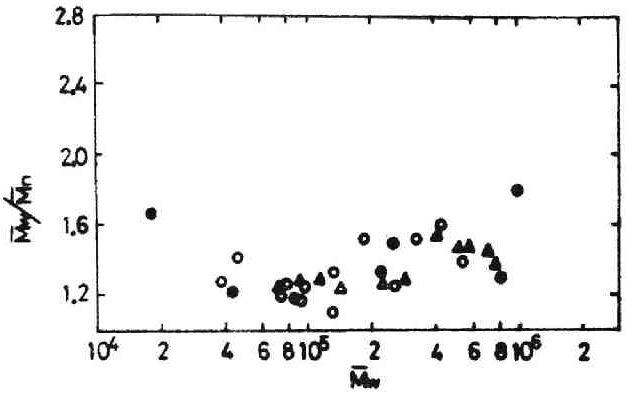

Fig. 8 D values of the fractions: (●) the fractions obtained from the polymer deposited in the 100 % decalin system; (○) in the 70 % decalin system; and (△) in the reversed desposition.

3.3 The state of deposited polymer on support

The state of deposited polymer was observed with a microscope at room temperature. As shown in Figure 9, the polymer is not uniformly spread on the support, but deposited in particle-form. Further this state has a similar appearance in the two types of support examined. The construction looks quite different from that demonstrated by Kenyon,[3] who assumed that the polymer is uniformly spread on the support in the order of decreasing molecular weight as shown in Figure 10.

As is evident from the diagram described in Chapter 2, the particles at a given fractionation temperature are in the state of liquid. Since the particles are found on the support far from one another, they may be in liquid droplets. The polymer concentration of the droplets is

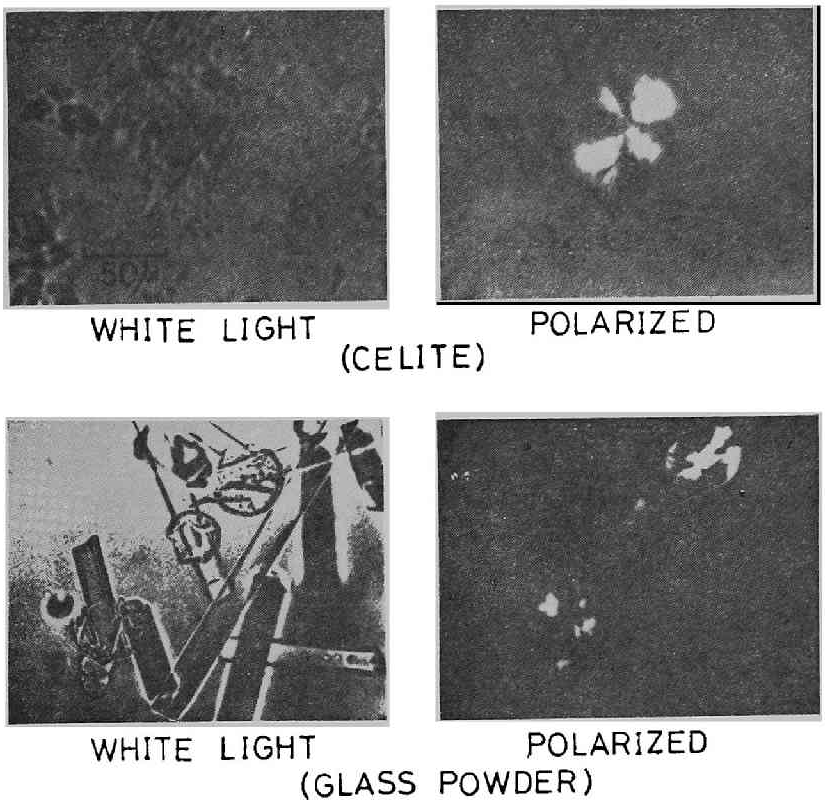

Fig. 9 Particles of crystalline polypropylene deposited on Celite and glass powder supports.

shown by one end of tie line in the phase diagram (cf. Chapter 2). On the other hand, the polymer concentration of the droplets may be estimated by simulation of the fractionation. Polymer concentration C_j of the j-th fraction is given by the following equation:

$$C_j = G_j/V' \qquad (1)$$

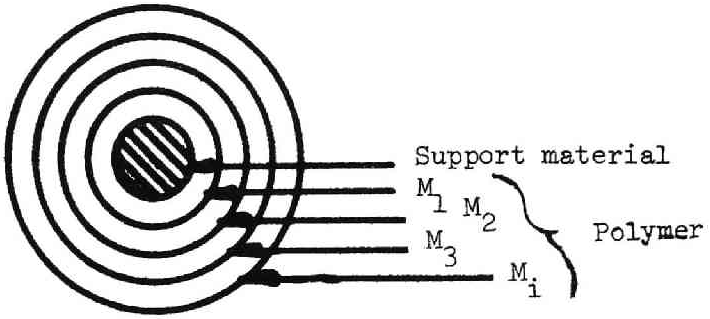

Fig. 10 Schematic diagram of deposited polymer presented by Kenyon; the M_1, M_2, M_3, --- M_i denote the molecular weights of polymer($M_1 > M_2 > M_3 \longrightarrow M_i$).

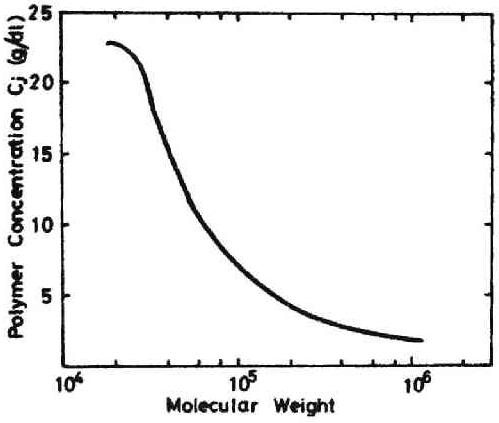

Fig. 11 Polymer concentration of liquid droplet in fractionation column as a function of molecular weight.

with

$$G_j = 1.0 - \sum_{k=1}^{j} \sum_{i=1}^{n} (f_i^E)_k \qquad (2)$$

$$V' = V_o/(1.0 + R) \qquad (3)$$

These symbols are the same as shown in Chapter 2. Figure 11 shows the result. The concentration decreases from 25 to 1.5 g/l with increase of molecular weight. The liquid droplets are regarded as a homologous solution. Thus, the fractionation process can be analyzed by the same principle as the solvent extraction of ordinary organic compounds, such as spray tower techniques. In these apparatus, it is well known that increasing contact surface of liquid droplets with solvent considerably improves the extraction efficiency. The time required for solute diffusing from center to surface of a liquid droplet is proportional to the square of the radius. That is, the diffusion of the solute obviously follows the equation of one-dimensional diffusion, as shown in eq.(4):

$$t \propto R_o^2/Do \qquad (4)$$

where t is the time for solute to diffuse from center to surface of the droplet of radius Ro, and Do is the diffusion constant. For the purpose of confirming the effect of particle size upon column fractionation, polymer particles having an average diameter of 100 μ were packed in the column together with Celite 545, and fractionated. Figure 12 shows the

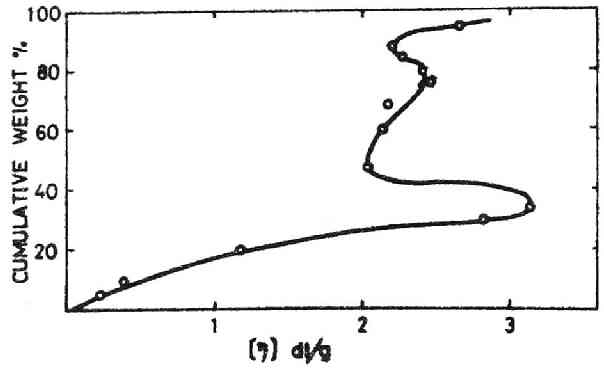

Fig. 12 Cumulative weight distribution curve obtained from polymer particles having an average diameter of 100μ (polymer load 5.0 g). The polymer particles were packed in the fractionation column by the method shown in Figure 4.

fractionation result. Only 30-40 % of the packed polymer was eluted in the order of increasing molecular weight. On the other hand, as shown in Figure 6, good fractionation was achieved when the polymer particles are one-36th in size of the above one. These results demonstrate that the size of polymer particles or liquid droplets is the most important factor for good fractionation. This concept is also in agreement with the fact that the extraction of polymer coated on wire gauze gave better results than that on aluminum leaf, as reported by Fuchs[8] and Beresniewicz.[9] Therefore, the depositing condition should be adjusted so as to make the particle size as small as possible in any case.

Next, how to reduce the particle size must be pursued. The particle size of deposited polymer under various conditions were determined with a microscope. As Figures 13 and 14 show, the deposited polymer particles on glass powder are smaller than those on Celite 545. The particle

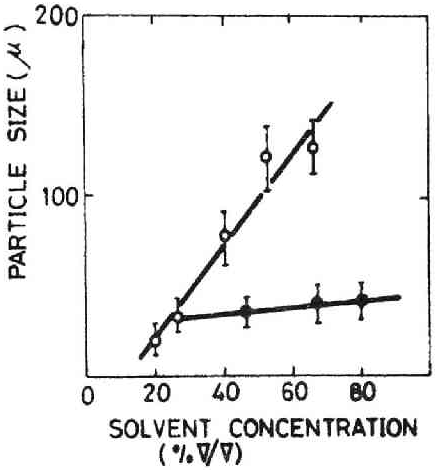

Fig. 13 Dependence of particle size on solvent ratio, determined in 0.04 g polymer per 1.0 g Celite 545 (O), and in 0.02 g polymer per 1.0 glass powder (●). Polymer concentration: 1.2 % V/V.

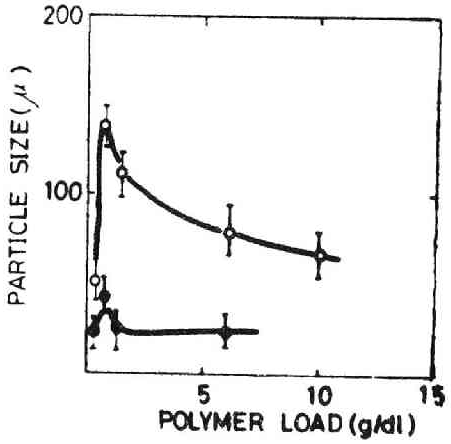

Fig. 14 Dependence of the particle size on polymer load, determined in the 60 % decalin system for (O) 10 g Celite 545 or (●) 21 g glass powder.

size is hardly dependent on solvent concentration in eluent and on polymer concentration. In the case of Celite 545, the particle size becomes smaller as the solvent concentration in eluent decreased. Therefore, the observation that the deposition from a thermodynamically poor solvent gave a good fractionation should be attributed to the effect of the particle size rather than that of the selective deposition. It is also noteworthy that the support has an important effect upon the size of deposited polymer and hence upon the fractionation efficiency. Further investigation should be required in connection with the influences of shape and dimension of these supports and of the polymer particles. Anyway, glass powder is a superior support for the fractionation of crystalline polypropylene, as far as we studied here concerning the deposited state of polymer.

REFERENCES

1.. S. Shyluk, J. Polym. Sci., 62, 317(1962)

2. R.A. Mendelson, J. Polym. Sci., Part A, 1, 2361(1963)

3. A.S. Kenyon and I.O. Salyer, J. Polym. Sci., 43, 427(1960)

4. M. Hamashima, S. Hattori, and E. Tomimura, Kobunshi Kagaku, 26, 298(1969)

5. K. Murata and S. Kobayashi, Kobunshi Kagaku, 26, 542(1969)

6. T. Ogawa, S. Tanaka, and T. Inaba, J. Appl. Polym. Sci., 17, 319(1973)

7. T. Ogawa, S. Tanaka, and S. Hoshino, J. Appl. Polym. Sci., 16, 2257(1972)

8. O. Fuchs, Makromol. Chem., 5, 245(1950)

9. A. Beresniewicz, J. Polym. Sci., 35, 321(1959)

Chapter 4 CHOICE OF SOLVENT AND NONSOLVENT FOR COLUMN FRACTIONATION OF POLYPROPYLENE

The effect of solvent-nonsolvent combination on fractionation results has not drawn much attention so far: there have been only a few papers concerned with this effect on fractionation of amorphous polymers.[1-3] These authors examined the effect only in regard to the changes in the molecular weight of each fraction with increasing the number of fractions. In this chapter we examine the effect of solvent-nonsolvent combination on the polydispersity of recovered fractions. This is particularly important when one performs column fractionation for a preparative purpose of obtaining narrow distribution fractions.

Another important aspect of this problem is concerned with the range of average molecular weights of the fractions obtained. For preparative purpose it is desirable to have narrow distribution fractions covering the molecular weight range as wide as possible. Presumably an adequate choice of solvent-nonsolvent combination and method of making solvent gradient of the eluent are important to attain this purpose. To this end it is desirable to establish the relation between molecular weight and eluent composition for a given combination. In this chapter the relation is examined for several polypropylene-solvent-nonsolvent systems using Caplan's method.[4]

4.1 Experimental procedure

Crystalline polypropylene for commercial usage (M.F.I. = 5.4) was used as sample. Decalin, α-chloronaphthalene, o-dichlorobenzene,

chlorobenzene, tetralin, n-hexadecane, and kerosene were adopted as solvents. Kerosene is of commercial grade (b.p. = 200°C, M = 158). Other solvents are of high grade commercially available. Methyl carbitol, ethyl carbitol, diethylene glycol mono-butyl acetate and butyl carbitol were used as nonsolvents. Butyl carbitol is of commercial high grade, and others are of commercial grade. To prevent degradation of the sample, Ionol was added to the solution throughout the fractionation processes. The same fractionation apparatus as described in Chapter 2 was used. For polymer deposition onto the support, the stationary method described in Chapter 2 was used.[5] A decalin-butyl carbitol mixture (70 : 30 by weight) was used as the depositing medium for all fractionations which are described in this chapter. The column temperature was kept at 161°C by refluxing cyclohexanol. The polymer was fractionated to 15 to 17 fractions. Other procedures are the same as described in Chapter 2.

A Shimadzu GPC Model-1A mounted with four columns of 10^6, 10^5, 10^4 and 10^3Å permeability limits was used for determining molecular weight and molecular weight distribution of the fractions. The experimental conditions have been already described in Chapter 2. When the molecular weight distribution is determined by GPC, the error known as the broadening effect is involved in the observed distribution curve. This error was corrected by a calibration curve which correlates the apparent and true extent of polydispersity as a function of GPC-elution volume. For this purpose, narrow distribution polymers (Pressure Chemical Co.) of known D values (D_t) were used, since the broadening effect is peculiar to the set of columns applied. From the observed chromatograms for the

polystyrenes, D values (D_g) were calcualted. Then the values of $(D_g - D_t)/D_t$ were plotted against their elution counts, as shown in Figure 1.

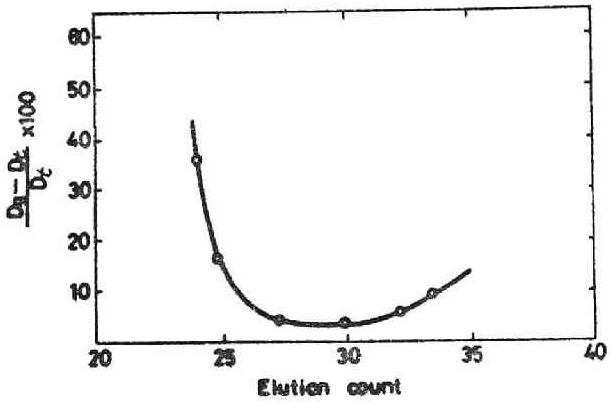

Fig. 1 Correction curve for observed D values in GPC.

4.2 Solvent and nonsolvent properties

In order to select appropriate solvent-nonsolvent combinations for the fractionation of polypropylenes, cloud point measurements were carried out. The measurements were made on 1 % polymer solution in various solvent-nonsolvent systems. The results are shown in Figures 2 and 3. These figures and the Figure 2 in Chapter 2 show that the solubility of polypropylene in these systems decreases in the following order:

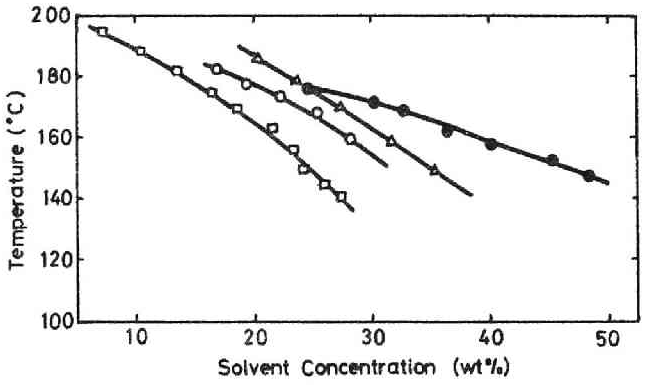

Fig. 2 Cloud points of crystalline polypropylene in solvent-nonsolvent (butyl carbitol) systems. □ : n-hexadecane, ○ : chlorobenzene △ :o-dichlorobenzene, ● : α-chloronaphthalene
Polymer concentration : 1.0 wt% polymer/(solvent + nonsolvent).

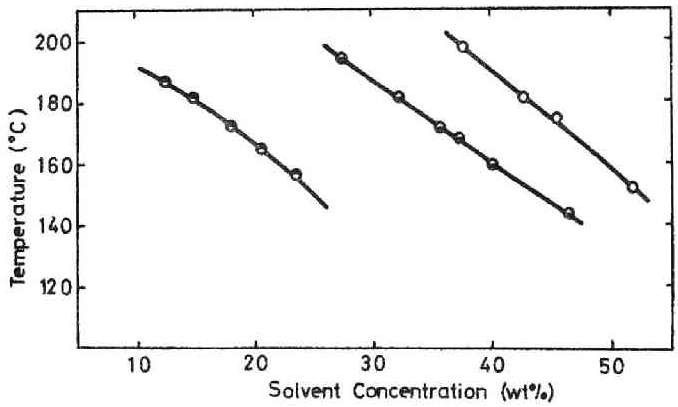

Fig. 3 Cloud points of crystalline polypropylene in solvent (decalin)-nonsolvent systems. ◓ : diethylene glycol monobutyl ethyl acetate, ◒ : diethylene glycol monoethyl ether (ethyl carbtiol), ○ : diethylene glycol monomethyl ether (methyl carbitol)
Polymer concentration: 1.0 wt% polymer/(solvent + nonsolvent).

n-hexane > decalin ≃ kerosene > tetralin > chlorobenzene

> o-dichlorobenzene > α-chloronaphthalene

That is to say: α-chloronaphthalene has the poorest solvent property among those examined here. On the other hand, the nonsolvent action of ethylene glycol derivative is as follows.

methyl carbitol > ethyl carbitol > diethylene glycol mono-butyl-

acetate > butyl carbitol

The order shows that methyl carbitol has the highest nonsolvent property among them. Other esters and glycols such as dioctyl sebacate, $C_4H_9O(CH_2CH_2O)_2C_4H_9$, and $C_4H_9OCH_2CH_2OH$ had weaker nonsolvent power than the above ethylene glycol derivatives. Polypropylene dissolved in these solvents at 160°C and became insoluble at the lower temperature. Therefore, they are not useful as the nonsolvent in polypropylene fractionation based on liquid-liquid phase equilibrium. In the present work, we selected the following solvent-nonsolvent systems for further study on the combination effect: they are decalin-butyl carbitol (D-B), decalin-ethyl carbitol (D-E), kerosene-butyl carbitol (K-B), and α-chloro-naphthalene-butyl carbitol (C-B) systems.

4.3 Molecular weight distribution of fractions

The molecular weight distribution of each fraction obtained by such various eluent systems was determined by GPC. The result obtained in K-B system is shown in Figure 4 and Table I. The corrected D value of the fractions ranges from 1.1 to 1.5, and the average is 1.24.

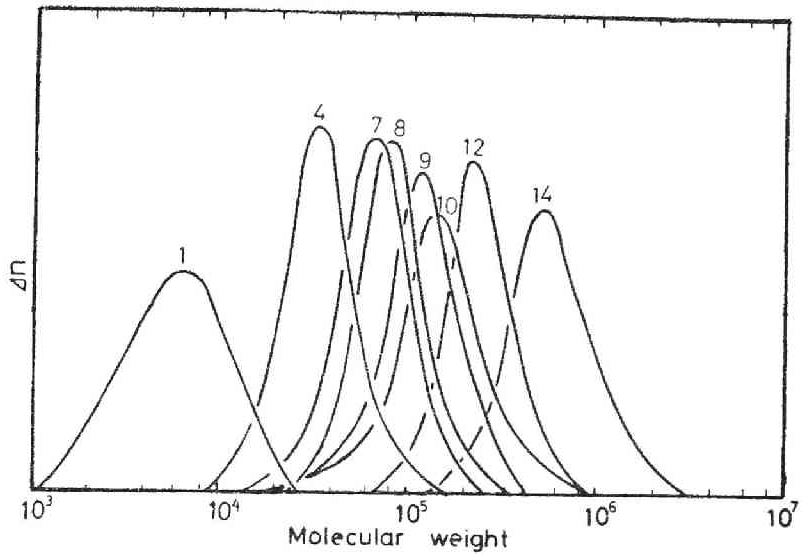

Fig. 4 Molecular weight distribution curves of the fractions obtained in kerosene-butyl carbitol system. The curves were obtained by GPC. The numbers indicate fraction number.

The results obtained by other eluent combinations are summarized in Table II. This table shows that the average of D values ranges from 1.14 to 1.24. These values demonstrate that the fractionations adopted here are generally excellent.

The simulation of the fractionation was carried out, for the sake of comparison, by using the relations between the elution point and molecular weight of the fractions shown in Figure 5, and in Figure 8 in Chapter 2. The solvent-nonsolvent systems differed from one another in the relation. Therefore, the simulation was initiated for each system from an arbitrarily chosen solvent concentration in such a way that an appropriate amount (usually more than 1 %) of polymer was obtained as the first fraction. Polymer was hypothetically fractionated to 16 fractions and the D values were calculated

Table I Molecualr weights and D values of the fractions obtained in kerosene-butyl carbitol system.

Fraction No.	$\bar{M}w \times 10^{-4}$	$\bar{M}n \times 10^{-4}$	D value	
			Observed	Corrected
1	0.70	0.49	1.49	1.38
4	3.89	3.09	1.26	1.22
7	7.44	5.99	1.24	1.20
8	9.38	7.59	1.24	1.20
9	13.2	9.98	1.32	1.27
10	18.7	12.3	1.52	1.46
12	26.8	22.1	1.21	1.14
14	61.6	44.9	1.37	1.22

for each fraction. The results are shown in Figure 6 and Table II. In Figure 6, the D values of the fractions are given as a function of molecular weight in the form of $(\bar{M}n\bar{M}w)^{1/2}$. These simulated values can be used only for evaluating approximate D values, because the combination effect is not completely taken into account in the simulation (cf. Section 2.2 in Chapter 2). The experimental D values are in good agreement with the simulated ones. The fact shows that these fractionation experiments were carried out completely according to molecular weight. From the above results it is evident that the average D value in D-E system is the smallest among the four systems tested, and that the D values of the fractions from this

Table II Fractionation results in various solvent-nonsolvent systems.

Eluent system	Experimental D value on average[a]	2σ[b]	$[\eta]$dl/g[c]	Simulated D value on average
C-B	1.18	0.03	8.55	1.16
D-B	1.22	0.10	7.74	1.14
D-E	1.14	0.05	14.5	1.13
K-B	1.24	0.06	8.38	------

a: $D = \bar{M}w/\bar{M}n$, the values of the first and last fractions were excepted from calculation due to large errors in GPC measurement,

b: σ is the standard deviation of the average D value,

c: the highest limiting viscosity number of the fractions obtained in each system.

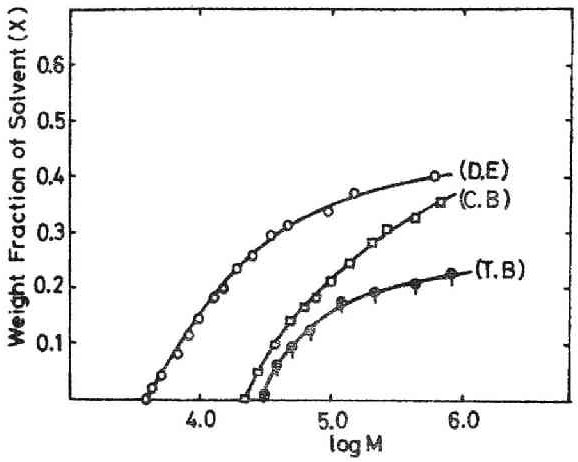

Fig. 5 The relation between molecular weight and eluent composition in various solvent-nonsolvent systems.
(D.E): D-E system, (C.B): C-B system,
(T.B): T-B system.

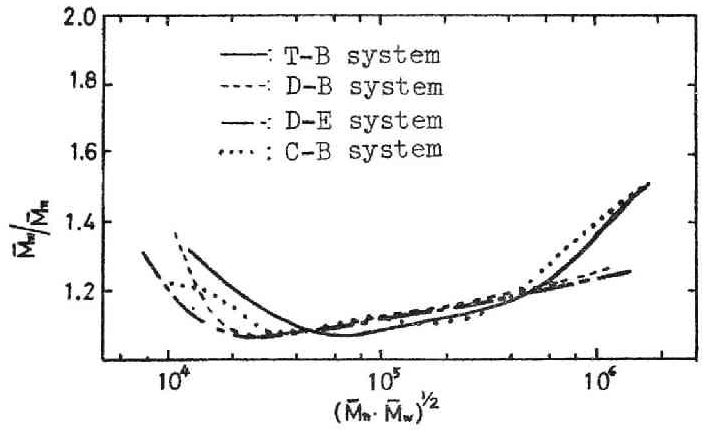

Fig. 6 The D value of fractions obtained by simulated fractionation.

system are smaller than those from other systems in substantially wide molecular weight range. Moreover, as shown in Table II, a fraction of the highest molecular weight among all the systems was obtained in this system. These results show that D-E system is most suitable for preparative purpose, as far as the molecular weight range and the D values of the fractions are concerned.

4.4 Treatment of fractionation results by Caplan's method

We have been looking for a suitable and simple method to correlate molecular weight with eluent composition in various eluent systems. After a number of trials, we found that a method proposed by Caplan[4] was most useful for this purpose. Caplan's method is based on an experimental finding, reported by Powers,[6] that the cloud point temperature for a ternary system polystyrene, toluene and decane was lowered linearly with increasing the volume fraction of toluene. Further assuming that the cloud point be identified with the elution point in fractionation, Caplan presented an empirical equation for the Θ temperature (Θ_t) of ternary system polymer, solvent and nonsolvent. This is given by

$$\Theta_t = \Theta_N - (\Theta_N - \Theta_S)\upsilon_1 \qquad (1)$$

where Θ_N and Θ_S are the Θ temperatures of the polymers in nonsolvent and solvent, respectively; υ_1 is the volume fraction of solvent. By referring to the well known Shulz-Flory equation describing the relation between Θ temperature and molecular weight, eq.(1) was converted to:

$$M^{-1/2} = (\Theta_N - T)/KT - (\Theta_N - \Theta_S)\upsilon_1/KT \qquad (2)$$

where T is the fractionation temperature; K is a constant. In the above derivation, it was assumed that the Shulz-Flory equation be valid for ternary systems polymer, solvent and nonsolvent. Therefore, utility of the equation is limited to qualitative descriptions of the relationship between M and υ_1.

In our experimental data we represented the eluent composition by weight fraction rather than the volume fraction. As shown in Figures 2 and 3, the plot of cloud point temperature against eluent composition gives similar tendency as confirmed by Powers[6] for cloud point vs. volume fraction relationship. Presumably Caplan's method is applicable to our systems by substituting weight fraction (W_s) for volume fraction (υ_1) in eq.(2). $M^{-1/2}$ was plotted against W_s with a series of solvent-nonsolvent systems as shown in Figure 7. The results are summarized in Table III. One can find that eq.(2) is a satisfactory approximation for these systems. Agreement of the data in different polymer loads is also good as indicated in C-B and K-B systems in Figure 7.

Let us consider how to obtain narrow distribution fractions covering the molecular weight range as wide as possible. In eq.(2), the greater the term Θ_N, the more we can magnify the difference between the molecular weights of adjacent fractions. On the other hand, the higher the Θ_S, the more the slope of the curve expressed by eq.(2) decreases, when Θ_N is kept constant. Under these conditions, the phase diagram (see Fig. 5 in Chapter 2) indicates that the difference between the solvent-nonsolvent ratios in the dilute and concentrated phases increases.

Table III Evaluation of the fractionation results based on Caplan's method

Eluent system	$(\Theta_N - \Theta_S)/K$	$(\Theta_N - T)/KT \times 10^2$
C-B	8.12	0.66
D-B	12.1	0.57
D-E	14.1	1.47
K-B	15.3	0.80

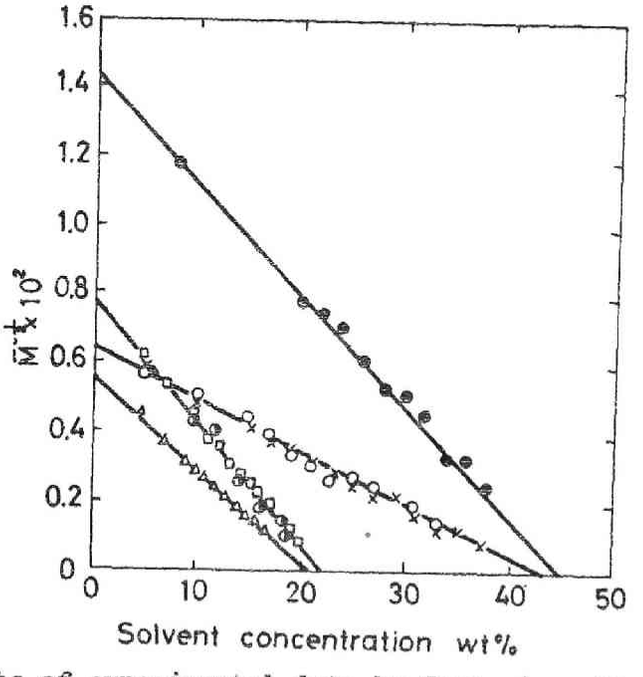

Fig. 7 Plots of experimental data by Caplan's method.

○, × : C-B system, polymer load 5 g, 9 g;

△ : D-B system, polymer load 5 g;

● : D-E system, polymer load 5 g;

◑, □ : K-B system, polymer load 5 g, 9 g.

This leads to more efficient fractionation. It may be concluded that a system having higher Θ_N and Θ_S values is preferable in principle for achieving an efficient fractionation. In this regard, D-E system satisfies this requirement. Horowitz[3] found that the use of butyl cellosolve-butyl carbitol system at 165°C gave a good result for the fractionation of crystalline polypropylene. As is commonly known, these two carbitols are nonsolvents for polypropylene. However, a certain difference between them is present in the solubility. It seems reasonable from our conclusion that butyl cellosolve works as the solvent and butyl carbitol as the nonsolvent in the above system. Horowitz himself did not speculate about this. As a conclusion, both solvent and nonsolvent should be poorer with regard to solubility for polypropylene, although other physical properties such as boiling point, viscosity and density must be considered for selecting them in a practical use.

REFERENCES

1. J.M. Hulme and L.A. Mcleod, Polymer, 3, 153(1967)

2. R.T. Traskos, N.S. Schneider, and A.S. Hoffman, J. Appl. Polym. Sci., 12, 509(1968)

3. R.H. Horowitz, Abstr. Amer. Chem. Soc., 145th Meeting New York, Div. Polym. Chem., Preprints, Vol. 4, 689(1963)

4. S.R. Caplan, J. Polym. Sci., 35, 409(1959)

5. T. Ogawa, Y. Suzuki, S. Tanaka, and S. Hoshino, Kobunshi Kagaku, 27, 356(1970)

6. P.O. Powers, Ind. Eng. Chem., 42, 2558(1950)

Chapter 5 EFFECTS OF STEREOREGULARITY ON FRACTIONATION OF POLYPROPYLENE

As is well known there are two different procedures in column fractionation method. One is the procedure involving solvent gradient elution at a given temperature (S.G. method), and the other is the one raising temperature with a fixed solvent or solvent-nonsolvent mixture (R.T. method). When we apply these methods for the column fractionation of crystalline polypropylene, the former is commonly used at an elevated temperature where liquid-liquid phase equilibrium is attained. Under such a condition polypropylene dissolves only according to molecular weight, because the solution properties are almost independent of tacticity in this system.[1,2] The fractionation with respect to molecular weight is possible. On the other hand, the latter is usually employed under such a condition that solid-liquid phase equilibrium exists. Polypropylene dissolves mainly according to tacticity under this condition, because the free energy of fusion is closely related to the dissolution temperature.[3,4] Here the fractionation will proceed mainly according to the difference in tacticity.

The fractionation of polypropylene by an R.T. method was first reported in detail by Wijga et al.[5] Similar experiements were performed also by other investigators.[6-9] However, concerning the fractionation mechanism of this method, no proper study has been done. This chapter deals with the fractionation behavior involving the solid-liquid equilibrium from the viewpoint of tacticity and molecular weight distribution of fractions.

5.1 Experimental conditions

5.1.1 Apparatus

As shown in Figure 1, the apparatus for the R.T. method consists of a column and an oil bath. The lower part of the column was packed to a height of 5 cm with coarse particles of sea sand (40 - 80 mesh). Then the upper part of the column was packed with Celite 545 to a height of 30 cm, on which polypropylene had been deposited. The top of the column was filled with glass fiber. The apparatus for the S.G. method was the same as described in Chapter 2.

5.1.2 Fractionation experiment and characterization

A crystalline polypropylene of M.F. = 5.4 was used. The sample of 5 g was dissolved in a decalin (269 g)-butyl carbitol (115 g) system. The solution was poured into Celite 545 (support material) heated to 160°C, and the polypropylene was deposited on it by cooling.[10] Fractionation was started from 30°C with decalin, and the column temperature was raised in increments. A change-over to a higher temperature setting was made after the eluent failed to show turbidity in excess acetone-methanol mixture (7 : 3).[5] The outline of the S.G. method is the same as described in Chapter 2.

A Shimadzu GPC Model-1A was employed to determine the molecular weights and D values of the fractions with a combination of four columns of crosslinked polystyrene gels of 1×10^6, 1×10^5, 1×10^4, and 1×10^3 Å permeability. Other experimental conditions were described in Chapter 2.

5.1.3 Differential scanning calorimetry

Some fractions were subjected to differential scanning calorimetry (DSC) to determine the melting point T_m and the relative heat of fusion ΔH_u.

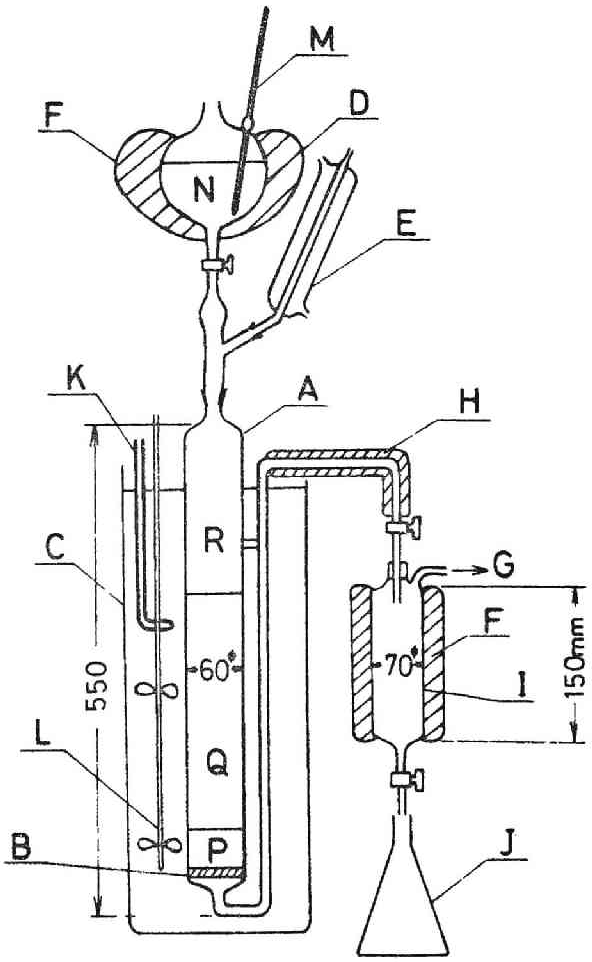

Fig. 1 Fractionation apparatus for the R.T. method.

(A) column body; (B) sintered glass filter (G4); (C) oil bath; (D) eluent reservoir; (E) reflux condenser; (F) heating mantle; (G) aspirator; (H) band heater; (I) adapter; (J) flask; (K) heater; (L) stirrer; (M) thermometer; (N) eluent; (P) sea sand (40-80 mesh); (Q) Celite 545, on which polymer is deposited; (R) glass fiber.

Fractions were dissolved in a hot decalin-ethyl carbitol mixture. The solution was cooled to room temperature and allowed to precipitate. The precipitate obtained in such a way is regarded to be in the same crystalline state as that deposited onto the support. The measurements were made by a Perkin Elmer DSC Model-1B with 10 mg sample at a heating rate of $10^{\circ}C$/min. The area under the DSC curve largely depends on the heating rate. However, the ratio of the areas determined by two different samples, i.e., the relative area, is almost independent of the heating rate, as shown in Figure 2. The relative area is a reasonable parameter for indicating the variation of the heat of fusion with tacticity or molecular weight.

5.1.4 Determination of tacticity parameter

To examine the tacticity dependence of fractionation, the tacticity index of fractions was determined by infrared method. The fractions were dissolved in hot xylene to make 5-10 wt% solution. The solution was poured on a microslide glass. The glass was cooled to room temperature and annealed at $120^{\circ}C$ for 6 hr under vacuum. This film was subjected to IR test. An intensity ratio (D_{998}/D_{974}) of 998 cm^{-1} band to that of 974 cm^{-1} in the infrared spectrum was used as the tacticity index.

5.2 Theoretical background

Each fractionation step in the R.T. method represents the process of dissolution of polymer from solid to eluent at a given temperature (cf. Fig. 3). Therefore, the properties of solid and solution of polypropylene must be known. The two phases and standard state should be defined for thermodynamic study. It is generally accepted that crystalline lamellae are the basic structural element of crystalline polymers in solid state. However, we cannot find any perfect crystals in actual polymers because of the presence of crystallographic

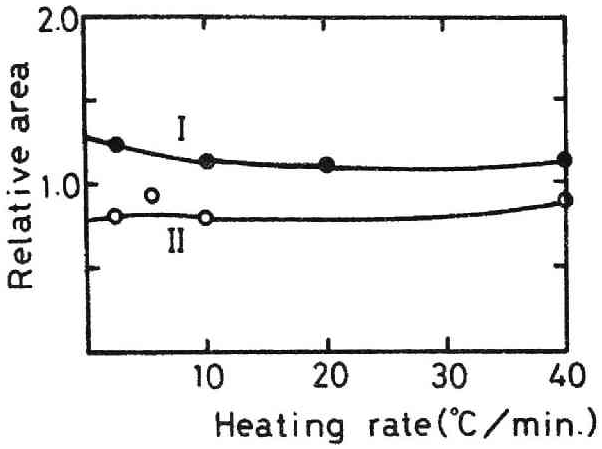

Fig. 2 Dependence of the relative area under the DSC curve on heating rate.
(I) : (peak area for M = 5.96 x 10^5)/(that for M = 2.07 x 10^5);
(II) : (peak area for M = 8.09 x 10^5)/(that for M = 5.96 x 10^5).

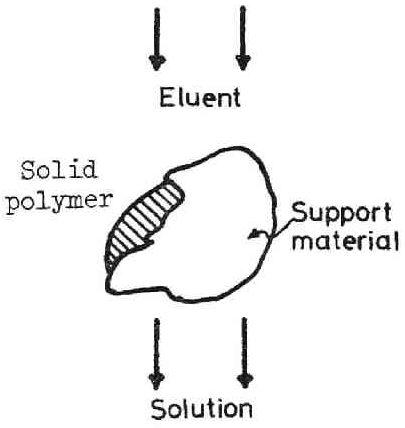

Fig. 3 Schematic representation of polymer deposited onto the support material.

defects,[12] and atactic units. Further, since the polymer is immersed in solvent during fractionation, the solid state should be very complicated.[10,13] In this study, for the sake of simplicity, the solid state polymer in solvent was assumed to have the same properties as the imperfect crystal in a solvent-free state.

When the fractionation experiment is carried out at a given temperature (T), the chemical potential of the solid state (μ_c) has to be equal to that of the dissolved polymer (μ). This relation is expressed by eq.(1).

$$\mu_c - \mu = (\mu_c - \mu_o) + (\mu_o - \mu) = 0 \tag{1}$$

At a certain temperature, μ_c becomes equal to the chemical potential of the melt polymer (μ_o) as expressed by eq.(2). This temperature is defined as the melting point (T_m) of the deposited polymer.

$$\mu_c - \mu_o = -(\Delta H_u - T_m \Delta S_u) = 0 \tag{2}$$

where ΔH_u and ΔS_u are the heat and entropy of fusion per unit mole, repsectively. According to Flory's equation for dilute solution of polymer,[14] the relation between T and T_m can be expressed by use of eqs.(1) and (2).

$$(1/T) - (1/T_m) = (R/\Delta H_u)(V_u/V_1)[(1 - 1/X)\upsilon_1 - (BV_1/RT)\upsilon_1^2 - \ln(1 - \upsilon_1)/X] \tag{3}$$

where V_u is the molar volume of structural unit; V_1 is the molar volume of solvent; X is the ratio of molar volume of polymer to that of solvent; υ_1 is the volume fraction of solvent; B is the thermodynamic interaction parameter for polymer-solvent systems; and T is the dissolution temperature, corresponding to the elution temperature of fractionation on large υ_1. In this equation ΔH_u does not necessarily represent that of a perfect crystal. In deriving eq.(3), the heat and entropy of fusion are assumed to be independent of temperature.

5.3 Elution behavior

When we discuss the R.T. method from the thermodynamic point of view, several parameters in eq.(3) must be determined. The peak position of the DSC curve was adopted as T_m of each fraction. The relation between T_m and molecular weight of the fractions is shown in Figure 4. Although it is somewhat doubtful whether the peak position represents the true T_m of the fraction, the only mutual relationship is of interest here and hence the use of the peak position would be satisfactory. Parameter B was estimated from the data given by Tamura et al [16] for decalin-polypropylene system. By assuming 15 for the B value, and 0.42×10^{-3} deg^{-1} for $R/\Delta H_u \times (V_u/V_1)$[16], the dependence of dissolution temperature on molecular weight was calculated through eq.(3). Figure 5 shows the result. The expremental points in the n-decane-polypropylene system[17] are also shown for reference. The calculated curves do not deviate very much from the experimental points in decalin-polypropylene system. Thus the B value adopted is pertinent. Under these conditions, the behavior of the elution temperature T was examined by assuming $\upsilon_1 = 0.99$ corresponding to solvent concentration in eluent.

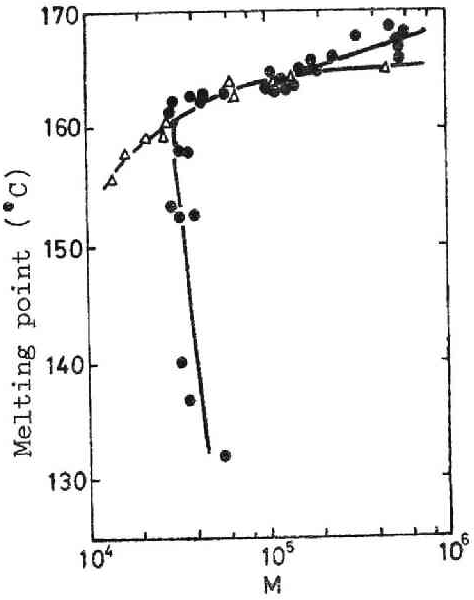

Fig. 4 Melting points of the fractions.

(●) : the fractions obtained by the R.T. method,

(△) : the fractions obtained by the S.G. method,

M ($=(\bar{M}n\bar{M}w)^{1/2}$) was determined by GPC.

As the first test, the elution temperature was calculated from the properties of solid state by assuming that ΔH_u was independent of molecular weight. The heat of fusion of polymer was fixed in such a way that the calculated elution temperature agreed with an experimental point at M = 5.0×10^4. As shown in Figure 6, the curve thus calculated by eq.(3) shows a slight increase with an increase of molecular weight. When the molecular weight of the fractions changes from 5×10^4 to 10^6, the difference of experimental elution temperature is 25°C, while that of the calculated temperature is only 2°C. This fact indicates that the fractionation

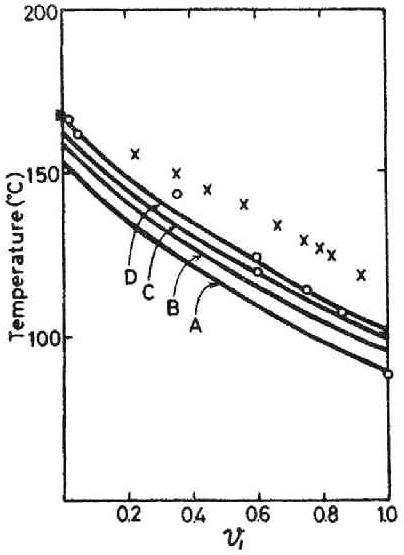

Fig. 5 Dissolution temperature of polypropylene.

(O) : the data obtained by Tamura et al.,[18] $M = 3.7 \times 10^5$ in decalin;

(X) : the data obtained by Hamada et al.[19], $M = 3.4 \times 10^5$ in n-decane.

Calculated curves obtained by using eq.(3),

(A): $M = 1 \times 10^4$; (B): $M = 2 \times 10^4$;

(C): $M = 5 \times 10^4$; (D): $M = 1 \times 10^6$.

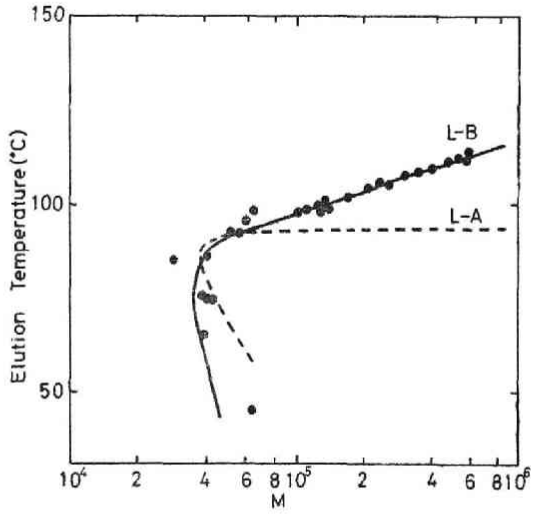

Fig. 6 Comparison of the calculated curves with the experimental results.

(L-A): the curve was obtained by assuming that ΔH_u is constant;

(L-B): the curve was obtained by considering that ΔH_u varies according to fractionation steps (cf. Fig. 7);

● : experimental points.

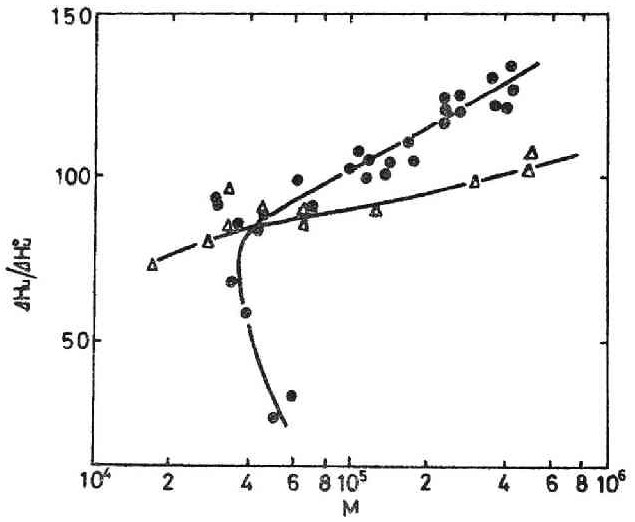

Fig. 7 The relative heat of fusion of the fractions.
(●): the fractions obtained by the R.T. method; (Δ): the fractions obtained by the S.G. method. The heat of fusion ΔH_u^o for $M = 10^5$ is conveniently assumed to be 100.

behavior cannot be explained by assuming ΔH_u = constant.

As the second test, it was assumed that ΔH_u varied in the order of increasing fractionation steps. The dependence of ΔH_u on molecular weight was obtained by measuring the area of the DSC curve, for which we arbitrarily assumed that $\Delta H_u^\Phi = 100$ for $M = 10^5$. Figure 7 shows the results. The dependence was more pronounced in the R.T. method than the S.G. method. When values of ΔH_u and T_m of the fractions obtained by the R.T. method were used, the calculated T versus M curve (see Fig. 6) agreed very well with the experimental points. Therefore, this fractionation is carried out depending on ΔH_u and T_m of polypropylene. The polypropylene was expected to be separated mainly according to tacticity. However, the polypropylene is apparently fractionated according to molecular weight also as shown in Figure 6. The extent of molecular weight fractionation in this method was examined by determining the D value of the fractions.

Table I The D value of the fractions obtained by the R.T. and S.G. methods.

Method	$\bar{M}w \times 10^{-4}$	$\bar{M}n \times 10^{-4}$	$\bar{M}w/\bar{M}n$
R.T.	7.40	2.92	2.53
R.T.	21.1	7.68	2.75
R.T.	21.1	9.99	2.11
R.T.	32.1	14.5	2.23
S.G.	6.22	4.68	1.28
S.G.	8.53	7.85	1.09
S.G.	9.63	8.56	1.13
S.G.	24.8	18.2	1.36

Table I shows the results. The D value obtained by averaging over those of the fractions is 2.4, while the average D value of the fractions obtained by the S.G. method is 1.23. Both values were found for the same original polymer having D = 4.6. Further, the R.T. method is different from the S.G. method in the behavior of melting point as shown in Figure 4. These facts suggest that the fractionation mechanism of the R.T. method is considerably different from that of the S.G. method, which allows polymer fractionation according almost completely to molecular weight.

These complicated phenomena can be understood as follows. It is generally accepted that the melting point and heat of fusion of crystalline polymers rise up to a certain value relevant to each with increase in molecular weight and also in tacticity.[18,19] Therefore, the elution temperature is a function of both molecular weight and tacticity, and

the relation among these three variables, i.e., molecular weight, tacticity and elution temperature, may be represented schematically by Figure 8. Let us assume an operation of fractionation which is performed at temperatures T_1, T_2 and T_3, as indicated in the figure. Basically the polymer species having low tacticity and low molecular weight is eluted at the low temperature T_1 together with that having high tacticity but lower molecular weight. The polymer species having high tacticity and high molecular weight is eluted only at the high temperature T_3. In other words, the tacticity of the fractions increases in the order of raising elution temperature. The molecular weight of the fractions increases as well. These results coincide with the experimental ones shown in Figures 6 and 9. Namely the commercial polypropylene is considered to be fractionated according to not only tacticity but also molecular weight due to polydispersity in molecular weight.

The relationship among the elution temperature, molecular weight and tacticity at temperature below 85°C shifts from the above described one. The fractions in this temperature region show lower melting points and smaller heat of fusion than expected. As a reason for the deviation, it is considered that the relative area and T_m determined by DSC method largely depend on the heating rate because of low tacticity.

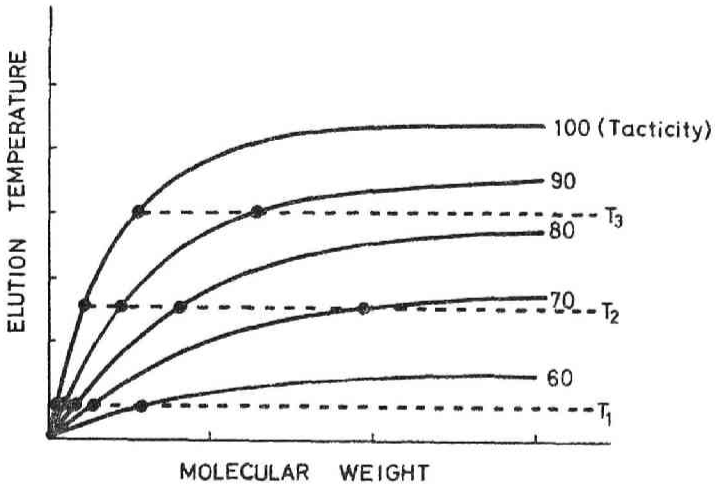

Fig. 8 A schematically represented relation among elution temperature, molecular weight and tacticity.

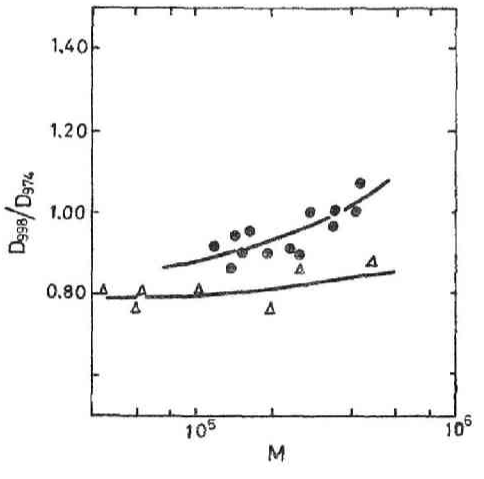

Fig. 9 Tacticity index of the fractions.

(●) : the fractions obtained by the R.T. method;

(Δ) : the fractions obtained by the S.G. method.

REFERENCES

1. A. Kotera, K. Takamizawa, T. Kamata, and H. Kawaguchi, Rep. Progr. Polym. Phys., 4, 131(1961)
2. P. Parrini, F. Sebastiano, and G. Messina, Makromol. Chem., 38, 27(1960)
3. P.J. Flory, R.R. Garret, S. Newman, and L. Mandelkern, J. Polym. Sci., 12, 97(1954)
4. E.M. Cernia, C. Mancici, and A. Saini, Kobunshi Kagaku, 24, 738 (1967)
5. P.W.O. Wijga, J. van Schooten, and J. Boerma, Makromol. Chem., 36, 115(1960)
6. M. Sato and O. Ishizuka, Kobunshi Kagaku, 23, 799(1966)
7. H. Sato, Kogyo Kagaku Zasshi, 65, 385(1962)
8. A. Saijyo, S. Hayashi, F. Hamada, and A. Nakajima, Kobunshi Kagaku, 24, 775(1967)
9. A. Nakajima and H. Fujiwara, Bull. Chem. Soc. Japan, 37, 909(1964)
10. T. Ogawa, Y. Suzuki, S. Tanaka, and S. Hoshino, Kobunshi Kagaku, 27, 356(1970)
11. J.P. Luongo, J. Appl. Polym. Sci., 3, 602(1960)
12. R.K. Eby, J. Appl. Phys., 34, 2442(1963)
13. A.S. Kenyon and I.O. Salyer, J. Polym. Sci., 43, 427(1960)
14. P.J. Flory,"Principles of Polymer Chemistry," Cornell University Press, Ithaca, N.Y., p.513(1953)
15. P.J. Flory and W.R. Krigbaum, Ann. Rev. Phys. Chem., 2, 383(1951)
16. K. Tamura, K. Nakatsuka, and R. Fujishiro, Bull. Chem. Soc., Japan, 39, 20(1966)

17. F. Hamada and A. Nakajima, Kobunshi Kagaku, 22, 577(1965)

18. P.J. Flory and A. Vrij, J. Am. Chem. Soc., 85, 3545(1963)

19. M.G. Broadhurst, J. Chem. Phys., 36, 2578(1962)

Chapter 6 FRACTIONATION OF ETHYLENE-PROPYLENE COPOLYMERS

Copolymers are generally composed of various species of different composition, molecular weight, and monomer sequence length. It is therefore important to separate a given copolymer into individual species, each having the same structural characterisitcs. Some reports concerning the fractionation of ethylene-propylene (EP) copolymers have been published.[1-4] However, they are concerned mainly with the fractionation results of copolymerization products, such as the molecular weight and composition heterogeneity, and not with the fractionation mechanism. Thus, many problems are still left unsolved. This chapter is devoted to establish the fractionation technique for EP-copolymers, associated with fractionation mechanism.

We consider three distribution characteristics with respect to chemical composition, molecular weight and monomer sequence length, according to which the polymer will be fractionated. Generally, fractionations according to the former two characteristics are carried out with a system based on liquid-liquid phase equilibrium. When the solubilities of parent homopolymers in a given eluent system differ from each other to a large extent, the fractionation will proceed mainly according to chemical composition (compositional fractionation); while if the homopolymers have similar solubility, the fractionation will proceed mainly according to molecular weight (molecular weight fractionation). In the case of copolymers the fractionation becomes more complicated. The solubility in any eluent system is always dependent more or less on both molecular weight and chemical composition. Thus the so-called cross fractionation is necessary. An additional complexity, specific to fractionation

of EP-copolymers, is that the elution behavior is affected by their degree of crystallinity, which varies essentially with the chemical composition and monomer sequence length, as is well known through the Flory theory.[6] However, when an eluent system based on solid-liquid equilibrium is found, the fractionation may be performed according largely to the difference in monomer sequence length, since solid-liquid equilibrium is not quite sensitive to the molecular weight. The chemical composition affects the equilibrium as well but it should be taken into consideration that random-type incorporation of ethylene monomers into propylene chain lowers the melting point to a great extent in comparison with block-type incorporation. In this chapter we will discuss fractionations of EP-copolymers based on these aspects.

6.1 Experimental conditions

6.1.1 Sample materials

Five copolymers were prepared in n-heptane with complex catalyst systems. A mixture of ethylene and propylene gases with fixed composition was bubbled into the reaction mixture for a certain period of time. The reaction was stopped by addition of iso-propanol containing 1 % HCl. The product was washed successively with methanol, water, and methanol, dried and used as a sample. Samples A (average ethylene content = 23.5 wt%) and B (59%) were prepared with an $AlEt_2Cl$-$VOCl_3$ system; and samples C (47 %), D (26 %) and E (24 %) were prepared with $AlEt_2Cl$-$TiCl_3$ (activated).

6.1.2 Cloud point determination

Cloud point determination was conducted on a polyethylene (PE) and a polypropylene (PP) fraction of narrow distribution in several solvent-nonsolvent combinations to establish suitable conditions for compositional and molecular weight fractionations. The molecular weight of PP fractions

was 2.0×10^5 and that of high density PE fraction 1.7×10^5. Polymer, solvent, and nonsolvent were weighed into a test tube, which was purged with nitrogen and sealed. Ionol (2,6-di-tert-butyl-p-cresol, 0.2 wt%) was added to all the solvents and nonsolvents used. The cloud point was determined by visual observation in an oil bath and was reproducible within $\pm$ 1.0°C.

The extent of compositional fractionation in a given solvent-nonsolvent system was examined by measuring the dependence of the cloud point composition on molecular weight. A Sofica 42000M light scattering instrument was employed. Measurements were performed in a xylene-butyl cellosolve system at 127°C. First a solution of a sample in xylene at 50 mg/dl was prepared by using narrow distribution samples (usually less than 1.3 in D value). The intensity of scattered light at 90° angle was recorded for 10 min after every 1.0 ml addition of butyl cellosolve to the method described in Chapter 3.

6.1.3 Column fractionation

Since a copolymer is characterized by various factors such as chemical composition and molecular weight, several measurements must be made for each fraction of the copolymer. A large scale fractionation apparatus (80 mm-diam. x 1000 mm-length) was designed, in which flow rate and temperature were regulated exactly. A schematic diagram of this apparatus is shown in Figure 1. The fractionation temperature was fixed in the vicinity of melting point of samples. Table I shows the temperature and melting point of samples. The column temperature was attained by circulating silicone oil at a constant temperature through a column of stainless steel. The solvent-nonsolvent systems adopted for eluent

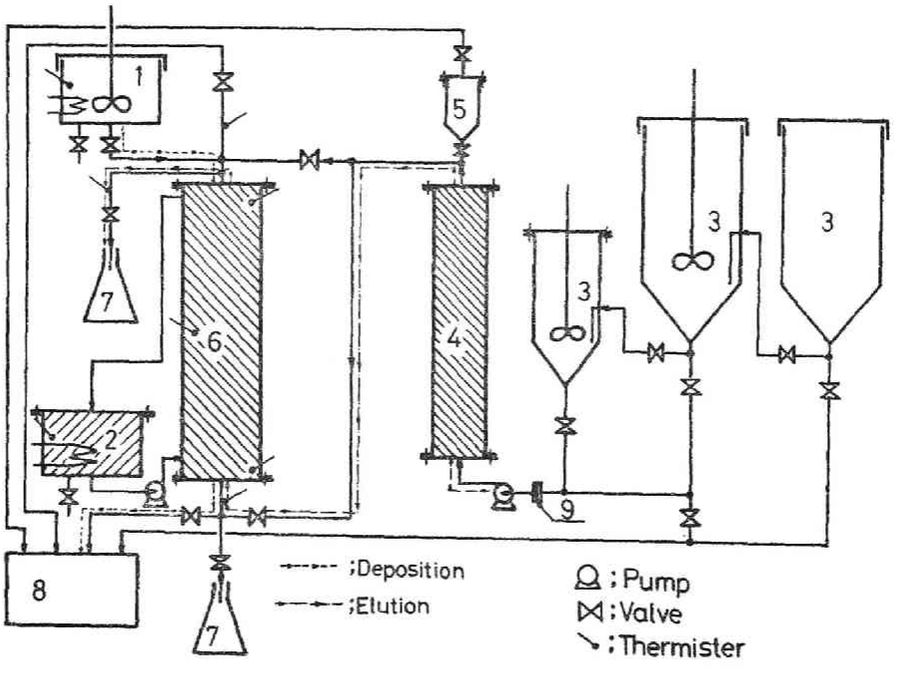

Fig. 1 Large scale fractionation apparatus: (1) vessel for dissolving sample in the deposition process; (2) oil bath; (3) eluent reservoir; (4) heating pipe for eluent; (5) degasser; (6) fractionation column (80 mm-diam x 1000 mm-length); (7) adapter; (8) drainage tank; (9) filter.

Table I Fractionation temperatures and melting points of samples.

Sample	Melting point[a] (°C)	Fractionation temperature(°C)
A	116	123
B	undetectable	119
C	120	120
D	117	117
E	120	120

a : the values were obtained by DSC.

were selected on the basis of the cloud points of PE and PP in those systems. The composition of eluent was varied stepwise or exponentially. Polymer deposition onto the support (Celite 545) was achieved by pouring the polymer solution into the column, and by lowering the column temperature at the rate of 0.3°C/min to room temperature. The solution was prepared beforehand in the vessel No.1 (see Fig. 1) at 170°C. After the eluent remaining in the column was replaced by nonsolvent, the column was heated to the fractionation temperature shown in Table I. The apparatus was maintained at that temperature for 8 hr. and the operation of fractionation was started. Other procedures are the same as described in Chapter 2[7,8].

6.1.4 Solvent extraction

The distribution of monomer sequence length in EP-copolymers was examined by solvent extraction. The extraction was carried out in a Soxhlet extractor by use of ethyl ether, n-hexane, cyclohexane, and n-heptane successively. These solvents were of commercially available high grade.

6.1.5 Infrared analysis

A Hitachi Model EPI-G_3 infrared spectrophotometer was used to determine ethylene content and monomer sequence length of EP-copolymers. The ethylene content was determined by Corish's method,[9] which is based on the ratio of the intensity at 1380 cm^{-1} to that at 1460 cm^{-1} arising from the methyl group, and the methyl and methylene groups, respectively. Blends of commercial PP and PE (Hizex) were used for constructing a calibration curve. In the determination of monomer sequence length, a film of 0.1 mm thickness was prepared with a hot press, and the intensity at 722 cm^{-1} was measured at 150°C with a heating cell to remove the effect of crystalline band. Block length of PE was evaluated according to Bucci's method.[10]

6.1.6 Molecular weight determination

Average molecular weights of EP-copolymer fractions were determined mostly by GPC. Experimental conditions were the same as described in Chapter 2. The location of the calibration curve for EP-copolymers was determined by assuming the additivity of contribution of the ethylene content from the two curves of PE and PP homopolymers. This assumption is considered to be reasonable from the standpoint of properties of such copolymers in a good solvent.[11] In this case, those of the homopolymers must be previously known. These curves were obtained from the curve of polystyrene by applying Benoit's universal calibration rule.[12-15] On applying this rule, one has to know the viscosity-molecular weight relations at the same temperature and in the same solvent as used for GPC. The relations were determined on PE and PP fractions and Pressure Chemical polystyrenes in o-dichlorobenzene at 135°C.[15] Figure 2 shows the double logarithmic plots, which are formulated as follows:

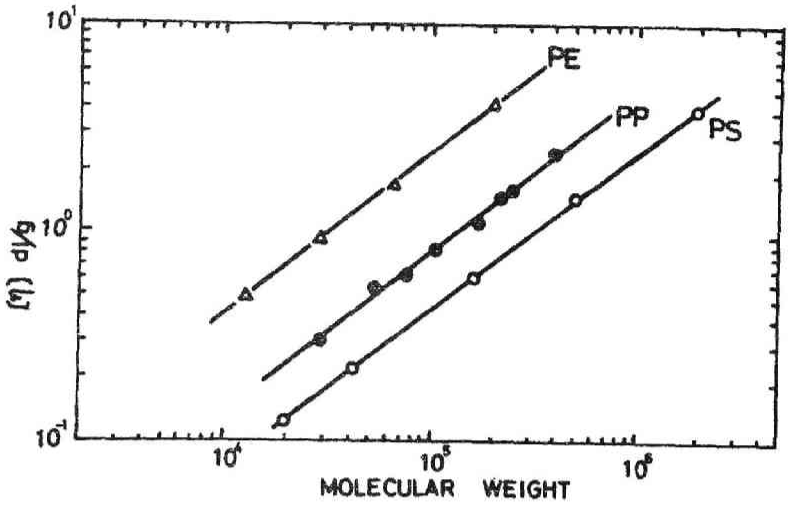

Fig. 2 Relations between molecular weight and limiting visocsity number for polyethylene (PE), polypropylene (PP), and polystyrene (PS) in o-dichlorobenzene at 135°C.

$$[\eta] = 4.9 \times 10^{-4} \times M^{0.74} \qquad \text{(PE)} \qquad (1)$$

$$[\eta] = 1.0 \times 10^{-4} \times M^{0.78} \qquad \text{(PP)} \qquad (2)$$

$$[\eta] = 7.4 \times 10^{-4} \times M^{0.75} \qquad \text{(PS)} \qquad (3)$$

Figure 3 shows the calibration curve obtained by using these relations.

Average molecular weights of some of the EP copolymer fractions were determined also by osmometry and light scattering. A Hewlett-Packard high speed membrane osmometer Model 502 was employed to determine the number average molecular weight. Determination was made at 130°C in

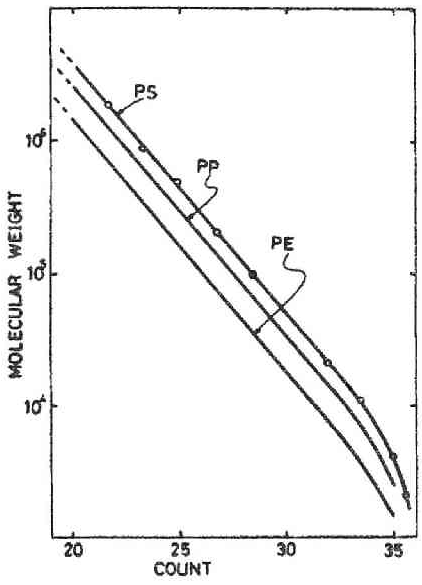

Fig. 3 GPC calibration curves of PE and PP deduced from that of PS.

tetralin solution containing 0.2 % Ionol (2,6-di-tert-butyl-p-cresol) with adequately conditioned ultracellafilters (allerfeinst).[7] A Sofica 42000M light scattering instrument was employed to determine the weight average molecular weight. Determination was made at 140°C in α-chloronaphthalene solution. A Millipore filter holder with two pieces of fluororesin filter paper VF-6 was used for filtration of the solution. The weight average molecular weight was calculated by the Zimm plot method. Specific refractive index increments (dn/dc) of the copolymer were approximated by the arithmetic mean (-0.190 ml/g) of those of PP (-0.188 ml/g)[16] and PE (-0.191 ml/g).[17]

A Perkin Elmer differential scanning calorimeter (DSC) Model-1B

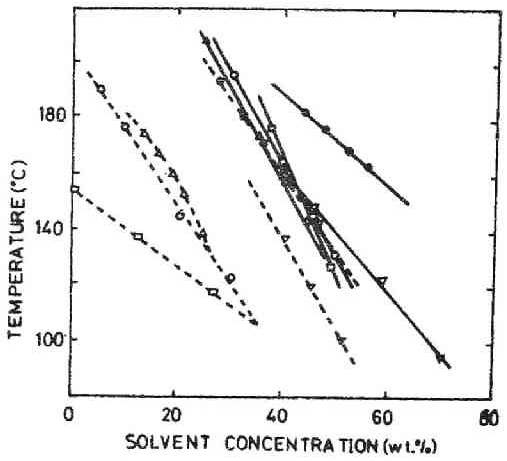

Fig. 4 Cloud points of PE and PP in various solvent-nonsolvent systems. Polymer concentration: 1.0 wt%.

-----: PP; ——— : PE.

□ : xylene-butyl cellosolve system; ○ : n-decane-butyl carbitol system; ▽ : tetralin-ethyl carbitol system; △ : decalin-butyl carbitol system; ● : decalin-ethyl carbitol system.

was used with a heating rate of 20°C/min with each 5-mg sample. The thermogram was corrected by the peak position of high purity indium.

6.2 Solubility of polymers

The solubility of PE, PP, and EP-copolymer was first investigated for selecting suitable solvent-nonsolvent systems. Cloud points of PE and PP in several solvent-nonsolvent systems were used as indication of

solubility. Figure 4 shows the results. As described in the introduction, an eluent having a large difference between the solubilities of PE and PP is suitable for compositional fractionation: among these systems examined here, the xylene-butyl cellosolve seems to be the most desirable system for this purpose. While an eluent in which the solubilities of both homopolymers are similar to each other is ideal for molecular weight fractionation. However, any systems do not exactly satisfy this requirement as shown in Figure 4. As far as we have examined, tetralin-ethyl carbitol system appears to be most recommendable.

To examine the extent of compositional fractionation, the dependence of cloud point on molecular weight was investigated in the xylene-butyl cellosolve system at 127°C. Figure 5 shows the results. Cosiderable dependence on molecular weight becomes remarkable in both PE and PP in the molecular weight range below about 10^5. In this region presumably EP-copolymers would be fractionated according to both chemical composition and molecular weight. However, in the molecular weight range above 10^5, the dependence on molecular weight is hardly noticeable. Since the cloud points of EP-copolymers are located between those of PE and PP, the fractionation is expected to proceed mainly according to chemical composition in this molecular weight range.

On the basis of these considerations, three types of separation, i.e., column fractionations in xylene-butyl cellosolve and in tetralin-ethyl carbtiol systems, and solvent extraction were conducted on EP-copolymers. Figure 6 shows these processes.

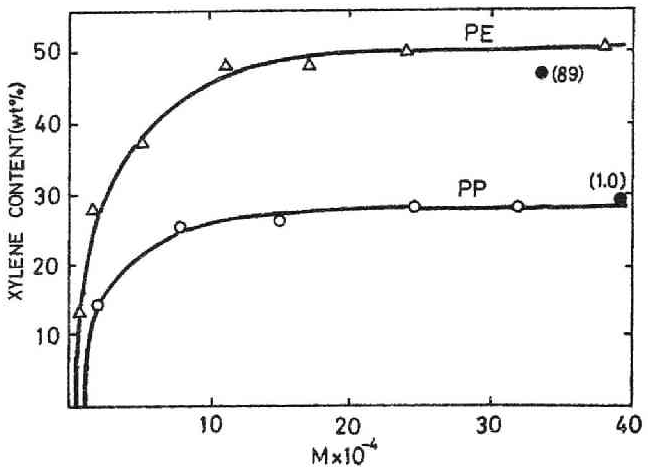

Fig. 5 Dependence of the cloud point composition on molecular weight in xylene-butyl cellosolve system at 127°C.
△ : PE; ○ : PP; ● : EP-copolymer, numbers indicate ethylene content (wt%).

6.3 Fractionation in xylene-butyl cellosolve system

Ethylene-propylene copolymers were fractionated in a xylene-butyl cellosolve system which is most suitable for compositional fractionation. Cumulative weight distribution curves for samples A, B and C are shown in Figures 7, 8 and 9. Table II lists the fractionation result of sample C. Partial inversion in the distribution curve was observed for sample C (see Fig. 9). This is probably due to the presence of a small amount of PP homopolymer in the sample. A similar behavior was observed in the case of isobutylene-styrene copolymer.[18] Since this fractionation depends mainly on chemical composition in the molecular weight range above 10^5,

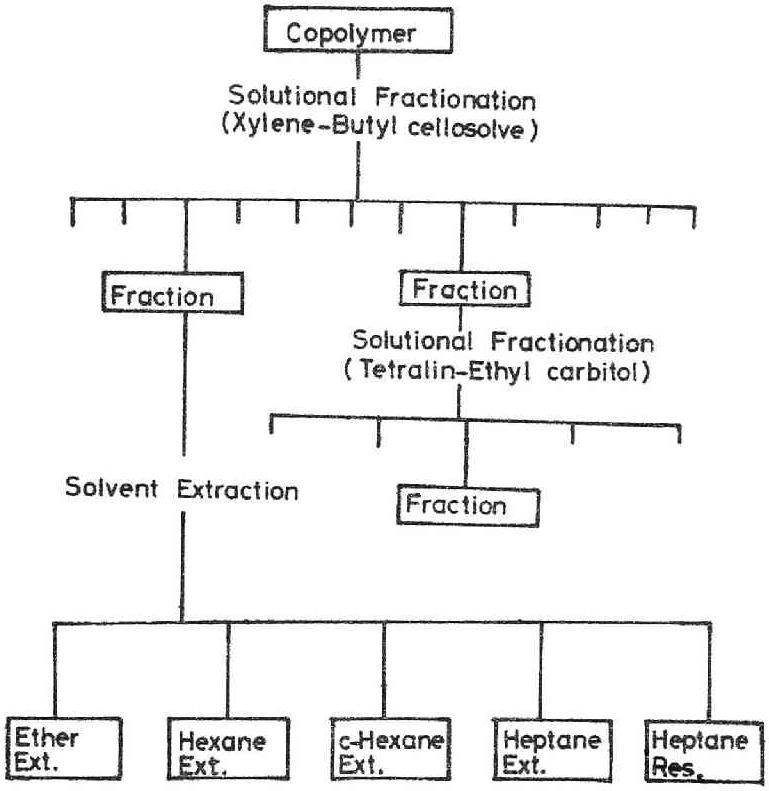

Fig. 6 Fractionation processes adopted in this study.

the fractions may still have broad molecular weight distribution. Thus, their molecular weight distributions were determined mainly by GPC. Table III shows the value of D ($=\bar{M}_w/\bar{M}_n$) of these fractions. These copolymer fractions have considerably large values of D (2.5 on average), while column fractionation of homopolymers usually gives fractions having D values less than 1.4 except the first and last ones. This fact may be an indication that compositional fractionation takes place.

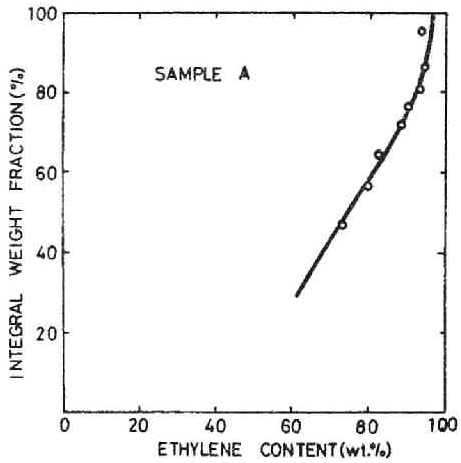

Fig. 7 Cumulative weight vs. ethylene content curve for sample A.

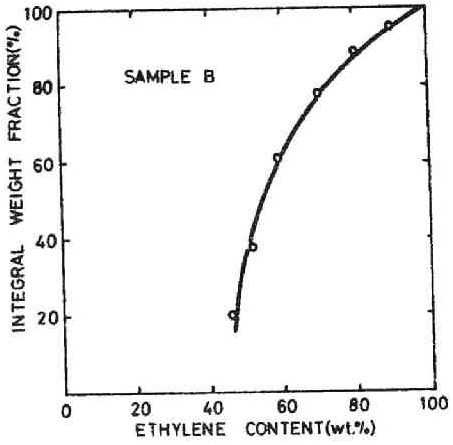

Fig. 8 Cumulative weight vs. ethylene content curve for sample B.

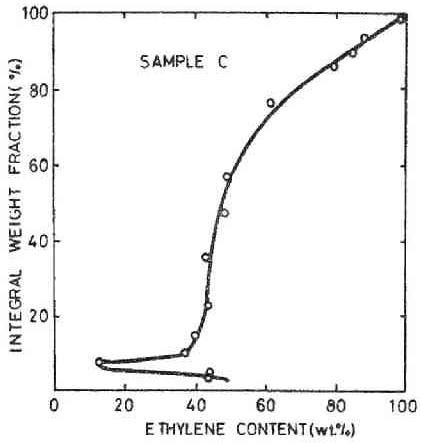

Fig. 9 Cumulative weight vs. ethylene content curve for sample C.

Assuming that each fraction is compositionally homogeneous, we can deduce the distribution of the original copolymer on both chemical composition and molecular weight from ethylene contents and GPC curves of all the fractions. The result for sample C is shown in Figure 10. The figure shows that this polymer has very broad distribution for both chemical composition and molecular weight. To explain Figure 10, an expression: distribution range was introduced, which means the upper and lower limits of molecular weights detectable by GPC curve. The shape of this distribution range is expected to vary considerably depending on copolymerization processes. Details concerning the shape of the distribution will be discussed in Chapter 7 in relation to the simulated fractionation of this copolymer.

Table II Fractionation results of sample C obtained by xylene-butyl cellosolve system.

Fr.No.	Xylene (wt%)	Weight fraction(%)	Cumulative weight	[η]dl/g	Ethylene content(wt%)
1	0	2.47	0.0123	------	------
2	5	2.10	0.0352	------	44.0
3	9	1.67	0.0540	0.180	45.3
4	12	2.81	0.0764	0.749	12.0
5	15	1.95	0.1002	1.32	36.7
6	18	6.99	0.1449	2.03	39.0
7	21	10.38	0.2316	3.21	44.0
8	24	12.60	0.3464	3.21	42.3
9	27	11.37	0.4662	3.84	48.0
10	30	8.71	0.5665	4.20	48.0
11	33	6.56	0.6428	4.40	------
12	36	5.78	0.7045	4.70	------
13	39	5.27	0.7597	4.90	61.3
14	42	4.48	0.8085	4.90	------
15	45	4.95	0.8556	------	79.3
16	48	4.24	0.9016	7.05	80.6
17	51	3.12	0.9384	8.40	86.7
18	54	4.51	0.9766	14.2	98.7

Table III Molecular weights and D values of fractions.

Fraction	Method	Ethylene content(wt%)	$\bar{M}w \times 10^{-4}$	$\bar{M}n \times 10^{-4}$	D ($=\bar{M}w/\bar{M}n$)
A-4 blend A-5 (7 : 3wt)	LS,OS	63.8	7.5	3.0	2.5
A-6	GPC	73.8	7.4	4.4	1.7
A-7	GPC	79.5	10.5	6.1	1.8
A-8	GPC	82.0	17.0	6.2	2.8
A-9 blend A-10 (7 :3 wt)	LS,OS	89.0	33.3	11.1	3.0
A-12 blend A-16 (7 : 3wt)	LS,OS	94.0	30.0	11.9	2.5
C-4	GPC	12	12.6	4.8	2.6
C-5	GPC	37	27.6	11.2	2.5
C-13	GPC	61	41.6	14.3	2.9
C-17	GPC	87	60.8	29.9	2.0

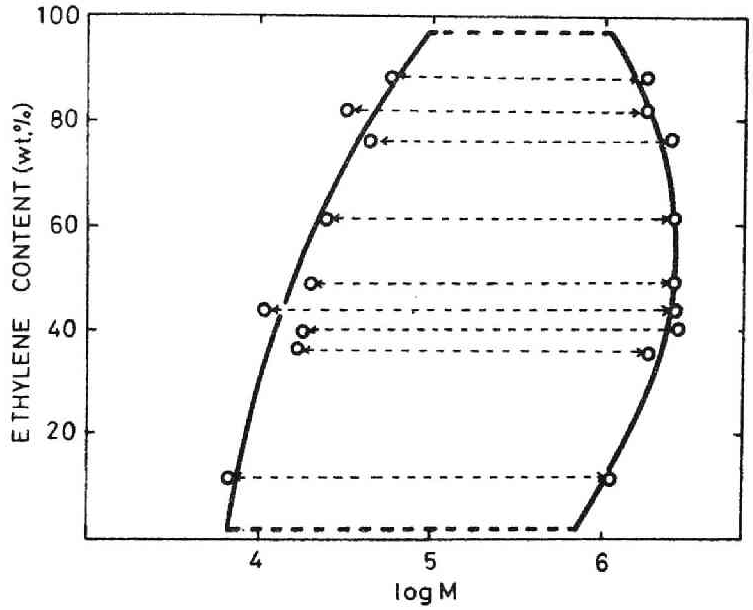

Fig. 10 Distribution range of chemical composition and molecular weight for sample C. The molecular weight range for each fraction was determined with the upper and lower limits of molecular weights detectable by GPC curve.

6.4 Fractionation in tetralin-ethyl carbitol system

Some of the fractions obtained by xylene-butyl cellosolve system were further fractionated by tetralin-ethyl carbitol system, which seems to be most advantageous for molecualar weight fractionation (cf. Fig. 4). The result is shown in Figure 11, where cumulative weight per cent is plotted against molecular weight as determined by GPC elution peak. Apparently the fractions are further fractionated according to the molecular weight difference. Therefore, the fractionation by this system

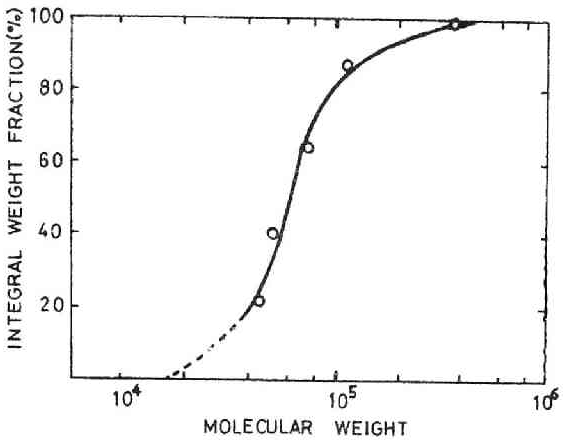

Fig. 11 Cumulative molecular weight distribution curve of the fraction obtained in xylene-butyl cellosolve system. The blend of the fractions Nos. 6 and 7 (1 : 1) was fractionated.

on all the fractions obtained in xylene-butyl cellosolve system leads, in principle, to the complete molecular weight distribution of the original copolymer. As described in the previous section, the molecular weight distribution of the original copolymer can also be easily estimated by the combination of the column fractionation in xylene-butyl cellosolve system and GPC. Therefore, the fractionation in tetralin-ethyl carbitol system might not be necessary. However, since the fractions obtained through these two steps of fractionations are presumably homogeneous in both chemical composition and molecular weight, the fractionation in this system is very useful for preparative purpose.

6.5 Solvent extraction

As described previously, the fractionation based on solid-liquid equilibrium is suitable for separation of EP-copolymer according to monomer sequence length. This fractionation, i.e., solvent extraction, is also influenced more or less by chemical composition and molecular weight. It is preferable to examine the distribution of monomer sequence length for the fractions prepared by the above two steps of fractionations. However, the characterization of such fractions is very difficult because of extremely small amount. Therefore, we subjected some fractions obtained in xylene-butyl cellosolve system to further solvent extraction experiments. They were successively extracted with a variety of solvents such as shown in Figure 6. The results are summarized in Table IV. Judging from the ethylene contents and the D values in this table, we may note that EP-copolymer is fractionated almost independent of either chemical composition or molecular weight. These extracts were tested by DSC to determine melting points and by IR spectroscopy to determine ethylene-sequence lengths. The latter was determined from the intensity of infrared absorption band in the region 700 - 850 cm^{-1} arising from the rocking mode of methylene groups. DSC thermograms of ether or n-hexane extracts showed no peaks, as in Figure 12. This implies that these extracts have highly random distribution of monomer sequence length. A melting peak of PE block at 119°C was detected in the n-heptane extract. The n-heptane residue showed a further melting peak of PP together with that of PE at 120°C. The same tendency was confirmed also for other samples. The infrared absorption band arising from $-(CH_2)\overline{\overline{\quad}}_{n>4}$ was used for evaluating block length of PE. Table V shows the results with theoretical values calculated by Bucci's method[10] assuming the samples as EP random copolymers. The table shows that

Table IV Solvent extraction of some fractions, which were obtained previously by the column fractionation in xylene-butyl cellosolve system.

	Ether extract	n-Hexane extract	Cyclohexane extract	n-Heptane extract	n-Hexane residue
			S-1		
Weight, %	9.3	15.6	none	74.0	1.1
Ethylene, wt%	60.0	47.0	-------	53.3	-----
D value	2.7	2.2	-------	3.4	-----
			S-2		
Weight, %	15.2	13.6	16.1	11.2	44.0
Ethylene, wt%	-----	37.3	40.0	39.0	31.3
D value	-----	2.3	3.3	3.2	3.2
			S-3		
Weight, %	17.8	25.7	13.7	20.8	22.0
Ethylene, wt%	-----	46.7	35.0	33.7	33.3
D value	-----	4.2	4.0	3.8	3.2

S-1: blend of the fractions Nos.10, 11 and 12 (1:1:1 wt%) of sample C, S-2: the fraction No.3 of sample D, S-3: blend of the fractions Nos.6 and 7 (1:1 wt) of sample E.

Table V Solvent extraction of a fraction obtained by xylene-butyl cellosolve system.

Fraction	$-(CH_2)_{n\geq 4}-$ content		
	Theoretical[a], (wt%)	Observed, (wt%)	Deviation, (wt%)
Ether extract	8.5	12.4	3.9
n-Hexane extract	11.0	17.6	6.6
Cyclohexane extract	10.5	18.3	7.8
n-Heptane extract	12.0	20.5	8.5
n-Heptane residue	15.5	24.0	8.5

a : the values were estimated from ethylene content by Bucci's method.[10]

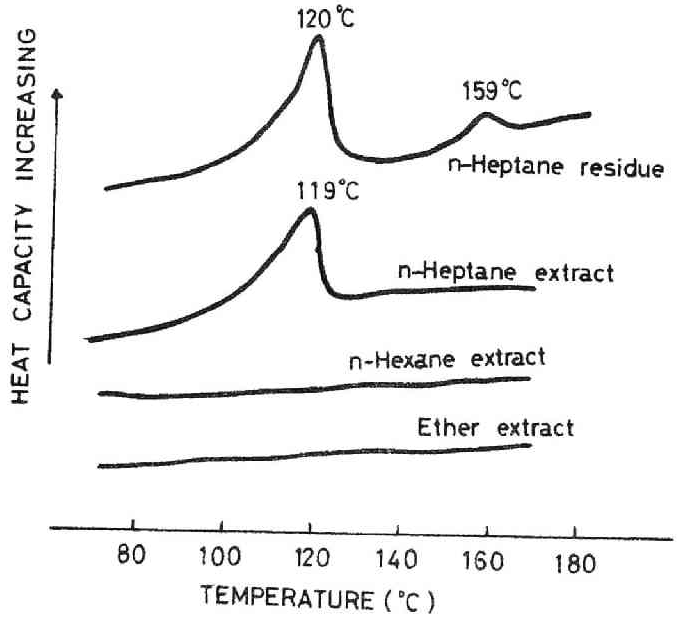

Fig. 12 Thermogram of extracts: blend of the fractions Nos. 10, 11 and 12 (1 : 1 : 1) of sample C (see Table IV) was extracted.

the deviation from the theoretical values increases with progress of solvent extraction. We may say that the sample was fractionated according to monomer sequence length.

6.6 Summary of fractionation of EP-copolymers

The above investigation is summarized as follows. Figure 13 shows schematically the fractionation processes from the standpoint of molecular structure. Cloud points of PE, PP and EP-copolymer were determined prior to the fractionation for the purpose of selecting appropriate systems for the compositional and molecular weight fractionations. We found that xylene-butyl cellosolve and tetralin-ethyl carbitol systems are suitable for these purposes. EP random type copolymers were fractionated successfully according to chemical composition by the column method in xylene-butyl cellosolve system. The compositional and molecular weight distributions of the original copolymer were drawn by using ethylene contents and GPC curves of the fractions. A few of the fractions were further fractionated according to molecular weight in tetralin-ethyl carbitol system. Fairly good fractionation was achieved. Furthermore, fractionation according to monomer sequence length was attained by solvent extractions using several solvents. The detailed characterization of EP random type copolymers are possible by the combination of these techniques.

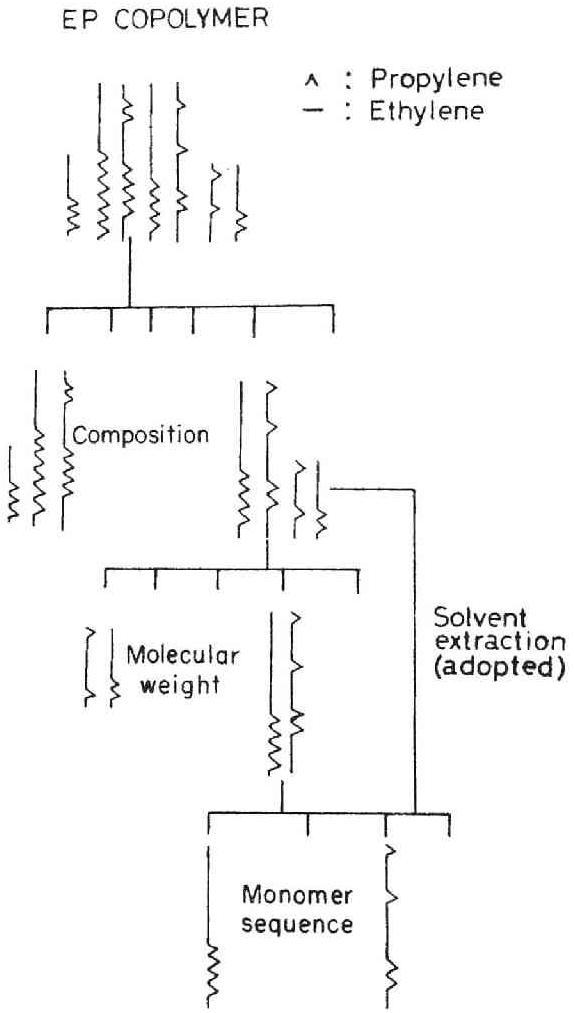

Fig. 13 Fractionation results expressed by molecular structure of EP-copolymer.

REFERENCES

1. G.W. Phillips and W.L. Carrick, J. Am. Chem. Soc., 84, 920(1962)
2. V.O. Fuchs, Makromol. Chem., 58, 65(1962)
3. V.I. Pilipovskii, I.K. Kartsev, G.V. Vinogradov, and S. Shibalovskaya, Soviet Plast., No. 5, 1(1969)
4. V.A. Klyushnikov, N.N. Severa, K.I. Kosmatykh, N.M. Domareva, N.A. Dominicheva, I.N. Andreeva, A.I. Barkova, Z.V. Akkhipova, and L.F. Shalaeva, Soviet Plast., No. 1, 5(1969)
5. H.W. Melville and B.D. Stead, J. Polym. Sci., 16, 505(1955)
6. P.J. Flory, J. Chem. Phys., 17, 223(1949)
7. T. Ogawa, Y. Suzuki, S. Tanaka, and S. Hoshino, Kobunshi Kagaku, 27, 356(1970)
8. T. Ogawa, Y. Suzuki, and T. Inaba, J. Polym. Sci., A-1, 10, 737(1972)
9. P.J. Corish and M.E. Tunnicliffe, J. Polym. Sci., Part C, 7, 187(1964)
10. G. Bucci and T. Simonazzi, J. Polym. Sci., Part C, 7, 203(1963)
11. H. Inagaki, "Kyojugotai no Gosei to Bussei (Polymerization and Physical Properties of Copolymers)", edited by T. Kuroda, M. Nagasawa, and Y. Yamashita, Kagakudojin (1967)
12. K.A. Boni, F.A. Soliemer, and P.B. Stickney, J. Polym. Sci., A-2, 6, 1579(1968)
13. H. Coll and L.R. Prusinowski, Polym. Lett., 5, 1153(1967)
14. T. Williams and I.M. Ward, Polym. Lett., 6, 621(1968)
15. T. Ogawa, S. Tanaka, and S. Hoshino, Kobunshi Kagaku, 29, 6(1972)
16. R. Chiang, J. Polym. Sci., 28, 235(1958)
17. E.E. Drott and R.A. Mendelson, Polym. Lett., 2, 187(1964)
18. J. Danon and J. Jozefonvicz, Eur. Polym. J., 5, 405(1969)

Chapter 7 SIMULATION ANALYSES OF FRACTIONATION OF ETHYLENE-PROPYLENE COPOLYMERIZATION PRODUCTS

As described in Chapter 6, ethylene-propylene copolymers can be fractionated according mainly to chemical composition or to molecular weight by adequate choice of solvent-nonsolvent systems in which the state of liquid-liquid phase equilibrium prevails. Strictly speaking, however, any fractionation process inevitably depends more or less on both chemical composition and molecular weight. More detailed consideration is required for understanding completely the fractionation behavior of copolymers. As far as we rely on only limited experimental data, this purpose can not be attained. Further, it is difficult to elucidate the molecular weight and compositional distributions for copolymers, especially when copolymerization products include homopolymers, i.e., polyethylene (PE) and polypropylene (PP). A guide line can be obtained by computer simulation method. This chapter mainly deals with simulation analyses of fractionation of the products based on the experimental results described in Chapter 6.

When one intends to discuss the fractionation from the viewpoint of simulation, many factors must be taken into consideration. These factors can be classified into two groups. One is those concerned with molecular characteristics of the copolymer and components homopolymers, such as average molecular weight, molecular weight distribution, average ethylene content, compositional distribution, tacticity, tacticity distribution, and monomer sequence length. In this place, the fractionation behavior was examined only with regard to chemical composition and molecular weight. The other is the factors concerned with the partition equilibrium of

polymer species between two liquid phases in each fractionation step, such as solubility, phase ratio of dilute and concentrated solutions, and partition coefficient. These factors must be considered in principle as a function of molecular weight, chemical composition, eluent composition, and so on. Since it is impossible to find a complete function including all these variables, certain approximations must be introduced. The values of all these factors should be similar to experimental ones as closely as possible for practical calculation. Under these conditions, hypothetical fractionation was carried out by a method similar to that described in Chapter 2. Pure EP and PE-PP blend are mainly described in this place as representative types of the copolymerization products.

The simulation results of pure EP agreed well with the experimental ones on random type copolymers. The results of PE-PP blends showed peculiar behavior with regard to both chemical composition and molecular weight. These peculiar behavior are very useful for distinguishing this blend from pure EP. Further, the various patterns of the behavior are considered to be a powerful tool for identifying complicated copolymerization products, as are NMR and IR spectra for identifying ordinary organic compounds. The simulation procedure and the results will be described in detail.

7.1 Basis of simulation

7.1.1 Molecular weight and compositional distribution

Concerning the factors related to molecular characteristics, we treated as follows. The distribution of original polymers, i.e., pure EP, PE and PP, must be known for simulating fractionation. With respect to these factors, we introduced the following assumptions: log normal distribution

function was adopted for the molecular weight distribution of homopolymers by considering the previously reported data.[2-5] It is given by

$$W(\ln M) = 1/(2\Pi\beta_h^2)^{1/2}\exp[(-1/2\beta_h^2)(\ln M - \ln M_o)^2] \qquad (1)$$

where $W(\ln M)$ is the weight distribution function, β_h is the standard deviation for $\ln M$, and $\ln M_o$ is the peak position of the distribution curve. This equation was applied to both PP and PE only by changing the values of parameters β_h and $\ln M_o$.

Among the factors which characterize pure EP, those for chemical composition and molecular weight are of principal importance. In simulation, the distributions were estimated from the knowledges such as experimental distribution curves and polymerization mechanism. For the molecular weight distribution, again log normal distribution function was assumed, because the polymerization mechanism of EP-copolymer is basically the same as that of PP and PE homopolymers.[2-5] Furthermore, as shown in Figure 1, GPC curve of an EP-copolymer suggests that the distribution can be approximated by log normal distribution function. For the chemical composition we assumed normal distribution function considering experimental results described in Chapter 6 and copolymerization data of Tosi et al.[6] Further, Figure 9 in Chapter 6 shows that chemical composition varies only slightly with molecular weight. Consequently a bivariate log normal-normal distribution function was assumed.

$$W(\ln M,\alpha) = 1/[2\beta_M\beta_\alpha(1-\rho^2)^{1/2}]\exp\{-1/2(1-\rho^2)[(\ln M - \ln M_o)^2/\beta_M^2 - 2\rho(\ln M - \ln M_o)(\alpha-\alpha_o)/\beta_M\beta_\alpha + (\alpha-\alpha_o)^2/\beta_\alpha^2]\} \qquad (2)$$

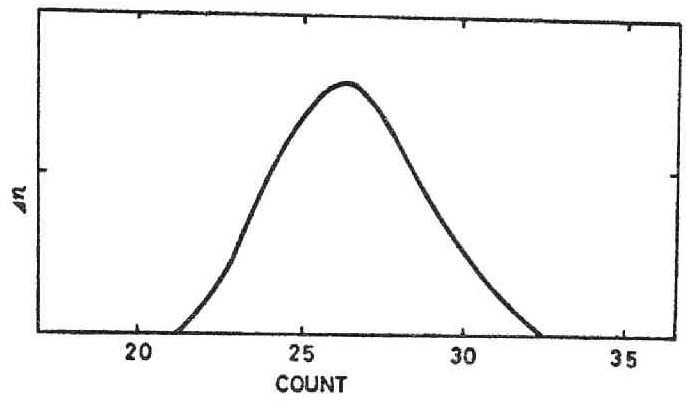

Fig. 1 GPC curve of an EP-copolymer.

Here $W(\ln M,\alpha)$ is the weight distribution function of a copolymer; $\ln M$ is log molecular weight and α is ethylene content; $\ln M_o$ and α_o are the peak positions of molecular weight and compositional distributions, respectively; and ρ is the correlation coefficient between molecular weight and chemical composition. Thus, we can also determine the molecular characteristics of original polymers, such as average molecular weights and average ethylene content, from eqs. (1) and (2) by an ordinary method.

7.1.2 Solubility of polymer

Concerning the factors related to phase equilibrium, we treated as follows. Elution point data were used to assess the solubility of polymer species at each fractionation step. As described in Chapter 4, generally the relation between molecular weight and eluent composition for PP at a given elution temperature is given by eq.(3).

$$M_c = 10^4(K_1 - K_2S)^{-2} \tag{3}$$

where K_1 and K_2 are constants; M_c is the molecular weight at elution point; and S is the weight fraction of solvent. A similar relationship, which was estimated by cloud point measurements, was used for PE. It is given by eq.(4).

$$M_c = 10^4\{[K_1 - K_2(S - K_3)]^{-2} + K_4\} \tag{4}$$

where K_3 and K_4 are another constants. Presumably M_c of pure EP lies between those of PP and PE as shown in Figure 5 in Chapter 6. We assumed M_c to shift with the monomer content α in the form:

$$M_c = 10^4\{[K_1 - K_2(S - K_3\alpha)]^{-2} + K_4\} \tag{5}$$

In other words, eq.(5) shows that a polymer species having molecular weight M_c and ethylene content α has the cloud point in the eluent of solvent concentration S. Our experimental data concerning the relation between Huggins constant and molecular weight of copolymer also suggest that such a treatment is actually valid.[7]

We assigned the values $K_1 = 0.57$, $K_2 = 2.79$, $K_3 = 0.22$ and $K_4 = 0.83$ for decalin-butyl carbitol system; and $K_1 = 1.47$, $K_2 = 3.25$, $K_3 = 0.19$ and $K_4 = 0.24$ for decalin-butyl carbitol system from the data described in Chapter 4 and from the cloud point measurements.

The effects of molecular weight and chemical composition on fractionation of EP-copolymers can be represented by the cloud point curves obtained from eq.(5) as shown in Figure 2 (dotted line). That is, all kinds of

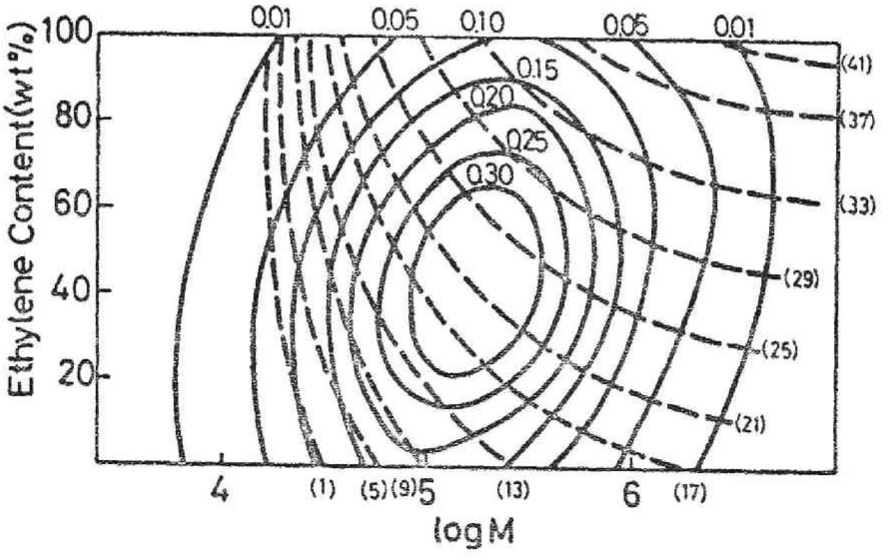

Fig. 2 Relations between molecular characteristics and eluent composition showing common cloud-point.

(------): the polymer species giving a common cloud-point composition such as shown by per cent decalin in the parenthesis;

(———): contour lines of polymer weight. Numbers indicate the relative weight.

Original polymer: $\bar{\alpha} = 0.49$, $\beta_\alpha = 0.362$, $\beta_M = 1.25$, $\ln M_o = 12.0$, $\rho = 0.25$, $\bar{M}n = 8.1 \times 10^4$, $\bar{M}w = 3.6 \times 10^5$.

polymer species on a dotted line have the common properties on fractionation, and elute in the same fraction. For example, PE with $M = 3.2 \times 10^4$ elutes together with PP with $M = 1.8 \times 10^6$ in the case of the dotted line (17). For lower solvent per cent in eluent, i.e., lower molecular weight region, the cloud point curve is almost independent of the ethylene content of copolymers. Accordingly, the fractionation may be performed mainly according to molecular weight. For higher solvent per cent in eluent, i.e., higher molecular weight region, the cloud point curve varies mainly with the ethylene content. Compositional fractionation can be attained in this region.

The distribution curve of the copolymer was assumed to have the form of eq.(2). As shown in Figure 3, the distribution curve is widely variable depending on the parameters included in the equation. On the other hand, we have already confirmed in Chapter 6 that random type EP-copolymer usually has a broad compositional and molecular weight distribution. In actual simulation the parameters in eq.(2) were adequately determined from such experimental results.

7.1.3 Partition of polymer between two liquid phases

For the partition relationship, a well-known equation derived from the Flory-Huggins theory[1] was used:

$$f^E = R\, f^R/[R + \exp(\sigma \cdot \gamma)] \qquad (6)$$

where f^E and f^R are the volume fractions of γ-mer in the dilute phase and in the original sample, respectively; R is the phase ratio of

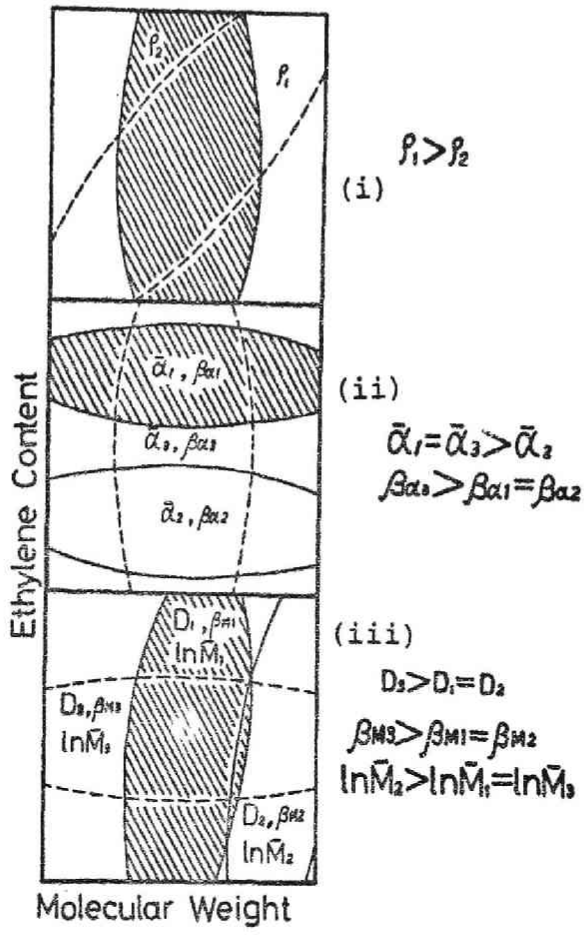

Fig. 3 Various distribution curves of pure EP, expressed by contour lines.

(i) The parameters other than ρ in eq.(2) were kept constant: (------) ρ_1; (————) ρ_2.

(ii) The parameters other than α and β_α in eq.(2) were kept constant: (————) α_1, α_2, $\beta_{\alpha 1}$, and $\beta_{\alpha 2}$; (------) α_3, $\beta_{\alpha 3}$.

(iii) The parameters other than β_M and ln M_o in eq.(2) were kept constant: (————) β_{M1}, ln M_1 (corresponding to ln M_o), β_{M2}, and ln M_2 (corresponding to ln M_o); (------) β_{M3}, ln M_3 (corresponding to ln M_o).

volumes of the dilute to the concentrated phase. A value of R = 200 seemed to be reasonable from the result of more accurately simulated fractionation of homopolymers as described in Chapter 2; the parameter o is the partition coefficient of γ-mer between the two liquid phases. The problem is how to define the γ-mer for the original product which usually consists of PE, EP-copolymers of varying ethylene content α, and PP components. For PE the γ-mer is the species having the degree of polymerization γ. For EP-copolymers and PP, the γ-mer is the species which has the same cloud point as the γ-mer of PE in a given eluent system (cf. Fig. 4). We assumed that all the species having M_E, M_{EP}, M'_{EP} ------, and M_P, i.e., the γ-mer, follow the same partition equilibrium, and assign the same value of σ and the same value of γ as well.

In practice when the solvent composition S is given, we first calculate γ for PE by eq.(4) (or eq.(5) with α = 1). Then we calculate σ by eq.(6) for this value of γ , assuming f^E/f^R equal to 0.5 in usual cases. To describe the partion behavior of a species having M_j and α_k (other than PE) in the eluent of the composition S, we use the same value of σ but have to reevaluate the value of γ , which is done as follows: we first calculate S', by eq.(5) with $M_c = M_j$ and $\alpha = \alpha_k$; then M'_c by eq.(4) for the S', and assign this M'_c or γ' as the value of γ for this species (cf. Fig. 5). That is, the γ value of a species having M_j and α_k is the M'_c of PE component which has the same cloud point composition as the given species. When we alter the solvent composition of the eluent, we repeat the above procedures.

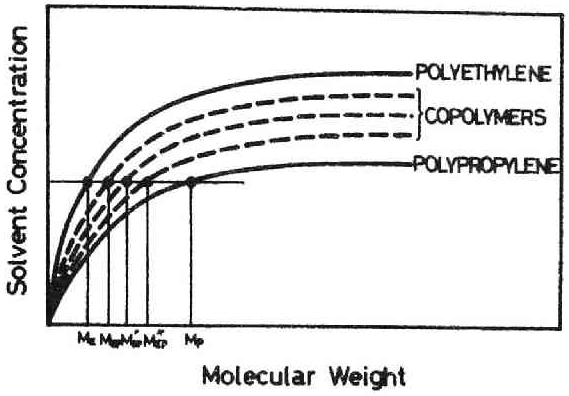

Fig. 4 Schematic solubility curves of polymers in a solvent-nonsolvent system.

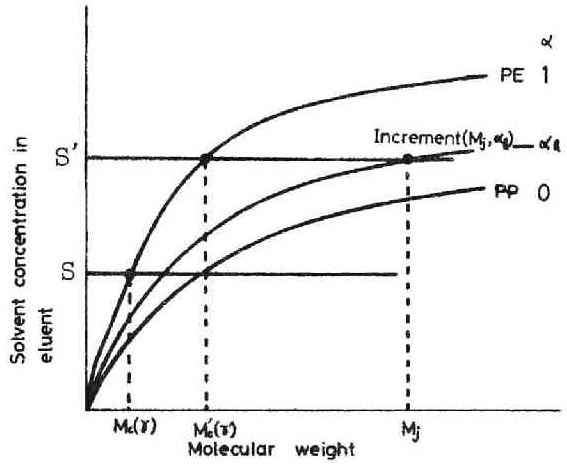

Fig. 5 The relation among $M_c(\gamma)$, $M_c'(\gamma')$, S, and S' in a given eluent composition S.

7.2 Procedure for simulating the fractionation

The fractionation process is the same as described in Chapter 2 (cf. Fig. 6). However, since the fractionation must be considered for component and chemical composition as well as molecular weight, the calculation process becomes more complicated comparing with that for homopolymers. The calculation process is shown in Figure 6 in the form of flow chart for computer calculation. For PP and PE, the molecular weight distribution curve was divided into K = 30 increments; the range of ln M was from 7 to 19. The distribution surface of an EP-copolymer was divided into K x N = 810 increments; the range of α was from 0 to 1.0, and the range of ln M was from 7 to 19. We define WPP, WEP and WPE by

$$WPP = \sum_{j=1}^{K} f_{PP}^{RO}(\ln M_j) \tag{7a}$$

$$WEP = \sum_{k=1}^{N} \sum_{j=1}^{K} f_{EP}^{RO}(\ln M_j, \alpha_k) \tag{7b}$$

$$WPE = \sum_{j=1}^{K} f_{PE}^{RO}(\ln M_j) \tag{7c}$$

where $f_{PP}^{RO}(\ln M_j)$, $f_{EP}^{RO}(\ln M_j, \alpha_k)$ and $f_{PE}^{RO}(\ln M_j)$ express the weights of j-th, (j,k)-th, and j-th increments of PP, EP and PE components, respectively, in the original polymer "RO". The above functions are normalized as follows:

$$WPP + WEP + WPE = 1 \tag{8}$$

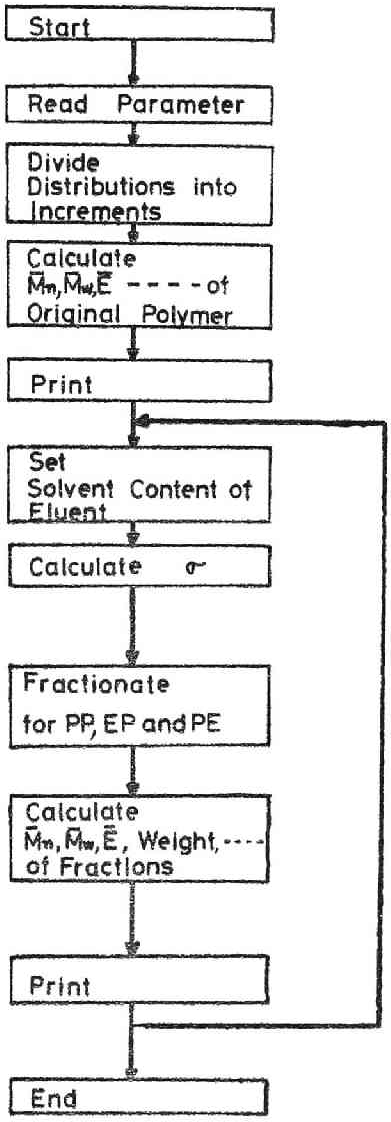

Fig. 6 Flow chart of simulated fractionation for EP copolymerization products.

Obviously the ratio of the PP, EP and PE components are

$$PP : EP : PE = WPP : WEP : WPE \tag{9}$$

The first fractionation step is performed by an eluent of an arbitrarily chosen composition S_1 on the original polymer defined by eqs.(8) and (9). We calculate the weight fraction $(f^E)_1$ of all the increments in the dilute phase by eq.(6), employing the parameter σ and γ as described before. Then we subtract $(f^E)_1$ from (f^{RO}) to obtain $(f^R)_1$. The next fractionation step is to be carried out for $(f^R)_1$ by an eluent of composition S_2, and so on. The solvent concentration in eluent was increased stepwise in increments of from 3.0 to 4.0 wt%, i.e., $S_i - S_{i-1} = 0.03 \sim 0.04$. The i-th fraction is obtained from the (i-1)-th residue $(f^R)_{i-1}$ which is given by

$$f^R_{PP}(\ln M_j)_{i-1} = f^{RO}_{PP}(\ln M_j) - \sum_{\ell=1}^{i-1} f^E(\ln M_j)_\ell \tag{10a}$$

$$f^R_{EP}(\ln M_j, \alpha_k)_{i-1} = f^{RO}_{EP}(\ln M_j, \alpha_k) - \sum_{\ell=1}^{i-1} f^E_{EP}(\ln M_j, \alpha_k)_\ell \tag{10b}$$

$$f^R_{PP}(\ln M_j)_{i-1} = f^{RO}_{PE}(\ln M_j) - \sum_{\ell=1}^{i-1} f^E_{PE}(\ln M_j)_\ell \tag{10c}$$

The weight $W(\ln M_j)_i$ of the polymer species having M_j regardless of α_k in the i-th fraction is calculated by the equation:

$$W(\ln M_j)_i = f^E_{PP}(\ln M_j)_i + \sum_{k=1}^{N} f^E_{EP}(\ln M_j, \alpha_k)_i + f^E_{PE}(\ln M_j)_i \tag{11}$$

The weight $W(\alpha_k)_i$ of the polymer species having α_k regardless of M_j in the i-th fraction is as follows:

For $\alpha_k = 0$,

$$W(\alpha_k) = \sum_{j=1}^{K} f^{E}_{PP}(\ln M_j)_i \tag{12a}$$

For $0 < \alpha_k < 1.0$,

$$W(\alpha_k)_i = \sum_{j=1}^{K} f^{E}_{EP}(\ln M_j, \alpha_k)_i \tag{12b}$$

For $\alpha_k = 1.0$,

$$W(\alpha_k)_i = \sum_{j=1}^{K} f^{E}_{PE}(\ln M_j)_i \tag{12c}$$

The number $(\bar{M}n)_i$ and weight $(\bar{M}w)_i$ average molecular weights, and the average ethylene content $\bar{\alpha}_i$ of the i-th fraction are given by eqs.(13), (14) and (15), respectively.

$$(\bar{M}n)_i = \sum_{j=1}^{K} W(\ln M_j)_i / \sum_{j=1}^{K} [W(\ln M_j)_i / M_j] \tag{13}$$

$$(\bar{M}w)_i = \sum_{j=1}^{K} M_j W(\ln M_j)_i / \sum_{j=1}^{K} W(\ln M_j)_i \tag{14}$$

$$\bar{\alpha}_i = \sum_{j=1}^{K} \alpha_k W(\alpha_k)_i / \sum_{j=1}^{K} W(\alpha_k)_i \tag{15}$$

The standard deviations of molecular weight σ_M and ethylene content σ_α of the i-th fraction are, respectively, given by eqs.(16) and (17).

$$(\sigma_M)_i = \{\frac{1}{\sum_{j=1}^{K} W(\ln M_j)_i} \sum_{j=1}^{K} W(\ln M_j)_i [\ln M_j - (\overline{\ln M_j})]^2\}^{1/2} \tag{16}$$

$$(\sigma_\alpha)_i = \left[\frac{1}{\sum_{k=1}^{N} W(\alpha_k)_i} \sum_{k=1}^{N} W(\alpha_k)_i (\alpha_k - \bar{\alpha}_i)^2\right]^{1/2} \qquad (17)$$

The above procedures are repeated until residual polymer components have been exhausted from the residual phase.

7.3 Fractionation experiment and characterization

Two copolymerization products designated as PEPB, EPA, and a mechanical blend designated as PEPA were subjected to column fractionation experiments. The results were compared with the simulated ones. The sample PEPA is a 45 : 55 (by weight) mixture of commercial PE and PP samples: the PE has $\bar{M}n = 2.6 \times 10^4$ and $\bar{M}w = 10 \times 10^4$, and the PP has $\bar{M}n = 7.9 \times 10^4$ and $\bar{M}w = 36 \times 10^4$. A 5-g sample was fractionated at 161°C in decalin-butyl carbitol system by using the column described in Chapter 2. The sample PEPB was prepared in n-heptane by successively introducing propylene, hyrodgen, and ethylene in the presence of $AlEt_2$-$TiCl_3$ (activated). The ethylene content of the product was 31 wt%. A 40-g sample was fractionated at 161°C in decalin-butyl carbitol system by using the apparatus described in Chapter 6. The sample EPA was a commercial high-impact polypropylene. The ethylene content was 8.6 wt%. A 10-g sample of EPA was fractionated at 164°C in decalin-butyl carbitol system.

Cumulative weight distribution curves were constructed from weight and limiting viscosity number of the fractions. The limiting viscosity number was determined at 135°C in decalin solution with an Ubbelohde-type viscometer. The ethylene content of the fractions was determined by Corish's method, which uses the ratio of the intensity at 1380^{-1} to that at 1460 cm^{-1} in infrared spectrum.[8,9]

7.4 Fractionation behavior of EP-copolymers

We assumed an original copolymer having a high average ethylene content (49 wt%) and a broad molecular weight and compositional distribution ($\bar{M}w/\bar{M}n$)= 4.44, and β_α = 0.362 in eq.(2)). The data in decalin-butyl carbitol system were adopted for the relation between eluent composition and molecular weight. A variety of the fractionation behavior were examined under the conditions in which WPP = 0 and WPE = 0 (eqs.(7a) and (7c)). The results are summarized in Table I. These will be evaluated below mainly from two points of view, i.e., compositional and molecular weight distributions of the original polymer and those of the fractions.

7.4.1 Compositional distribution

As shown in Figure 7, the compositional distribution of each fraction is broad. In particular the fractions obtained from eluents containing 1 and 5 % decalin show no definite peak: the distributions are generally broader than any other fractions. The compositional distribution becomes narrower for the fractions with higher molecular weight. This tendency is particularly obvious in Figure 8, in which the standard deviation of composition is plotted against molecular weight variable. Compositional fractionation becomes predominant in the range above $(\bar{M}n\bar{M}w)^{1/2} = 2 \times 10^5$. On the other hand, we predicted from the cloud point behavior as described in Chapter 6 that compositional fractionation would predominate in the range above $M = 10^5$. This discrepancy is due to the fact that the fractions have broad molecular weight distributions.

Table I Hypothetical fractionation of ethylene-propylene copolymers.

Original copolymer: $\bar{M}n = 8.08 \times 10^4$, $\bar{M}w = 36.2 \times 10^4$, $\bar{M}w/\bar{M}n = 4.48$, $\bar{\alpha} = 49$ wt% .

Fr. No.	Solvent wt%	Polymer weight %	$\bar{M}n \times 10^{-4}$	$\bar{M}w \times 10^{-4}$	$\bar{M}w/\bar{M}n$	$\bar{\alpha}_i$ %	$(\sigma_\alpha)_i$ %
1	1	6.86	1.78	3.87	2.18	30.7	21.0
2	5	5.91	3.18	6.30	1.98	29.4	19.8
3	9	6.48	4.95	9.47	1.91	30.0	19.5
4	13	8.08	7.06	13.8	1.95	31.7	19.5
5	17	10.4	9.64	19.9	2.06	34.8	19.5
6	21	12.9	12.7	27.7	2.18	40.2	19.4
7	25	14.3	16.4	36.7	2.24	48.4	18.5
8	29	13.7	21.2	47.4	2.24	59.0	16.9
9	33	11.1	28.2	61.0	2.16	71.2	14.5
10	37	7.16	42.3	82.2	1.94	83.8	11.1
11	41	2.38	85.1	153.	1.80	93.3	6.6

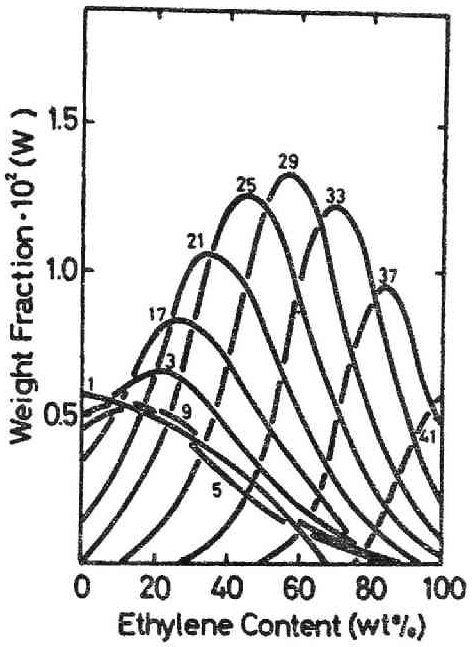

Fig. 7 Compositional distribution curves of the fractions obtained from the same original polymer as described in Figure 5. Numbers indicate per cent decalin in eluent (simulation).

The compositional distribution curve of the origianl polymer was drawn by Shulz's method[10] from the simulated fractionation data. Figure 9 shows the curve together with the experimental data points obtained in Chapter 6. The agreement between the calculated and experimental curves is fairly good.

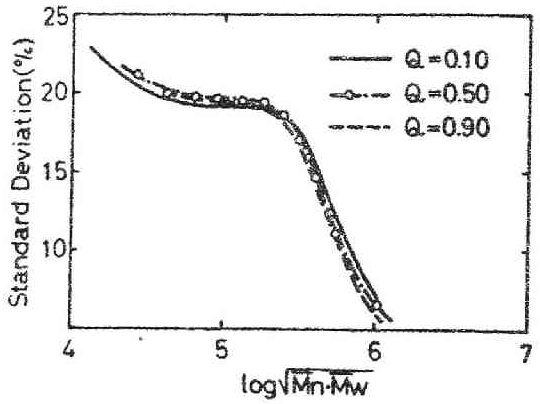

Fig. 8 Compositional distribution of the fractions expressed as standard deviation. The original polymer is the same as described in Figure 2. The Q values indicate f^E/f^R, which was fixed for each run of fractionation.

7.4.2 Molecular weight ditribution

Figures 10 and 11 show the molecular weight distribution curve and the D value of the fractions, respectively. The D value of the copolymer fractions is 1.5 - 2.5. Apparently the distribution is broader than that of fractionated homopolymers, for which the D value is usually less than 1.3 as described in Chapter 4. Accordingly the overlapping of the distribution curve is considerable. On the other hand, we described in Chapter 6 that the average D value of the fractions obtained experimental was 2.5, which is in good agreement with the simulated value. In Figure 11, D value vs. molecular weight of the fractions gives a minimum. This

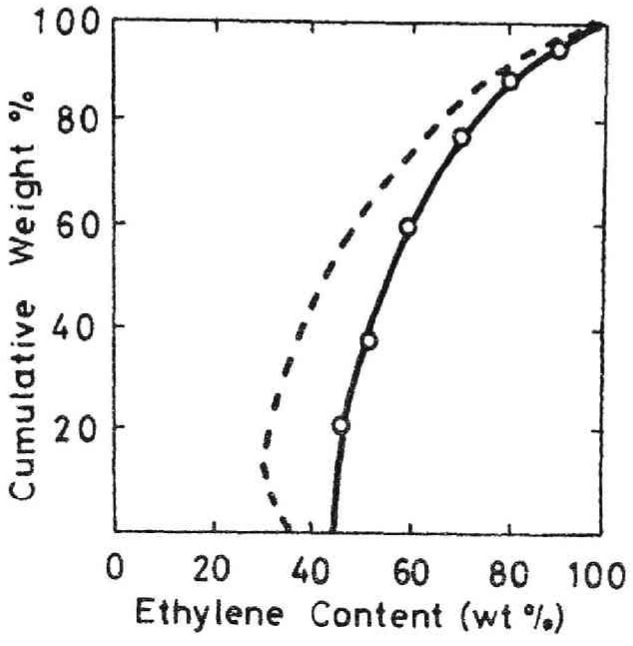

Fig. 9 Cumulative weight vs. ethylene content curves of the copolymer.

(————): simulated curve, $\bar{\alpha}$ = 0.59, β_{α} = 0.200, β_{M} = 1.25, ln M_{o} = 12.0, ρ = 0.25;

(--------): simulated curve obtained from the same original polymer as described in Figure 2;

(O): experimental point, $\bar{\alpha}$ = 0.59.

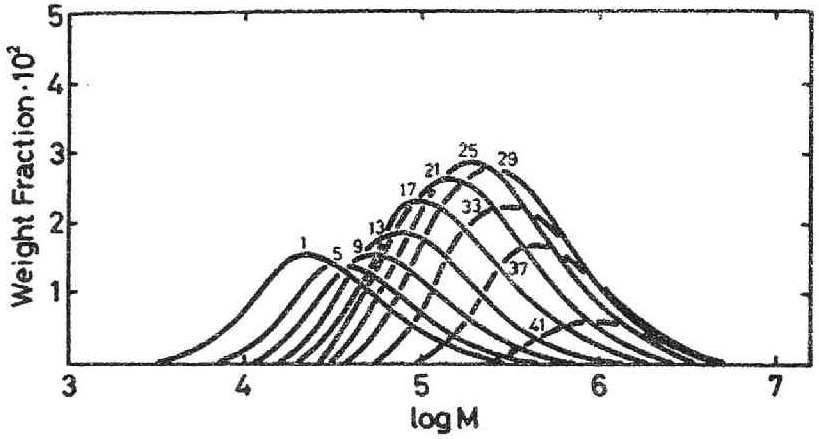

Fig. 10 Molecular weight distribution curves of the fractions obtained from the same original polymer as described in Figure 2. Numbers indicate per cent decalin in eluent.

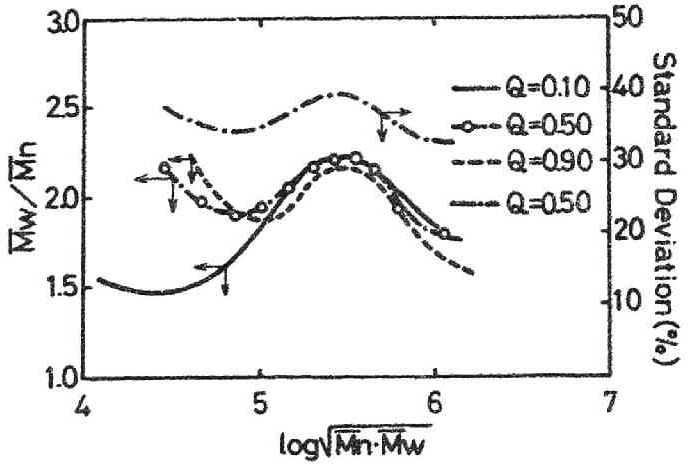

Fig. 11 D value and standard deviation $(\sigma_M)_i$ of each fraction obtained from the same original polymer as described in Figure 2.

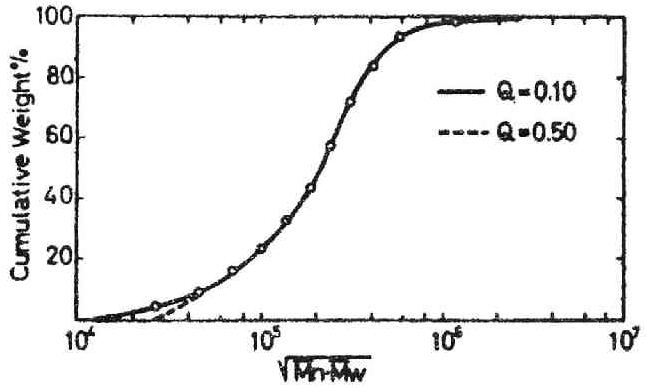

Fig. 12 Cumulative weight vs. molecular weight curves of the original polymer. Its molecular characteristics are the same as described in Figure 2 (simulation).

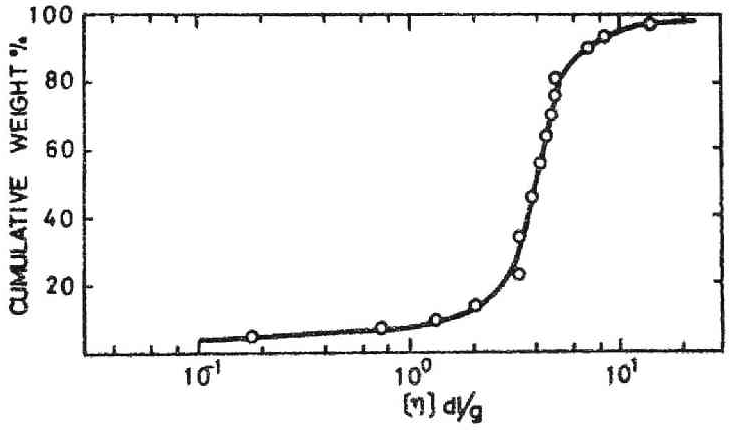

Fig. 13 Cumulative weight vs. limiting viscosity number curve for the sample designated as sample B in Chapter 6 (experiment).

pattern may be due to the fact that the distributions of molecular weight and chemical composition affect the fractionation to different extents.

The simulated molecular weight distribution curve of the original polymer was compared with the experimental one. Figure 12 shows a cumulative weight distribution curve drawn by Schulz's method from the simulation data. Figure 13 shows the experimental distribution curve, which was drawn by the data listed in Table II in Chapter 6. Apparently, the results are qualitatively in good sgreement with each other. In addition, even if the parameter Q (= f^E/f^R) is varied from 0.1 to 0.9, there is no essential difference in the qualitative features of the results (cf. Figs. 8, 11 and 12). This parameter causes no serious problem. As a conclusion, the simulation provides a very good representation of the actual fractionation results of copolymers.

7.5 Fractionation behavior of PE-PP blends

As described in the introduction of this chapter, there are various types of copolymerization products. This section deals with PE-PP blend which is the simplest of the products. We assume the component homopolymers to have broad molecular weight distribution, i.e., $\bar{M}w/\bar{M}n$ = 4.8, so as to facilitate the comparison with experiments. The blend is composed of PE and PP in the ratio 45 : 55. A simulated fractionation was carried out by use of the relation between eluent composition and molecular weight in decalin-butyl carbitol and decalin-ethyl carbitol systems. The calculation was done under the condition WEP = 0 (eq.(7b)). The results are summarized in Table II.

Table II Simulated fractionation of PE-PP blend.

Original blend: $\bar{M}n = 3.69 \times 10^4$, $\bar{M}w = 24.3 \times 10^4$,

$\bar{M}w/\bar{M}n = 6.58$. PE : PP = 45 : 55, by weight.

Fr. No.	Solvent wt%	Polymer weight %	$\bar{M}n \times 10^{-4}$	$\bar{M}w \times 10^{-4}$	$\bar{M}w/\bar{M}n$	$\bar{\alpha}_i$
1	1.0	16.4	1.15	3.30	2.87	48.1
2	4.0	8.93	2.34	7.39	3.16	23.3
3	7.0	8.01	4.81	12.7	2.64	12.7
4	10.0	8.86	7.98	19.5	2.44	11.3
5	13.0	10.3	9.39	29.0	3.09	15.4
6	16.0	10.2	10.1	45.1	4.46	18.3
7	19.0	7.14	10.8	70.1	6.49	23.0
8	22.0	4.67	6.27	59.9	9.55	59.2
9	25.0	3.51	4.66	18.8	4.03	92.1
10	28.0	4.36	6.01	6.82	1.13	98.9
11	31.0	4.98	8.16	8.63	1.06	100.
12	34.0	5.50	12.4	13.2	1.06	100.
13	37.0	4.69	22.1	24.4	1.10	100.
14	40.0	2.33	48.9	58.2	1.19	100.
15	43.0	0.182	158.	200.	1.26	100.

7.5.1 Compositional distribution and elution behavior

Since the evaluation of compositional distribution of the fractions is meaningless, only the distribution curve of the original blend is discussed. Figure 14 shows the cumulative weight vs. ethylene content curves for several blends, which were constructed from simulation data by Schulz's method.[10] Remarkable variation of ethylene content in the fractions is observed at around 70 % cumulative weight in the case of the blend of 45 wt% PE. Such a pattern is also found in the simulation of the blends with other ethylene contents. This behavior was evidenced by fractionation experiment as shown in Figure 15. Remarkable variation of ethylene content of the fractions at a certain cumulative weight or elution point is important feature for PE-PP blend.

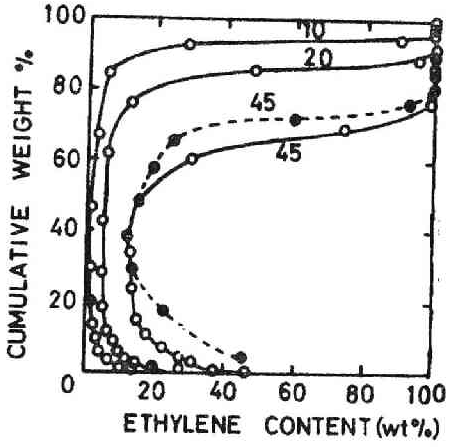

Fig. 14 Cumulative weight vs. ethylene content curves for PE-PP blends (simulation). Numbers indicate ethylene content of the blends by weight: (-----) the relation between polymer composition and molecular weight for the decalin-butyl carbitol system was used; (————) the same relation for the decalin-ethyl carbitol system was used. PE component: $\ln M_o$ = 10.8, β_h = 1.25; PP component: $\ln M_o$ = 12.0, β_h = 1.25.

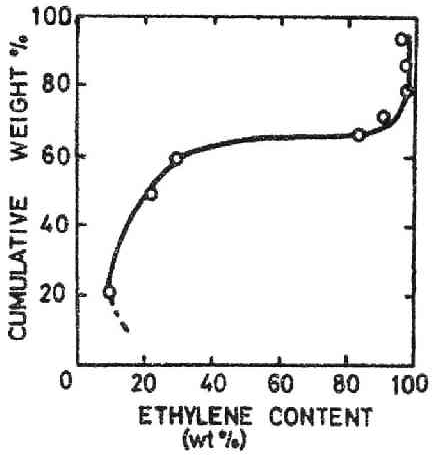

Fig. 15 Cumulative weight vs. ethylene content curve which was obtained for the sample PEPA in decalin-ethyl carbitol system (experiment).

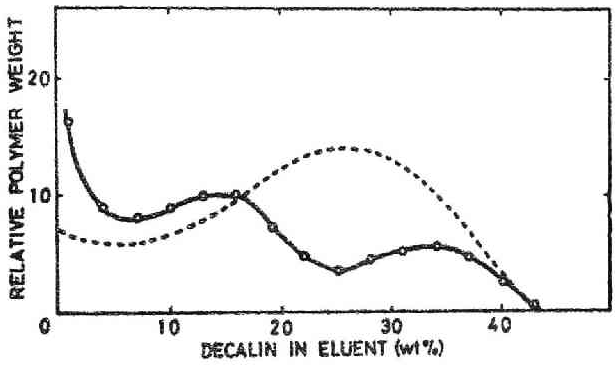

Fig. 16 Relative polymer weight eluted vs. eluate composition curves (simulation).

(————): PE-PP blend, the molecular characteristics are the same as described in Figure 14. PE : PP = 45 : 55.

(--------): EP-copolymer, $\bar{\alpha}$ = 0.49, other molecular characteristics are the same as described in Figure 2.

Figure 16 shows the relation between the weight of fraction and eluent composition. Two peaks were observed in the curve of this blend. One at 15 % decalin was assigned to PP, and the other at 34 % to PE in view of fractionation behavior of a single homopolymer. However, only one peak was observed in the case of pure EP (dotted curve in Figure 16). These behavior are also useful for distinguishing PE-PP blend from pure EP, although they are sensitive to some extent to the method of applying the solvent gradient.

7.5.2 Molecular weight distribution

The fractions from this blend gave peculiar molecular weight distribution curves. Figure 17 shows the molecular weight distribution curves of the fractions. Those obtained with the eluents of 1 % to 22 % decalin indicate two peaks. One in a lower molecular weight region arises from PE component, and the other in a higher molecular weight region arises from PP component. The fractions obtained by the eluent of higher decalin content show a single peak due to PE component, because PP component has already been eluted completely. As shown in Figure 18, the D value of the fractions also varies abnormally with the fraction number, reflecting the above fractionation behavior. The D value of the intermediate fractions is extremely high. The maximum is caused by the fact that the PP component having higher molecular weights and the PE component having lower molecular weights are included together in each fraction. While the D value for the latter half of the fractions is below 2.0 as in the case of homopolymers.[11,12] Such a pattern could not be detected in the simulation of pure EP. It is possible to distinguish homopolymer blends from copolymer by observing such peculiar behavior.

Next the distribution of the blend was evaluated in cumulative form.

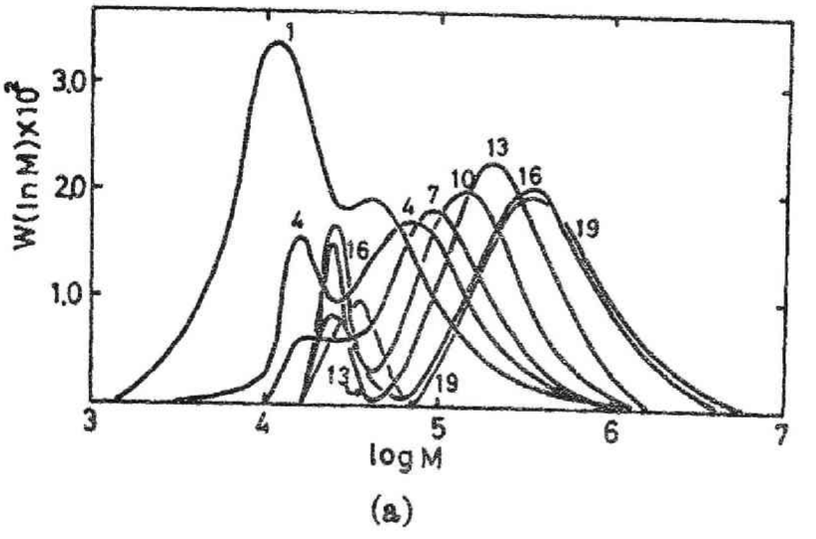

(a)

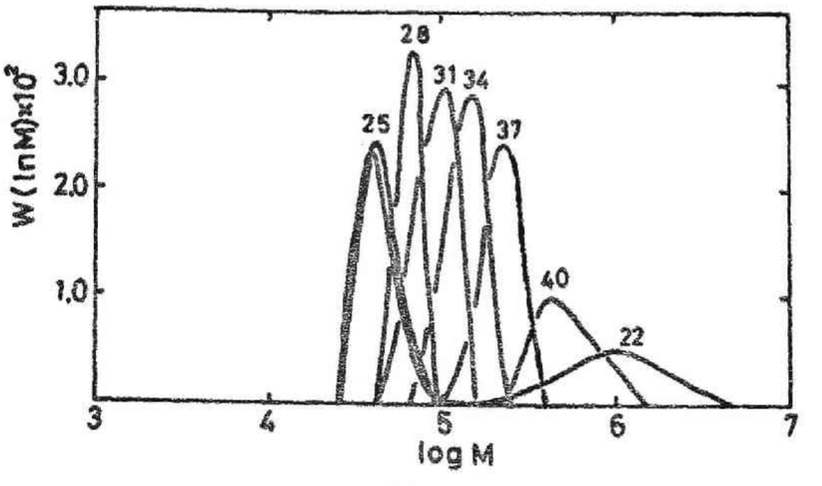

(b)

Fig. 17 Molecular weight distribution curves of the fractions for PE-PP blend. Its molecular characteristics are the same as described in Figure 14 (PE : PP = 45 : 55 by weight). Numbers indicate per cent decalin.

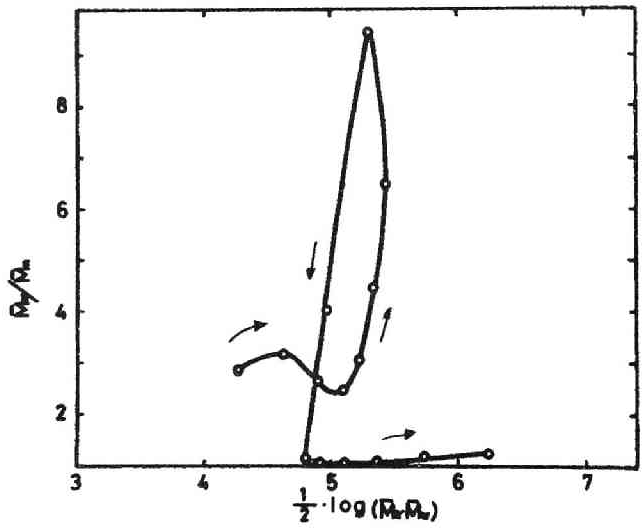

Fig. 18 D values of the fractions obtained from the blend having 45 wt% in ethylene content (simulation). The blend is the same as described in Figure 14.

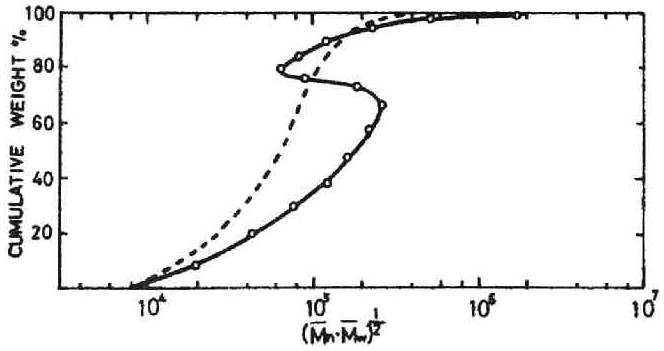

Fig. 19 Cumulative weight vs. molecular weight curves (simulation).

(———): PE-PP blend. Its molecular characteristics are the same as described in Figure 14 (PE : PP = 45 : 55).

(-------): EP-copolymer with $\bar{\alpha}$ = 0.49. Other molecular characteristics are the same as described in Figure 2.

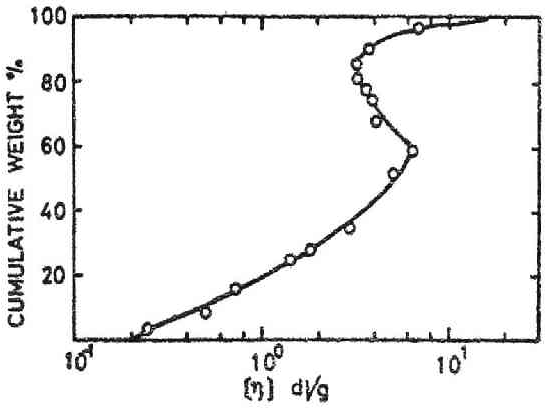

Fig. 20 Cumulative weight vs. limiting viscosity number curve for the sample PEPA (experiment).

As is evident from Figure 19, the reversal of the distribution curve occurs. Figure 20 shows the corresponding experimental curve. Such a pattern could be observed neither in simulation nor in the experiment in the case of pure EP. The reversal in the cumulative curve corresponds to the inflection point from the PP-rich fraction to the PE-rich fraction, as listed in Table II.

7.5.3. PE-PP type products obtained by experiment

On the basis of the above results, we carried out the characterization of an unknown sample PEPB. Figures 21 and 22, respectively, show the plots of the cumulative weight against the ethylene content and also the limiting viscosity number [η], which were obtained by experiment. The curves show the behavior similar to the simulated ones illustrated in Figures 14 and 19. Figure 23 shows the elution behavior concerning the polymer weights of fractions, obtained by experiment. This curve is also in qualitative agreement with the simulated one shown in Figure 16.

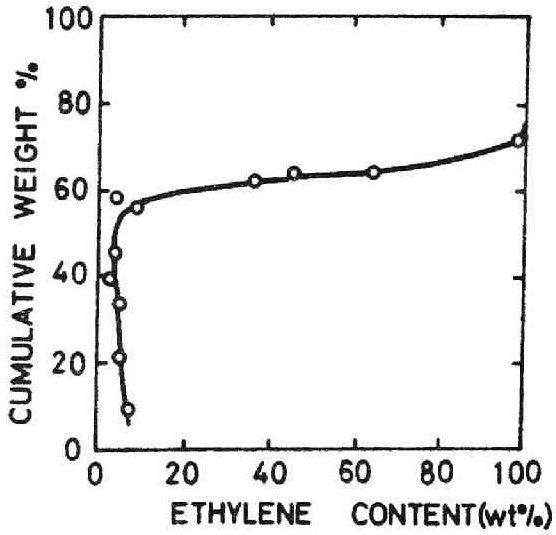

Fig. 21 Cumulative weight vs. ethylene content curve for the sample PEPB (experiment).

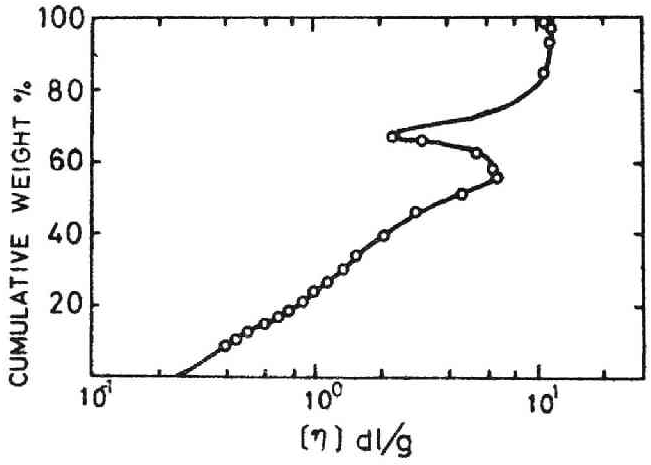

Fig. 22 Cumulative weight vs. limiting viscosity number curve for the sample PEPB (experiment).

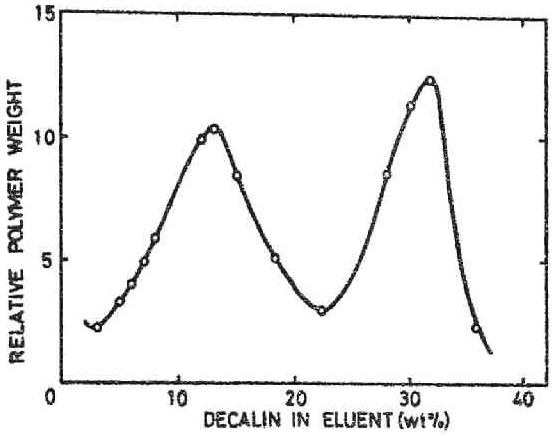

Fig. 23 Relative polymer weight of the fractions vs. eluent composition for the sample PEPB (experiment).

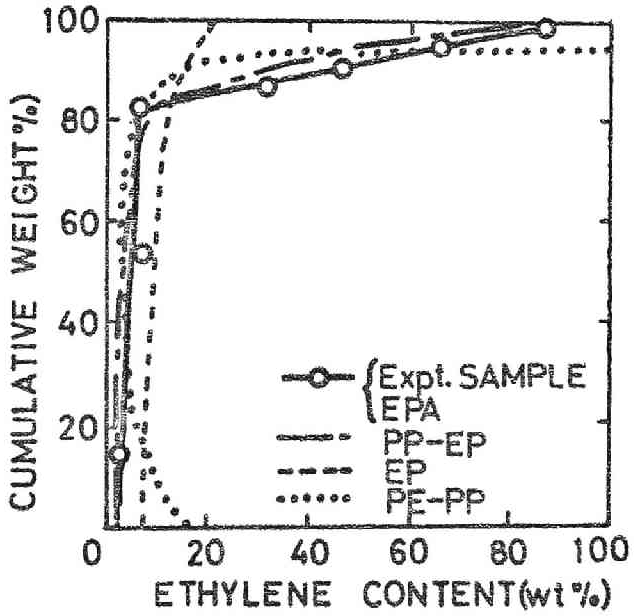

Fig. 24 Cumulative weight vs. ethylene content curves obtained by experiment and simulation for the sample EPA.

It is concluded that the sample PEPB consists of PE and PP, but contains virtually no EP, although the sample was prepared seemingly by copolymerization. A blend of homopolymers having similar molecular weights should be identified by dissolution or precipitation fractionation. However, it is generally difficult to draw a definite conclusion from only such experiments, and the identification may be attained with the aid of simulation.

7.6 Fractionation behavior of various blends of PP, EP and PE other than PE-PP blend

These types can be classified into three types, i.e., PP-EP, PP-EP-PE and EP-PE blends. The fractionation behavior of these blends varied in a very complicated way with respect to the kinds and ratios of components, and have been already reported in detail by us.[13] All fractionation data obtained experimentally, which were not explained as pure EP or PE-PP blend, were understood by comparing them with the calculated behavior. A representative case is shown in Figure 24 in the form of cumulative weight vs. ethylene content curves. The sample is one of the most important commercial polymers, called high impact polypropylene. The simulated curves in Figure 24 were obtained by considering the average ethylene content of the sample (8.6 wt%). Clearly the curve for chemical composition is not in agreement with that calculated for pure EP. If the experimental curve is compared with that of PE-PP type, the difference between the experimental and simulated curves exceeds the estimated experimental errors. Therefore, the sample is not of PE-PP type either. The experimental curve resembles most closely the simulated one for PP-EP type in the weight ratio 82 : 18. They might

have to be compared with those of PP-EP-PE type. However, the sample is expected to contain only a minute amount of PE component, if any present, in comparison with EP component. Similarly the curves other than the curve shown in Figure 24 for the same sample were also consistent with those of PP-EP type. Consequently, the sample EPA is constituted of PP and EP components in the weight ratio 82 : 18.

7.7 Conclusions for fractionation of copolymerization products by simulation

The bahavior of solution fractionation, as related to ethylene-propylen copolymerization products, was examined by computer simulation. The products were classified into five types, i.e., pure EP, PE-PP blend and other types of blends composed of PE, EP, PP components, i.e., PP-EP, PP-EP-PE, and EP-PE blends. The molecular weight and compositional distributions of fractions were found to vary in a complicated manner. In particular, the compositional fractionation was predominant in the latter half of fractions, when the simulated fractionation was performed on an original polymer having a broad compositional distribution. Since the solution properties of EP-copolymers are generally almost independent of the difference in monomer sequence,[7] these results are considered to be valid for both block and random copolymers.

The curves of cumulative weight against the ethylene content or the molecular weight of fractions for PE-PP blend revealed very peculiar patterns. Thus we can easily distinguish homopolymer blends from the copolymer by observing such peculiar patterns, and the component ratio of blends is inevitably determined. Further, these patterns for pure EP and PE-PP blend were proved experimentally.

In the case of other types of blends composed of PP, EP and PE components, the distribution patterns were much more complicated than those for pure EP and PE-PP blend. The determination of blend type and component ratio for such products can also be made if the results are studied from various points of view. In fact, all fractionation data obtained experimentally, which were not explained as pure EP or PE-PP blend, were understood as the results in terms of these blends.

REFERENCES

1. M.L. Huggins and H. Okamoto, in Polymer Fractionation, M.J.R. Cantow. Ed., Academic Press, New York, 1967, Chap. A.
2. H. Wesslau, Makromol. Chem., 20, 111(1956)
3. H. Sato, Kogyo Kagaku Zasshi, 65, 385(1962)
4. R.A. Mendelson, J. Polym. Sci., Part A, 1, 2361(1963)
5. T. Ogawa, Y. Suzuki and T. Inaba, J. Polym. Sci., Part A-1, 10, 737(1972)
6. C. Tosi, A. Valvassori and F. Ciampelli, Europ. Polym. J., 5, 575(1969)
7. H. Tanaka, T. Ogawa, and S. Hoshino, Paper No. 20C-14 presented at the SPSJ 19th Symposium on Macromolecules, Kyoto (1970)
8. T. Ogawa, S. Tanaka, and T. Inaba, J. Appl. Polym. Sci., 17, 319(1973)
9. P.J. Corish and M.F. Tunnicliffe, J. Polym. Sci., Part C, 7, 187(1964)
10. G.V. Schulz, Z. Physik. Chem., B47, 155(1940)
11. T. Ogawa, S. Tanaka, and S. Hoshino, J. Appl. Polym. Sci., 16, 2257(1972)
12. K. Kamide and K. Sugamiya, Makromol. Chem., 156, 259(1972)
13. T. Ogawa and T. Inaba, J. Appl. Polym. Sci., 18, 3345(1974)

Chapter 8 ONE-POINT METHOD FOR NUMBER-AVERAGE MOLECULAR WEIGHT DETERMINATION

For constructing molecular weight distribution curve from fractionation data, one has to determine molecular weights of large number of fractions. Therefore, it is desirable to have a rapid method of molecular weight determination. For this purpose one often uses intrinsic viscosity method. Especially the one-point intrinsic viscosity method is well-known as a rapid method.[1-3] However, the intrinsic viscosity method is a relative method and gives somewhat ambiguous average molecular weights for polydisperse samples. A much simpler and reliable method is preferable. Of cource such a simple and rapid method of determining molecular weight is useful for many other purposes such as quality control of commercial polymer production.

Recently osmotic mesurement has become rapid and easy by the development of high-speed membrane osmometers. One-point determination is possible by using these instruments. The method is especially straightforward, for it gives the number-average molecular weight $\bar{M}n$. This chapter is concerned with an one-point method by osmometry.

Osmotic pressure is generally expressed by eq.(1) in the virial expansion:

$$\Pi/C = (RT/\bar{M}n) \times (1 + \Gamma_2 C + \Gamma_3 C^2) \qquad (1)$$

where Γ_2 and Γ_3 are the second and the third virial coefficients, respectively. Accordingly when Γ_2 and Γ_3 are known at a given

temperature, $\bar{M}n$ can be determined from Π at a given concentration. And by setting $\Gamma_3 = 1/4\Gamma_2^2$ in accordance with Stockmayer's theory,[5] eq.(1) can be reduced to eq.(2):

$$(\Pi/C)^{1/2} = (RT/\bar{M}n)^{1/2} \times (1 + \Gamma_2 C/2) \qquad (2)$$

In this case, if only Γ_2 is known, $\bar{M}n$ of a sample can be determined by a single measurement of osmotic pressure. On the basis of this idea, the one-point method was investigated.

8.1 Experimental procedure

Polypropylene fractions having narrow molecular weight distribution (D = 1.3) was used to determine molecular weight dependence of the second virial coefficient. Commercial polypropylene homopolymers were used for the test of this method. A Hewlett Packard high-speed membrane osmometer Model 502 was employed. Determinations were made at 130°C on tetralin solutions containing 0.2 % Ionol with a pretreated Ultra-cellafilter (Sartrius Co., allerfeinst), which had been successively treated with water, isopropanol and finally tetralin.[6]

As shown in Figure 1, a plot of Π/C displayed a downward curvature owing to the third virial coefficient. Therefore the extrapolation of Π/C to C = 0 involves certain ambiguity. On the other hand, as shown in Figure 1, extrapolation of plot of $(\Pi/C)^{1/2}$ against C was linear, and a better extrapolation to C = 0 is possible. Thus, the form of eq.(2) was adopted for the one-point osmotic pressure measurement.

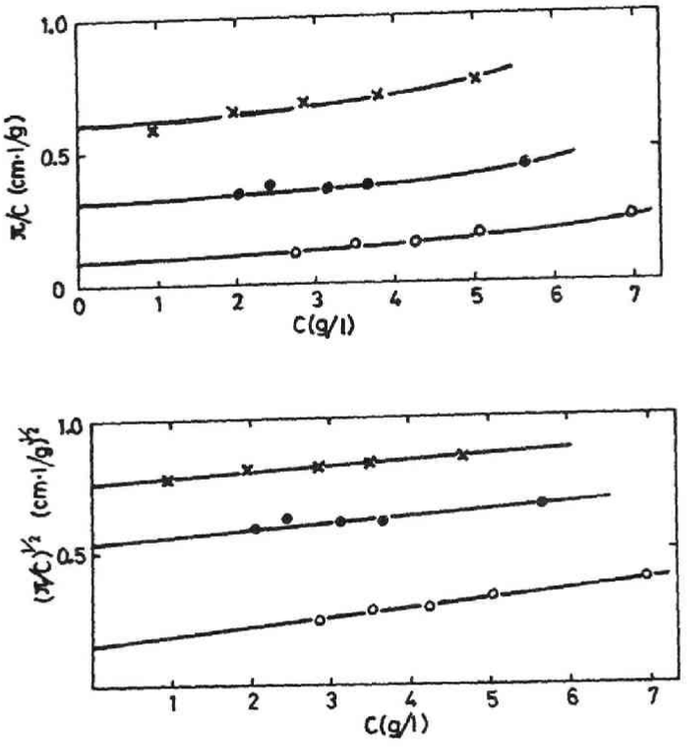

Fig. 1 Comparison of extrapolation methods of determining reduced osmotic pressure Π/C at $C = 0$.

8.2 Determination of the second virial coefficient

From the theoretical and experimental points of view, it is well-known that Γ_2 in eq.(2) highly depends on molecular weight.[7-9] The dependence was examined at 130°C in tetralin by using the fractions having narrow molecular weight distribution. The result is shown in Figure 2. Log $\Gamma_2/\bar{M}n$ decreases linearly with log $\bar{M}n$ in this figure, and Γ_2 is given by

$$\Gamma_2 = 1.15 \times 10^{-5} \bar{M}n^{0.76} \quad (1/g) \tag{3}$$

Substitution of the above equation for eq.(2) yields eq.(4):

$$\Pi = (RTC/\bar{M}n) \times (1 + 0.575 \times 10^{-5} C\bar{M}n^{0.76})^2 \tag{4}$$

In eq.(4), though $\bar{M}n$ can be determined by eq.(4) at a known concentration, the use of the relationship of Π for $\bar{M}n$ is tedious. It is simpler to determine $\bar{M}n$ graphically. Figure 3 shows the Π versus $\bar{M}n$ relationships at several concentrations.

8.3 Experimental errors in applying this method

The usefulness of this method depends greatly on how high the accuracy can be kept. Thus the errors in this method will be discussed in detail. There are three major sources of errors which would be involved in determining $\bar{M}n$ of crystalline polymers by the one-point method with a Hewlett-Packard membrane osmometer. The first one is the error inherent to the osmometer, especially due to adjusting the meniscus of solution.

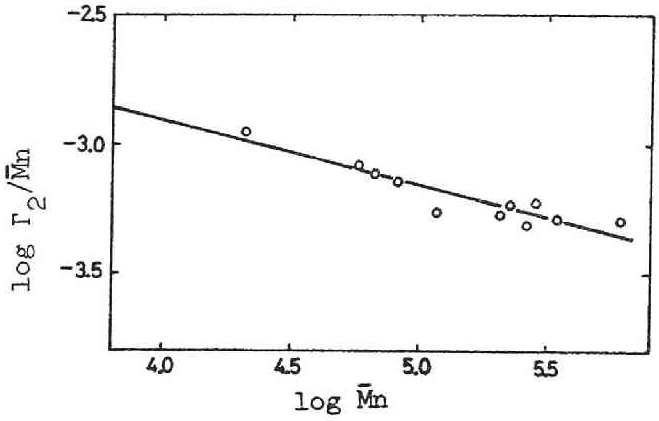

Fig. 2 Dependence of $\Gamma_2/\bar{M}n$ on log $\bar{M}n$. The fractions having narrow molecular weight distribution were used.

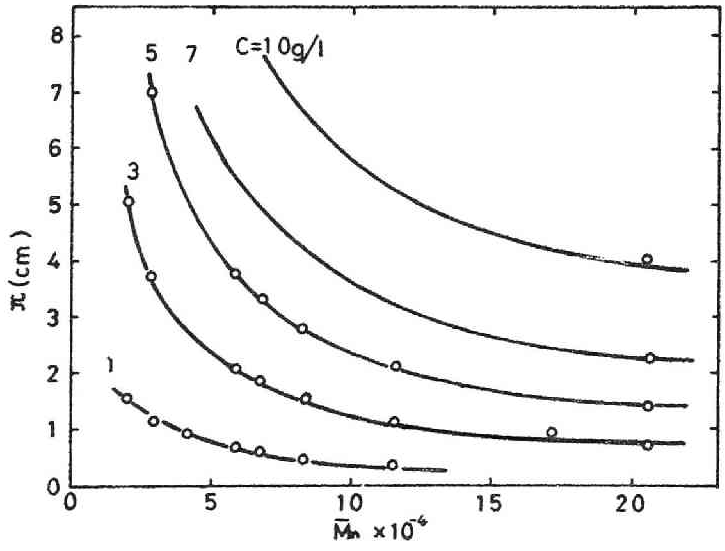

Fig. 3 Relation between Π and $\bar{M}n$ at given concentrations. (O): experimental points.

and solvent levels in glass stack of the instrument; the second one is due to the experimentation, particularly the accuracy of adjusting polymer concentration; and the third one is inherent to the one-point method itself, i.e., due to the insufficient knowledge of the second virial coefficient. The variation in fitting the solution level in the glass stack affects directly to the reading of the Π-values. The evaporation of solvent which causes the variation of polymer concentration is unavoidable especially when crystalline polypropylene is handled at high temperature. Further the uncertainty in weighing sample results in the same error. The ambiguity of the second virial coefficient is caused mainly by the difference in molecular weight distribution of sample.

The maximum error of $\delta M/\bar{M}r$ is given by eq.(5) based on the theory of errors:

$$\frac{\delta M}{\bar{M}n} = \frac{1}{\bar{M}n}\left\{\left|\frac{\partial M}{\partial \Pi}\,\delta\Pi\right| + \left|\frac{\partial M}{\partial C}\,\delta C\right| + \left|\frac{\partial M}{\partial \Gamma_2}\,\delta\Gamma_2\right|\right\} \qquad (5)$$

where $\delta\Pi$, δC and $\delta\Gamma_2$ are the variations of Π, C, and Γ_2, respectively. The error due to the variations of Π, i.e., fitting the solution level, is expressed as eq.(6) by partial differential of eq.(2)

$$(1/\bar{M}n)(\partial M/\partial \Pi) = -(4\bar{M}n/RTC) \times (2 + \Gamma_2 C)^{-2} \qquad (6)$$

It is generally expected that $|\delta\Pi| = 0.01$ cm. As shown in Figure 4, the error in this case is within 5 %. Accordingly it is worth little consideration. Next, the error due to the variation of C is expressed as

$$(1/\bar{M}n)(\partial M/\partial C) = (1/C) \times [1 + 2C(2 + \Gamma_2 C)^{-1}] \qquad (7)$$

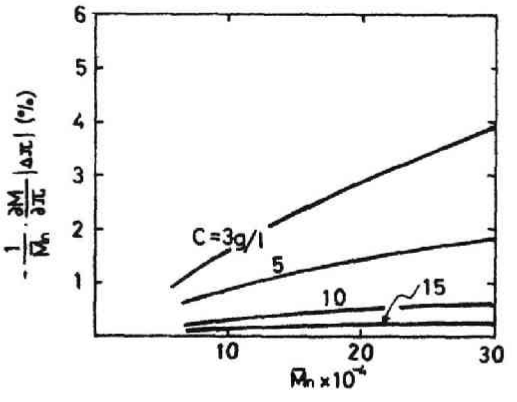

Fig. 4 Effect of the variation in fitting the solvent level in the meniscus of the glass stack on $\bar{M}n$.

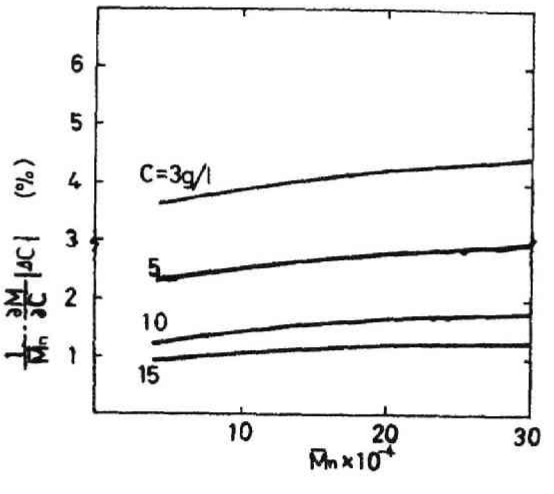

Fig. 5 Effect of the variation of polymer concentration C on $\bar{M}n$.

The variation of polymer concentration is mainly caused by uncertainty in weighing sample and by evaporation of solvent. Therefore, it is expected that $|\delta C| = 0.2$ g/l. The error in this case is shown in Figure 5. Obviously the error increases when the measurement is performed in dilute solution, but in general it is hardly worthy of attention.

Third the error due to the variation of the second virial coefficeint is expressed as:

$$(1/\bar{M}n)(\partial M/\partial \Gamma_2) = 2C(2 + \Gamma_2 C)^{-1} \qquad (8)$$

Γ_2 is expected to depend not only on molecular weight but also on molecular weight distribution. The effect of the latter is very important, because the determination is usually made on samples having different molecular weight distributions. The $\Gamma_2/\bar{M}n$ values were determined for polypropylene samples having broad molecular weight distributions. Table I shows the result. Samples having D-value from 2 to 4 give usually 0.2 higher value of log $\Gamma_2/\bar{M}n$ than that of narrow distribution polymers. In this case, as shown in Figure 6, the effect of Γ_2 on $\bar{M}n$ cannot be neglected. Therefore, the value 0.2 in log $\Gamma_2/\bar{M}n$ must be added to eq.(3), when this method is applied to commercial polypropylenes. The one-point method data after correction are shown in Table II together with the values determined by the ordinary method. In this table the relative error was calculated on the basis of the values which were determined by the ordinary method. On account of the error due to the variation of solution level, the measured values at the concentration of 0.1 g/l often deviate from those by the ordinary method. However, with this exception, the

Table I The effect of the molecular weight distribution on $\Gamma_2/\bar{M}n$

Sample	$\bar{M}n \times 10^{-4}$	$\bar{M}w/\bar{M}n$	$\log \Gamma_2/\bar{M}n$ (observed)	$\log \Gamma_2/\bar{M}n$ (calculated by eq.(3))	$\Delta\log \Gamma_2/\bar{M}n$ [a]
A	6.53	4.3	-2.99	-3.12	+0.13
B	6.53	-----	-3.01	-3.12	+0.11
C	7.28	-----	-3.07	-3.13	+0.06
D	7.65	3.1	-2.95	-3.13	+0.18
E	8.88	2.8	-3.03	-3.15	+0.12
F	9.65	2.1	-2.91	-3.16	+0.25
G	12.6	2.5	-3.01	-3.19	+0.18
H	14.6	2.4	-2.87	-3.20	+0.33
Average					+0.17

a: $\Delta\log \Gamma_2/\bar{M}n = \log \Gamma_2/\bar{M}n$ (observed) - $\log \Gamma_2/\bar{M}n$ (calculated)

Table II $\bar{M}n$ of commercial polypropylene determined by one-point and ordinary methods.

Sample	One-point method								Ordinary method
	1.0 g/l		3.0 g/l		5.0 g/l		7.0 g/l		
	$\bar{M}n \times 10^{-4}$	Error,%	$\bar{M}n \times 10^{-4}$	Error,%	$\bar{M}n \times 10^{-4}$	Error,%	$\bar{M}n \times 10^{-4}$	Error,%	$\bar{M}n \times 10^{-4}$
A	5.3	-18.5	6.6	+1.5	6.9	+6.2	7.0	+7.7	6.5
B	6.7	+1.5	6.9	+4.5	6.8	+3.0	7.1	+7.6	6.6
C	12.7	+74.0	7.6	+9.6	8.0	+9.6	----	----	7.3
D	6.9	-10.4	7.6	-1.3	7.5	-2.6	7.4	-3.9	7.7
E	8.4	-5.6	8.2	-7.9	9.9	+11.2	----	----	8.9
F	13.0	-3.2	12.8	+1.6	11.8	-6.3	----	----	12.6

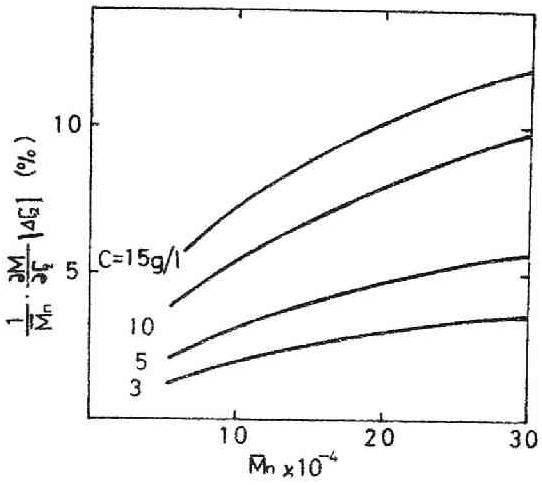

Fig. 6 Effect of the variation of the second virial coefficient Γ_2 on $\bar{M}n$.

agreement between the values by the one-point and ordinary methods is satisfactory.

This method is much preferred for amorphous polymers, which can be handled at ordinary temperature. The preparation of membrane suitable for high temperature operation is not easy. Therefore, the measurement of osmotic pressure for crystalline polymers such as commercial polypropylenes is accompanied by difficulty to some extent. Nevertheless the method seems to be satisfactory for rapid determination of their number-average molecular weights.

REFERENCES

1. M.L. Huggins, Ind. Eng. Chem., 35, 980(1943)
2. R.Z. Naar, H.H. Zabusky, and R.F. Heitmiller, J. Appl. Polym. Sci., 7, 330(1963)
3. J.H. Elliot, K.H. Horowitz, and T. Hoodock, J. Appl. Polym. Sci., 14, 2947(1970)
4. R. Koningsveld and C.A.F. Tuijnman, Makromol. Chem., 38, 39(1960)
5. W.H. Stockmayer and E.F. Casassa, J. Chem. Phys., 20, 1560(1952)
6. T. Ogawa, Y. Suzuki, and T. Inaba, J. Polym. Sci., Part A-1, 10, 737(1972)
7. A. Kotera, K. Takamizawa, T. Kamata, and H. Kawaguchi, Rep. Progr. Polym. Phys., 4, 131(1961)
8. T.A. Orofino and P.J. Flory, J. Chem. Phys., 26, 1067(1957)
9. E.F. Casassa, J. Chem. Phys., 31, 800(1959)

SUMMARY AND CONCLUSION

We attempted to establish a method of characterization of crystalline polypropylene and ethylene-propylene copolymers, which are commercially most important thermoplastic materials. For this purpose we introduced column fractionation technique. Various patterns of fractionation behavior for homopolypropylenes and ethylene-propylene copolymerization products were examined by experimental and simulation techniques in relation to the heterogeneity of the polymers such as molecular weight and compositional distributions.

In Chapter 2, experimental conditions and simulation method were studied for homopolypropylnes. The polymers can be fractionated according to molecular weight in the vicinity of 160°C, where the fractionation system is in liquid-liquid phase equilibrium. Simulation of the fractionation was carried out by computer on the basis of Flory-Huggins' theory. These results show that molecular weight distribution of original polymer constructed from fractionation data is apparently narrower than the true one. This artifact is attributed to the overlapping of distributions of the fractions, because these fractions are more or less polydisperse in molecular weight.

In Chapters 3 and 4, fractionation conditions of homopolypropylenes were examined in detail to attain better fractionation. Particularly attention was focused to depositing conditions and deposition state of the polymers on support surface. So-called selective deposition, in which high molecular weight species are deposited first and low molecular weight species later, has been considered so far to be important for achieving good fractionation. However, we found that this is not so. Rather,

we found that polymer is not uniformly spread as a film but deposited as small particles on support surface. This fact is largely different from the idea in the past. Better fractionation can be achieved by polymer particles of smaller size.

The fractionation of homopolypropylenes was carried out by several solvent-nonsolvent combinations. Almost all fractions obtained showed D values less than 1.4: the recovery of such narrow distribtuion fractions of homopolypropylenes by fractionation has been never reported previously. Especially use of solvent and nonsolvent of both poor in solubility gave better fractionation results. By such a combination, narrow distribution fractions usually 1.05 - 1.20 in D value can be obtained over a wide molecular weight range. This is particularly important for preparative fractionation.

In Chapter 5, we described the fractionation based on the system in solid-liquid phase equilibrium. The fractionation was carried out by raising column temperature stepwise. This method was expected to separate polypropylene according to tacticity. However, the fractionation behavior was always more or less influenced by molecular weight, when commercial polypropylenes were fractionated. This can be understood as a behavior similar to the influence of molecular weight on compositional fractionation of copolymers, which was described in Chapters 6 and 7. Especially in a lower molecular weight region the effect of molecular weight on solubility is pronounced. Therefore, commercial polypropylenes having broad molecular weight distribtuion are seemingly fractionated according to both molecular weight and tacticity.

In Chapter 6, fractionation conditions of random type ethylene-propylene copolymers were examined in detail through cloud-point and melting-point measurements. The distributions of molecular weight, chemical composition

and monomer sequence length were examined by using appropriate solvent-nonsolvent systems under other selected conditions. Generally these showed broad distributions concerning the above characteristics.

In Chpater 7, simulation analyses of the fractionation were carried out for several different types of copolymerization products which include homopolymers as by-products. Efforts were devoted to elucidate the components and composition of all types of the products from fractionation data. The products were classified for convenience into five types: pure ethylene-propylene copolymer (EP), polyethylene-polypropylene blend (PE-PP), polypropylene-copolymer blend (PP-EP), polypropylene-copolymer-polyethylene blend (PP-EP-PE), and copolymer-polyethylene blend (EP-PE). The fractionation behavior was examined with regard to molecular weight and chemical composition. The simulation was performed by considering the factors affecting fractionation behavior such as molecular weight, chemical composition and partition coefficient of polymer species between two liquid phases. The simulation results of pure EP was in good agreement with experiments on random type copolymers. EP-PP type gave peculiar patterns with regard to both molecular weight and compositional distributions. These patterns are very useful for distinguishing this blend from the copolymers. An example for this blend was found in actual copolymerization products. The fractionation behavior can be used for elucidating the component and composition of other types of blends. In fact all the fractionation results obtained experimentally were understood by the above simulation. In addition, we found that most commercial high impact polypropylenes belong to PP-EP type.

In Chapter 8, one-point osmometry, i.e., the method of determining $\bar{M}n$ by one-point measurement of osmotic pressure was investigated to develop a simple and rapid method of determining molecular weights. A high speed membrane osmometer was used for this purpose. This method could be applied to commercial polypropylenes within 5 % error by correcting the effect of molecular weight distribution on the second virial coefficient.

ACKNOWLEDGMENTS

The author wishes to express his deep gratitude to Professor H. Inagaki of Institue for Chemical Research, Kyoto University, for giving him the chance of writing the thesis and for detailed criticism of the manuscript. The author is greatly indebted to Dr. T. Kotaka of the Inagaki Laboratory, for valuable discussion and detailed criticism of the manuscript. Acknowledgments are due to the other members of the Inagaki Laboratory, especially to Dr. T. Miyamoto, Dr. H. Suzuki and Mr. N. Donkai for their helpful suggestions.

The author wishes to express his appreciation to the management of the Ube Industries Ltd., for supporting this study. Grateful acknowledgment is made especially to Dr. S. Tokiura, Manager of the Hirakata Plastics Research Laboratory, Mr. T. Inaba and Dr. S. Hoshino, Heads of the Special Research Section in the Research Laboratory for valuable discussions and their constant encouragement, without which this study would not have been completed. Appreciation is also tendered to Mr. Y. Suzuki, a Head of the Special Research Section, for advice in experiments. The experimental work in this study was greatly assisted by the continued efforts of Mr. S. Tanaka and Mr. T. Terada.

Thanks also to my wife Akiko for her patience and understanding during this endeavor.

List of Papers

Each chapter of this dissertation was described on the basis of the following papers published by the author: Chapter 2 concerns (1) and (2); Chapter 3 (3); Chapter 4 (4) and (5); Chapter 5 (6); Chapter 6 (7); Chapter 7 (8), (9) and (10); Chapter 8 (11).

(1) T. Ogawa, Y. Suzuki, S. Tanaka, and S. Hoshino, "On the Column Fractionation of Large Amount of Isotactic Polypropylene," Kobunshi Kagaku, 27, 356(1970)

(2) T. Ogawa, Y. Suzuki, and T. Inaba, "Determination of Molecular Weight Distribution for Polypropylene by Column Fractionation and Gel-Permeation Chromatography," J. Polym. Sci., Part A-1, 10, 737(1972)

(3) T. Ogawa, S. Tanaka, and T. Inaba, "Polymer Deposition onto the Support in Column Fractionation," J. Appl. Polym. Sci., 17, 779(1973)

(4) T. Ogawa and S. Hoshino, "Cloud Points in Isotactic Polypropylene-Solvent-Nonsolvent Systems," Kobunshi Kagaku, 28, 348(1971)

(5) T. Ogawa, S. Tanaka, and S. Hoshino, "Effects of the Combination of Solvent and Nonsolvent on the Fractionation of Polypropylene," J. Appl. Polym. Sci., 16, 2257(1972)

(6) T. Ogawa and S. Hoshino, "Fractionation of Polypropylene by the Rising Temperature Method," J. Appl. Polym. Sci., 17, 2235(1973)

(7) T. Ogawa, S. Tanaka, and T. Inaba, "Fractionation of Ethylene-Propylene Copolymers," J. Appl. Polym. Sci., 17, 319(1973)

(8) T. Ogawa, S. Tanaka, and T. Inaba, "Analysis of Fractionation of Ethylene-Propylene Copolymers," J. Polym. Sci., Polym. Phys. Ed., 12, 785(1974)

(9) T. Ogawa, S. Tanaka, and T. Inaba, "Analysis on the Fractionation of Polyethylene-Polypropylene Blends," J. Appl. Polym. Sci., 18, 1351(1974)

(10) T. Ogawa and T. Inaba, "Analysis of the Fractionation of Ethylene-Propylene Copolymerization Products," J. Appl. Polym. Sci., 18, 3345(1974)

(11) T. Ogawa, S. Tanaka, and S. Hoshino, "One-Point Method for Determination of Number-Average Molecular Weight," J. Appl. Polym. Sci., 17, 2435(1973)

A little part of the following papers was quoted to prepare the dissertation.

(1) T. Ogawa, S. Tanaka, and S. Hoshino, " The Effect of Pearmeable Low Molecular Weight Polymer through the Membrane on the Number-Average Molecular Weight with Osmometry, " Kobunshi Kagaku, 28, 8(1971)

(2) T. Ogawa, S. Tanaka, and S. Hoshino, "Calibration Curve for Polypropylene in Gel Permeation Chromatography," Kobunshi Kagaku, 29, 6(1972)